Pedaling-related brain activation in people post-stroke: an fMRI study

Nutta-on Promjunyakul
Marquette University

PEDALING-RELATED BRAIN ACTIVATION IN PEOPLE POST-STROKE: AN FMRI STUDY

by

Nutta-on Promjunyakul, P.T., M.Sc.

A Dissertation submitted to the Faculty of Graduate School,

Marquette University,

in Partial Fulfillment of the Requirements for

the Degree of Doctor of Philosophy

Milwaukee, Wisconsin

December 2012

ABSTRACT

PEDALING-RELATED BRAIN ACTIVATION IN PEOPLE POST-STROKE:

AN FMRI STUDY

Nutta-on Promjunyakul, P.T., M.Sc.

Marquette University, 2012

This study aimed to enhance our understanding of supraspinal control of locomotion in stroke survivors and its relationship to locomotor impairment. We focused mainly on the locomotor component of walking, which involves rhythmic, reciprocal, flexion and extension movements of multiple joints in both legs. Functional magnetic resonance imaging (fMRI) was used to record human brain activity while pedaling was used as a model of locomotion. First, we examined the spatiotemporal characteristics of hemodynamic responses recorded with fMRI and found that they were different in stroke survivors and control subjects. However, these differences were not substantial enough to require altering the normal canonical hemodynamic response function to obtain valid measurements of pedaling-related brain activity. During pedaling, stroke survivors and control subjects showed activity in the sensorimotor cortex and cerebellum. Stroke survivors had reduced volume of activation in those regions, however the signal intensity was similar between the groups. In stroke survivors, sensorimotor cortex activity was symmetrically distributed across the damaged and undamaged hemispheres; while cerebellum activity was lateralized to the damaged hemisphere. These brain activation patterns were different from those observed during non-locomotor movements, where volume of activation was unchanged but signal intensity was reduced in stroke survivors. We conclude that neural adaptations for producing locomotor and non-locomotor movements post-stroke are not the same and that the spinal cord and cerebellum might have a compensatory role in producing hemiparetic locomotion. Finally, we examined the relationship between locomotor performance and pedaling-related brain activity measured with fMRI. We found no relationship between the brain activation symmetry and locomotor symmetry, suggesting that the brain activation from each hemisphere was not directly responsible for control of the contralateral leg. However, our stroke survivors demonstrated poor locomotor performance and decreased volume of activation measured during pedaling, suggesting that impaired locomotion was associated with reduced volume of activation. Signal intensity of brain activity was associated with rate of pedaling in stroke survivors, suggesting that increased signal intensity in the active brain areas may compensate for reduced volume of activation in the production of hemiparetic locomotion.

ACKNOWLEDGEMENTS

Nutta-on Promjunyakul, PT, M.Sc.

I would like to thank my advisors, Drs. Sheila Schindler-Ivens and Brian Schmit for giving me their oversight and invaluable time throughout my project. I would also like to thank my committee members, Drs. Kristina Ropella, Scott Beardsley, and Daniel Rowe, for their constant guidance, enthusiasm, and advice.

I thank all of my colleagues at Marquette University who have assisted me in the research process. Thanks to Matthew Verber who taught me fMRI analysis; Dr. Naveen Bansal who helped me with statistical analysis; Ryan McKindles, Matthew Chua, and Eric Walker, David Seck and Cara Lewellyn for their help with data analysis; and Brett Arand for proofreading my work. A special thank you to Ruth Swedler, for her support and encouragement. Last but not least, thanks to Krishnaj Gourab, Dominic Nathan, Prajakta Sukerkar and Megan Conrad for their helpful opinions and moral support.

Additionally, I would like to extend my gratitude to my funding sources for this dissertation: National Center for Medical and Rehabilitation Research at the National Institute of Child Health and Human Development (NICHD-NCMRR #K01HD00600693) and the Ralph and Marion Falk Medical Research Trust.

Finally, I am especially grateful to have my family, my boyfriend, Nathaniel Blair, and his family who has provided constant encouragement and support throughout my graduate studies.

TABLE OF CONTENTS

LIST OF TABLES

LIST OF FIGURES

ABBREVIATIONS

AFNI=analysis of Functional NeuroImages

AFO= ankle-foot orthotic

ANOVA=one-way analysis of variance

AP-GRF=anteroposterior ground reaction force

ASL=arterial spin labeling (ASL)

BA6= Brodmann's area 6

BOLD=blood oxygen level-dependent

CPGs=central pattern generators

DICOM=digital imaging and communication in medicine

EEG=electroencephalography

fMRI= functional magnetic resonance imaging

FOV=field of view

KINSYM=Between-limb symmetry of walking kinetics

KINSYM(+)=Between-limb symmetry of walking propulsive impulse

KINSYM(-)=Between-limb symmetry of walking braking impulse

KINSYM(net)=Between-limb symmetry of walking net impulse

LI=laterality index

LSD=least significant difference

M1= primary motor area

M1/S1=primary sensorimotor area

MANOVA=multivariate analysis of variance

NIRS=near infrared spectroscopy

PEDSYM=Symmetry of mechanical work produced during pedaling

PEDSYM(+)=Symmetry of positive mechanical work produced during pedaling

PEDSYM(-)=Symmetry of negative mechanical work produced during pedaling

PEDSYM(net)=Symmetry of net mechanical work produced during pedaling

PMA=premotor area

Pre-SMA=pre-supplementary motor area

r=Pearson correlation coefficients

ROC=rate of change of amplitude

S1=primary somatosensory

S2=secondary somatosensory area

SD=standard deviation

SLR=step length ratio

SMA=supplementary motor area

SMC-Cb=sensorimotor cortex and cerebellum combined

SP=electrical silence period

TCD=transcranial doppler

TE=echo time

TES= transcranial electrical stimulation

TMS=transcranial magnetic stimulation

TR= repetition time

TSR=temporal symmetrical ratio

CHAPTER 1: LITERATURE REVIEW

1.1 INTRODUCTION

Stroke is a brain injury condition caused by disruption of the cerebral blood vessels. Each year, approximately 800,000 individuals in the US experience a new or recurrent stroke (Lloyd-Jones et al., 2009), often resulting in persistent residual walking impairment and preventing them from regaining their normal lifestyle. Lord et al. reported that 40% of post-stroke patients who were discharged continued to have significant impairment in walking (Lord et al., 2004). Desrosiers et al. demonstrated that at the time of discharge the average walking speed was 0.43±0.35 m/s (Desrosiers et al., 2003), which is adequate for household, but not community ambulation (Perry et al., 1995). Based on this information, stroke survivors still show gait deficits after a certain period of rehabilitation, suggesting that the current rehabilitation may not be adequate and improved approaches for gait rehabilitation are needed.

An important first step in formulating novel rehabilitation strategies to improve post-stroke gait rehabilitation is to better understand the role that the brain plays in human walking and how a stroke, and the subsequent functional reorganization in the brain, contributes to persistent gait impairment. Walking is composed of many components, such as locomotor movement, balance, and body weight support, which are deeply integrated for successful walking. However, each component has different neural controls for normal walking, and may therefore exhibit independent control and recovery post-stroke.

In this study, we aimed to enhance our understanding of supraspinal control of locomotion in stroke survivors and its relationship to locomotor impairment. We focused mainly on the locomotor component of walking, which involves rhythmic, reciprocal, flexion and extension movements of multiple joints in both legs. Studying the locomotor component of walking allowed us to examine the brain activation associated with locomotor movement without concern for the stroke subjects' impaired balance and body weight support. Functional magnetic resonance imaging (fMRI) was used to record human brain activity. A pedaling paradigm was used for examining the brain activation associated with locomotor movement. An understanding of the roles of functional reorganization in the brain after stroke and its contributions towards the severity of locomotion impairments can be used to guide treatment planning.

This chapter provides a literature review outlining neural control of locomotion, brain reorganization induced by locomotion in stroke survivors, instrumentation using fMRI, and locomotor impairments in stroke survivors and their relationship to brain reorganization. The goal of this chapter is to provide relevant background information regarding the supraspinal control of locomotion and to explain the rationale for enhancing our understanding of the role of brain reorganization in controlling locomotion post-stroke.

1.2 NEURAL CONTROL OF LOCOMOTION

Walking is a self-propelled rhythmic movement, which needs to be goal-directed and adjustable to changes in the environment with optimal expenditure of neural effort and metabolic energy. This task appears to be a stereotyped action involving repetitions of the same movement, which may mistakenly be thought of as a simple task. However, walking is a complex task biomechanically, as it requires skilled coordination in a timely manner between the two legs in order to produce a bilateral, reciprocal alternation of hip, knee, and ankle joints, while maintaining balance and body weight bearing. To achieve this complex movement, the activity of all muscles involved has to be precisely scaled with respect to each other so that the end-point is within the desired range (Hansen et al., 2001).

The underlying neural networks, which are responsible for the generation and control of the muscle activity during walking, must be organized to ensure that the overall activity of the muscles is scaled and timed correctly, yet still provide considerable flexibility of the individual muscle to adjust to unexpected situations. This is achieved through the integrated activity of spinal neuronal circuits, sensory feedback signals, and descending supraspinal motor commands.

Our understanding of human neural control of locomotion evolved from animal models, which are considered simpler versions of human locomotion and are much more extensively studied. However, we now know that the neural control of locomotion in animal models is not simply a less complex version of the human model, but they do indeed share some similarities. This section provides evidence for the existence of the

spinal rhythmic-generating center, the role of sensory feedback, and supraspinal inputs in the control of walking in humans.

1.2.1 Spinal cord

The spinal cord is the lowest level of the hierarchical central nervous organization. Neuronal networks in the spinal cord, known as central pattern generators (CPGs), can generate basic rhythmic locomotor movement (Brown 1911; SHERRINGTON 1910; Whelan 1996). Evidence of central pattern generators exists in all species, but it likely contributes to the control of locomotion to a different level in different species. In lower species, the neuronal network is complete in itself, meaning that it can generate rhythmic locomotor movement with the absence of supraspinal inputs and sensory feedback (Belanger et al., 1996; Duysens and Van de Crommert 1998). The higher the species is, the greater the amount of supraspinal inputs it requires. For example, cats that are given a spinal cord transection, referred to as spinal cats, can generate a complete automatic hindlimb stepping movement on a treadmill. Spinalized marmoset monkeys, which have a more complex neural control of locomotion than cats, have a spinal network that produces rhythmic alternating activity of the legs, but the pattern is not as robust as that seen in the cats. In humans the generation of rhythmic activity following complete spinal cord injury is rare, and even with considerable effort or interventions functional locomotion has not been observed in the absence of supraspinal inputs.

Classic experiments in spinal cats show that they can generate a stepping pattern with their hind limbs when placed on a motorized treadmill and provided body support. This movement is well coordinated, with alternating activity of the hind limbs and gait adaptation to the speed of the treadmill belt (Barbeau and Rossignol 1987; Forssberg and Grillner 1973). Electromyography recorded in the spinal cats demonstrates similar bursting activity of the flexor and extensor muscles to the intact cats (Barbeau and Rossignol 1987). The spinal cat's recovery is spontaneous during the acute phase and the rhythmic movement continues to improve in coordination and more closely resembles healthy functioning cats with time and training. This suggests that there is a complete spinal pattern-generating neuronal network. The most convincing evidence that the intrinsic neural networks in the spinal cord are solely able to generate rhythmic output was obtained from spinalized and deafferented cat experiments, where the locomotor-related afferent input is completely eliminated. Under this condition, the motor nerve activity recorded at the ventral root demonstrates rhythmic activity between agonist and antagonists reciprocally, which is termed fiction locomotion (Grillner and Zangger 1975; Grillner and Zangger 1979).

Acute spinalized and deafferented monkeys demonstrate stepping and rhythmic alternating activity in antagonistic muscles. However, this locomotor pattern is not as robust as seen in the cat (Barbeau and Rossignol 1991; Barbeau, Chau, Rossignol 1993). Fedirchuk et al. observed a much more robust muscle activity when they stimulated the brain stem, suggesting that, in monkeys, the central pattern generator relies more on supraspinal control to produce proper basic locomotor patterns compared to cats (Fedirchuk et al., 1998).

In humans, compelling evidence for the existence of a central pattern generator in the spinal cord comes from studies of gait development in human infants and the hierarchical organization of the central nervous system. Forrsberg demonstrated that human infants produce an automatic stepping pattern immediately after birth if held erect and moved over a horizontal surface. However, their movement lacked some of the mature characteristics compared to human adults (Forssberg 1985). This immature rhythmic movement is likely controlled by the central pattern generator since the pattern could also be seen in anencephalic infants (Yang, Stephens, Vishram 1998).

Other compelling evidence for the central pattern generator comes from patients with both incomplete and clinically complete spinal cord injuries (Bussel et al., 1988; Calancie et al., 1994; Dietz et al., 1995; Dietz et al., 1995; Dimitrijevic, Gerasimenko, Pinter 1998; Wernig and Muller 1992). For example, Calancie et al. showed that a patient with incomplete spinal cord injury at the cervical level, when lying with his hip extended, could generate a rhythmic, alternating, and forceful movement, involving all the lower extremity muscles (Calancie et al., 1994). Dimitrijevic et al. demonstrated that subjects with complete spinal cord injury at the thoracic and cervical levels could induce patterned, locomotor-like electromyography when non-patterned electrical stimulation was applied at the lumbar level. They were also able to generate a repetitive flexor withdrawal movement (Dimitrijevic, Gerasimenko, Pinter 1998). Dietz et al. also demonstrated a modulated electromyography pattern in patients with complete cord injury during treadmill walking, but no real movement was shown (Dietz et al., 1995). Although these studies demonstrated the existence of the central pattern generator in

humans and its potential in producing a rhythmic locomotor pattern, the spinal center could not solely generate functional locomotion.

1.2.2 Peripheral sensory feedback

Peripheral afferents play an important role in adapting and updating the muscle activity of walking during unperturbed locomotor movements, and allow for corrective reflexes and adjustment of stepping patterns when unexpected perturbations arise (Nielsen 2003). While spinal networks are capable of generating a rhythmic locomotor pattern, peripheral afferents are thought to regulate the movement. Proprioception regulates the timing and amplitude of the stepping patterns through the muscle's mechanoreceptors, and sensory input from the skin (cutaneous reflex) allows stepping to adjust to unexpected perturbations.

The two critical proprioceptive inputs that affect the timing of the phases during gait are the position of the hip and the load on extensors muscles. Previous work has shown that holding the hip in extension at an angle close to initiation of the swing prevents a transition from stance-to-swing phase (Grillner and Rossignol 1978), whereas assisting hip flexion during the swing phase advances the onset of ankle extensor activity and initiates the swing-to-stance phase (McVea et al., 2005). The other important muscle afferent is the load receptor of the extensors, which is important for stance phase. Duysens and Pearson demonstrated that an additional load on the ankle extensors during the stance phase in spinal cats increases extensor muscle activity and prevents the initiation of the swing phase. In contrast, removal of the load promotes the initiation of

the swing phase (Duysens and Pearson 1980). In humans, the sensory contribution to the excitatory drive of the motorneurons seems to be similar to cats (Hultborn and Nielsen 2007) for both joint position (Dietz, Muller, Colombo 2002; Marchand-Pauvert and Nielsen 2002; Marchand-Pauvert and Nielsen 2002) and loading (Dietz, Muller, Colombo 2002; Sinkjaer et al., 2000). These observations suggest that proprioception is essential peripheral afferent feedback for walking and maintaining an ongoing pattern, including phase transitions.

Cutaneous reflexes allow stepping to adjust to unexpected obstacles at specific parts of the gait cycle. Previous studies in cats have shown that mechanical (tactile) stimulation of the dorsum of the foot during the early part of the swing phase initiates knee flexion, and subsequently the swing phase (Forssberg, Grillner, Rossignol 1977; Forssberg 1979). This is known as a stumbling corrective reaction. The underlying mechanism involved is that the stimulus applied to the dorsal side of the paw produces excitation of the flexor motoneurons and inhibition of the extensor motoneurons.

In humans, the load-dependent cutaneous reflex has also been observed and was consistent with animal studies reporting that loading is important in controlling gait cycles. Gordon et al. (2009) have shown that, in both spinal cord injury and healthy control subjects, ankle loading increases hip extension moments during stance phase (Gordon et al., 2009). Additionally, Bastiaanese et al. demonstrated that reflex amplitudes increased with body unloading and decreased with body loading, suggesting that load receptors might be involved in the regulation of cutaneous reflex responses in response to different locomotor patterns (Bastiaanse, Duysens, Dietz 2000). Wu et al. (2011) have showed that applying electrical stimulation over the upper thigh muscles

enhanced hip and knee extension and flexion torque responses during stance and swing phases, respectively (Wu et al., 2011). We can conclude from these observations that cutaneous reflexes exist in both cats and humans, and are important in the regulation of gait.

1.2.3 Supraspinal inputs

Although supraspinal input is not essential for producing the basic rhythmic locomotor movement in spinal cats, it is involved in gait initiation and speed regulation. Shik et al. demonstrated that gait initiation could be evoked by electrical stimulation at the mesencephalic locomotor region located in the brainstem of decerebrated cats. They also showed that increased intensity of the electrical stimulation increases the speed of walking (Shik, Severin, Orlovskii 1966). This finding together with the previous finding that spinal cats without supraspinal inputs adapt to different speeds of the treadmill belt (Barbeau and Rossignol 1987; Forssberg and Grillner 1973), suggests that supraspinal inputs and the pyramidal tract play a facultative role during normal walking. However, while walking in a more complicated environment, such as avoiding obstacles or walking on a ladder, supraspinal control plays a crucial role for cats to adjust to the environment. This was supported by studies in healthy cats that demonstrate increased peak discharge frequency of the primary motor cortex as cats modified their gait to step over obstacles (Drew 1988; Drew 1993).

Unlike animals, humans require supraspinal inputs for functional walking because people with clinically complete spinal cord injuries, in the absence of supraspinal inputs,

have never regained functional walking (Dietz, Colombo, Jensen 1994; Dietz et al., 1995). Further evidence of the existence of supraspinal control during locomotor tasks comes from transcranial magnetic stimulation (TMS) and functional brain imaging studies.

Transcranial magnetic stimulation is a technique that directly stimulates excitatory monosynaptic projections from the motor cortex to the spinal motoneurons via corticospinal pathways (Burke, Hicks, Stephen 1990) and inhibitory intracortical connections (Ziemann, Rothwell, Ridding 1996), and can be measured as motor evoked potentials in the associated muscles. Previous studies using TMS demonstrate the modulatory role of the corticospinal input on the tibialis anterior and soleus during different phases of pedaling (Pyndt and Nielsen 2003) and walking (Capaday et al., 1999; Petersen, Christensen, Nielsen 1998; Petersen et al., 2001; Schubert et al., 1999). These studies also demonstrate greater activation of the motoneurons during walking than at rest or during a tonic contraction. Stronger evidence of the contribution of the motor cortex to locomotion came from Petersen et al (2001) when they demonstrated that below-threshold brain stimuli during walking was corresponded with a suppressive ongoing ankle dorsiflexor activity (Petersen et al., 2001). The motor cortex might not be involved in timing the motor bursts during the step cycle though, as Capaday et al. showed that magnetic stimulation of the motor cortex at various phases of the step cycle did not reset the cycle (Capaday et al., 1999). Later, a concern arose that TMS could not only activate neurons with monosynaptic connections to the motoneurons in the associated muscle, but also activate pathways with polysynaptic connections (Burke, Hicks, Stephen 1990). This implies that the measured motor evoked potential might reflect not only excitability

at the cortical level, but also at the subcortical level. Petersen et al. therefore used transcranial electrical stimulation (TES), which more selectively activates the axons of the cortical cells in the white matter, to rule out contribution of the subcortical structures. They found that only the subthreshold TMS generated the suppressive muscle activity during walking, not the TES, suggesting that the reduction of the muscle activity was caused by a reduction in the corticospinal drive and less likely by a subcortical structure (Petersen et al., 2001).

Functional brain imaging studies during real time locomotion and immediately after locomotion, such as walking or pedaling, have shown that bilateral primary motor (M1), primary somatosensory (S1), supplementary motor area (SMA), premotor area (PMA) and the cerebellum are involved in controlling locomotor movement (Christensen et al., 2000; Fukuyama et al., 1997; Harada et al., 2009; Mehta et al., 2012; Mihara et al., 2007; Miyai et al., 2001; Suzuki et al., 2004; Suzuki et al., 2008; Williamson et al., 1997). Other brain regions that contribute to locomotion include the visual cortex and striatum (Fukuyama et al., 1997). Electrocortical studies also demonstrate modulation of the motor cortex throughout the pedaling and gait cycle (Gwin et al., 2011; Sakamoto et al., 2004). Different speed and load of the rhythmic movement modifies the amount of cortical control (Christensen et al., 2000; Jain et al., 2012; Mehta et al., 2012). These results suggest that the sensorimotor cortex; including M1, S1, SMA, and PMA, and cerebellum control locomotion. The results also suggest the visual cortex and basal ganglia might be involved in bipedal locomotor activity in humans.

The M1 and S1, which are directly connected to the spinal cord via corticospinal pathways and the posterior column-medial lemniscus pathway, respectively, are

responsible for execution of steady-speed locomotion (Suzuki et al., 2008). The role of M1 in controlling locomotion is supported by a study using chronically implanted micro-electrodes to obtain the firing rate of motor cortical neurons during walking in cats. This study reported that during slow walking, 56% of motor neurons discharged faster than at rest and 80% showed frequency modulation time-locked to the gait cycle. Fourteen percent of the motor neurons demonstrated a linear relationship between the discharge rate and the speed, which ranged from 0.37 to 1.43 m/s (Armstrong and Drew 1984). This suggests that M1 contributes to control of locomotion.

The Primary somatosensory area is important in integrating sensory inputs from visual, vestibular, and somatosensory systems, and subsequently uses this information to modify locomotor output. This idea is supported by studies that show a transcortical contribution to cutaneous reflexes elicited during walking (Christensen et al., 1999). Additional evidence comes from passive pedaling studies that demonstrate roughly equivalent cortical activation during passive and active pedaling (Christensen et al., 2000; Mehta et al., 2012). Both of these studies conclude that sensory feedback from the moving limbs may play a substantial role in maintaining locomotor-related brain activity.

The other parts of the sensorimotor cortex are the SMA and PMA. These areas are associated with preparation for walking during both the rest and walking period. Suzuki et al. showed that during preparation for walking cued by a verbal instruction, increased activity of PMA and SMA are observed. During the preparation for walking, the activity of PMA and SMA is greater than initiating walking without any cue (Suzuki et al., 2008), suggesting that SMA and PMA are responsible for planning of locomotion. The SMA may also be involved in controlling the rate of movement. Mehta et al.

demonstrated a greater activity of the SMA during variable and fast pedaling as compared with slow pedaling (Mehta et al., 2012), suggesting that SMA might play a role in controlling rate of locomotion.

The cerebellum is a complex structure which is important for producing coordination, precision, and accurate timing of movement. It receives ipsilateral sensory inputs of limb and joint position from the spinal cord via spinocerebellar pathways and from other parts of the brain. This sensory information is integrated and is used to fine tune motor activity (Fine, Ionita, Lohr 2002). The cerebellar vermis and lobule IV-V and VIII play roles in motor control. The cerebellar vermis is thought to have a role in producing rhythmic locomotor movement. A decerebrate cat study has shown that stimulation of the hook bundle of Russell, which is located in the white matter of the cerebellar vermis, evokes a well-coordinated rhythmic locomotor pattern while the decerebrate cat walks on a treadmill. The pattern was comparable to the pattern produced when a stimulation was applied to the mesencephalic locomotor regions in the same animals (Mori et al., 2000). Both lobule IV-V and VIII, located in the anterior lobe of the cerebellum, are associated with sensorimotor tasks (Stoodley and Schmahmann 2009). The cerebellar vermis (Coffman, Dum, Strick 2011) and lobules (Kelly and Strick 2003; Ramnani 2006) are bidirectionally connected to contralateral M1 and S1 areas via the cerebellocortical loop of the sensorimotor network (Kelly and Strick 2003; Molinari, Filippini, Leggio 2002). This evidence demonstrates that the cerebellum is important for sensorimotor tasks, including locomotion, and works closely with the cortex and spinal cord.

These studies provide evidence that neural control of locomotion in humans and animals are not exactly the same, but they do share similarities. In humans, supraspinal regulation plays a larger role in controlling locomotion compared to animals. The main functions include regulating the spinal center, refining the motor pattern in response to feedback from the peripheral inputs, and controlling the overall speed of locomotion.

1.3 LOCOMOTOR-RELATED BRIAN REORGANIZATION AFTER STROKE

Neural plasticity after a stroke may cause brain functional reorganization during locomotor tasks, such as pedaling and walking, suggesting stroke survivors produce different brain activation patterns compared to healthy individuals. Previous work suggests that impaired locomotion after stroke is associated with asymmetrical activation of the primary somatosensory (S1) and primary motor (M1) cortical areas, and additional recruitment of the secondary motor areas, such as PMA, SMA, pre-SMA, and prefrontal area (Lin, Chen, Lin 2012; Miyai et al., 2002; Miyai et al., 2006), which are normally not as active as the S1 and M1 in healthy individuals when measured with the same brain imaging technique (Miyai et al., 2001; Suzuki et al., 2004; Suzuki et al., 2008). With improved locomotor ability caused by increased time post-stroke and/or rehabilitation, S1 and M1 activities become more symmetrical because of a reduction in activity on the undamaged side and an increase in activity on the damaged side (Miyai et al., 2003; Miyai et al., 2006), and a decrease in overall cortical activity (Miyai et al., 2006). These observations have led to the conclusion that asymmetrical activity in the S1 and M1 (undamaged>damaged) may contribute to impaired walking performance post-stroke and

that restoration of symmetry in this region may be responsible for recovery. Moreover, decreasing activity of the abnormally increased activity in the secondary motor areas during recovery after stroke suggests that these regions may be involved in compensation for cortical damage, also contributing to recovery.

Non-locomotor movement - unilateral paretic foot movement - was previously used as a model of locomotion for fMRI studies to provide insight into locomotor-related brain reorganization. Previous studies suggest that impaired locomotion in people post-stroke is associated with bilateral activation of S1 and M1 (Kim et al., 2006; Luft et al., 2005; You et al., 2005) and reduced brain activities in the same areas when compared to healthy individuals (Dobkin et al., 2004; Luft et al., 2005). With locomotor recovery, S1 and M1 activities become more lateralized to the damaged hemisphere due to a reduction in activity on the undamaged side and an increase in activity on the damaged side (Kim et al., 2006; Luft et al., 2005; You et al., 2005). Specifically, increased S1 and M1 activity of the damaged side is observed. (Carey et al., 2004; Luft et al., 2005). From these observations, we conclude that bilateral activation of S1 and M1 and decreased cortical activities during non-locomotor movement may critically impact locomotor impairments. Meanwhile, shifting activity of S1 and M1 from bilateral to ipsilesional activity suggests that a restoration of the brain regions may contribute to locomotor recovery.

1.4 INSTRUMENTATION: Functional Magnetic Resonance Imaging (fMRI)

FMRI is a brain imaging technique that maps local physiological or metabolic consequences of altered neuronal activity of the brain (Boynton et al., 1996). Blood-

oxygen level dependent (BOLD) imaging is the most common fMRI technique. It is sensitive to localized susceptibility changes that accompany alterations in blood oxygenation (Ogawa et al., 1990). This technique provides a spatial resolution of a few millimeters, with a temporal resolution of a few seconds (limited by the hemodynamic response itself) (Matthews and Jezzard 2004).

The contrast in MR images is the signal difference between any two types of tissue. It is determined by the hydrogen atoms which are abundant in the water molecules of the brain tissue, and the differences in fundamental nuclear magnetic processing known as relaxation (Matthews and Jezzard 2004). In order to determine the relaxation, the following steps must occur. In the absence of an external magnetic field, hydrogen atoms in free space have their spin axes aligned randomly. In the presence of an external magnetic field, the spin axes of hydrogen atoms are mostly aligned along the magnetic field. Applying a radio frequency to excite the system from a low to high energy state causes these hydrogen atoms to absorb energy (Heeger and Ress 2002). This is known as the "excitation" state. After the excitation, the radio frequency is removed and the hydrogen atoms emit energy until they gradually return to their equilibrium state (Heeger and Ress 2002). This is known as the "relaxation" state. This relaxation is characterized by the "relaxation time", which is determined by the proton density (water density-dependent) that is different for every tissue. The MR scanner measures the sum total of the emitted energy at the three primary interest relaxation times, T1, T2 and T2*.

The T1 relaxation time (spin-lattice or longitudinal relaxation time) is a tissue-specific time constant for protons and is a measure of the time taken to realign the protons with an external magnetic field. T2 relaxation time (spin-spin or transverse

relaxation time) is another tissue-specific time constant for protons and is a measure of the time taken to dephase the protons after the radiofrequency is removed. The main application for these two relaxation times is to create anatomical images for detecting structural abnormalities. The images from these two techniques are known as T1-weighted and T2-weighted images (Huettel, Song, McCarthy 2004). The T2* relaxation time is comprised of spin-spin interaction (T2) and changes in spin precession frequencies due to the presence of inhomogeneities of the magnetic field caused by the changes in blood oxygenation ratio (Huettel, Song, McCarthy 2004). Oxyhemoglobin is weakly diamagnetic and has little effect on the surrounding magnetic field, whereas deoxyhemoglobin is paramagnetic and introduces an inhomogeneity into the nearby magnetic field (Pauling and Coryell 1936). The greater inhomogeneity results in decreased signal intensity. An increase in the concentration of deoxyhemoglobin, according to the metabolic demands of active neurons, causes a decrease in signal intensity. The main application of this MR image is to create functional images, whose activity determining neural activity associated with a given task (Matthews and Jezzard 2004). These are known as T2*-weighted or BOLD contrast images.

The changes in the concentration ratio of oxyhemoglobin to deoxyhemoglobin cause the alterations of signal intensity (Ogawa et al., 1990), known as the hemodynamic response or BOLD response. Boynton et al. (1996) showed that the hemodynamic response extends in time in proportion to the duration of neural activity and also increases in amplitude in proportion to the change in intensity of neural activity, suggesting an approximately linear relationship to the underlying neuronal activity (Boynton et al., 1996). The hemodynamic response is sensitive to changes in regional blood perfusion,

blood volume, and blood oxygenation that accompanies neuronal activity (Noll and Vazquez 2004).

1.4.1 The quantitative relationship between neural activity and blood oxygen level-dependent (BOLD) contrast

The hemodynamic response related to a transient increase in neuronal activity during an event-related experimental task involves three main phases: pre-undershoot, rising edge, and trailing edge. The pre-undershoot is an initial, small decrease in signal intensity below baseline, which is noticeable at 2s post-stimulus onset (Ances 2004; Fransson et al., 1998). It results from an increase in deoxyhemoglobin, attributable to a brief uncoupling between blood flow and oxygen utilization (Ances 2004; Roc et al., 2006). The rising edge is a large increase above baseline and reaches its peak intensity at about 5 to 6s post-stimulus onset (Fransson et al., 1998). The rise is a consequence of an influx of cerebral blood flow and blood volume in order to bring in glucose and oxygen to the active neuron regions (Huettel, Song, McCarthy 2004). The trailing edge happens once the stimulus has been removed. The signal intensity is slowly decreased to its baseline as a consequence of decreased blood flow with nominal change in volume. This trailing edge phase includes post-undershoot at roughly 10s post-stimulus onset. In the next 10 to 20s after the post-undershoot, the BOLD signal completely returns to its baseline as blood volume decreases and vascular physiology returns to baseline.

In block-design experiments involving alternating blocks of sensorimotor activation and rest, there is an additional plateau phase between the rising and trailing edges. In this phase, the signal intensity remains elevated as long as the activity

continues. This is associated with a constant rate of cerebral blood flow and neural oxygen consumption. The spatiotemporal profiles of the hemodynamic response are varied with the properties of the evoking stimulus (Hund-Georgiadis et al., 2003), underlying neuronal activity (Thierry et al., 2003), and vascular properties (Rossini et al., 2004; Rother et al., 2002). It is important to note that within a subject, different brain regions show different hemodynamic response profiles (Miezin et al., 2000).

1.4.2 Alterations of hemodynamic response as an effect of cerebrovascular diseases

The hemodynamic response depends mainly on the cerebral blood flow, which is tightly related to the vascular properties of the brain. Insufficient vascular tone could cause changes in response to autoregulation to preserve blood for the active neurons (Rossini et al., 2004; Rother et al., 2002). As a result, disruptions of the cerebrovascular system could lead to alterations of the spatiotemporal profiles of the hemodynamic response. Several investigators have reported delayed time to peak, decreased amplitude, and prolonged initial dip of hemodynamic responses measured from people post-stroke (Altamura et al., 2009; Bonakdarpour, Parrish, Thompson 2007; Newton et al., 2002; Pineiro et al., 2002; Roc et al., 2006). Specifically, the delayed time-to-peak ranged from 2 to 19.5s (Bonakdarpour, Parrish, Thompson 2007; Carusone et al., 2002; Roc et al., 2006). The amplitude of the hemodynamic response is at least 30 percent lower in people post-stroke (Pineiro et al., 2002) and the reduction in amplitude can be greater than 60 percent (Carusone et al., 2002; Hamzei et al., 2003). Others have shown that hemodynamic responses in this population are negative instead of positive for the entire

duration of task performance (Fridriksson et al., 2006; Roc et al., 2006) or attenuated in amplitude with task repetition (Mazzetto-Betti et al., 2010). The abnormalities in hemodynamic responses are also documented in people without stroke who have complete or partial occlusion of cerebral vasculature (Carusone et al., 2002; Hamzei et al., 2003; Murata et al., 2006; Rother et al., 2002), suggesting that the change occurred before people had a stroke.

The hemodynamic response is important for fMRI analysis because it serves as an expected function in the model of the signal change. Using an inappropriate hemodynamic response function could result in poor signal detection with BOLD-fMRI and, subsequently, could lead to misinterpretation of the sites and the amount of task-specific neuronal activation. Previous studies have demonstrated that detection of brain activity with BOLD-fMRI is improved after canonical functions are modified to account for stroke-related changes in hemodynamic responses (Altamura et al., 2009; Bonakdarpour, Parrish, Thompson 2007). We conclude from these observations that using an appropriate hemodynamic response function is important for fMRI signal detection.

1.5 SEVERITY OF LOCOMOTION IMPAIRMENTS

The severity of locomotor impairments is determined by gait speed and symmetry between the two legs. Previous work has shown that stroke survivors walk slower (Perry et al., 1995; Turns, Neptune, Kautz 2007) and lack symmetry (Balasubramanian et al., 2007; Dettmann, Linder, Sepic 1987). Walking velocity is widely used as an indicator of

locomotor impairment. However, speed alone may not be sufficient to determine severity of walking impairments. This is due to a compensatory action by the non-paretic leg, which can result in a relatively functional walking velocity despite poor coordination of the paretic leg (Buurke et al., 2008; Den Otter et al., 2006). Likewise, during pedaling, stroke survivors are likely to be able to pedal at the same rate as healthy individuals because the crank is coupled, resulting in time- and trajectory-controlled movement. This allows the non-paretic leg to compensate for the paretic leg.

In addition to velocity, stroke survivors have poor gait symmetry in both spatiotemporal and kinetic characteristics of walking. Symmetry of spatial and temporal characteristics are represented by the step length ratio (SLR) and temporal symmetrical ratio (TSR), respectively (Alexander et al., 2009; Patterson et al., 2008). The kinetic characteristic of walking can be measured by the impulses calculated from anteroposterior ground reaction force (AP-GRF) (Balasubramanian et al., 2007). Propulsive impulse is the net positive, anteriorly directed force generated by the legs to propel the body forward. Bowden et al. showed that in order to maintain a given speed, the paretic leg created less propulsive impulse accompanied by a compensatory increase in propulsion of the non-paretic leg (Bowden et al., 2008). In addition, the braking impulse, which is a net negative, posteriorly directed force generated to decelerate the body center of mass, is significantly increased on the paretic leg compared to the non-paretic leg (Bowden et al., 2008). The combination of the propulsive and braking impulses by the paretic leg results in a negative net impulse in people post-stroke.

Mechanical measures of pedaling performance can characterize locomotor impairment as well. Previous work has shown that even though stroke survivors can

pedal at a given rate and load, they demonstrate asymmetrical mechanical work between the two legs (Brown, Kautz, Dairaghi 1997; Kautz and Brown 1998). Compared to the non-paretic leg, the paretic leg produces less positive work, which is a propulsion force to propel the crank against the load. In addition, the paretic leg produces more negative work, which is a resistance to the crank propulsion (Kautz and Hull 1993). As a result, the net mechanical work of the paretic leg is reduced compared to the non-paretic leg. This suggests that net mechanical work done could capture the locomotor deficits caused by stroke.

Previous studies have shown that asymmetrical and slow locomotion in people post-stroke might be attributed to changes in brain activity. Miyai et al. (2003 and 2006) have shown that improved swing phase symmetry during walking was positively correlated with a more symmetrical activity of the sensorimotor cortex (Miyai et al., 2003; Miyai et al., 2006). Lin et al. (2012) have also demonstrated that increased symmetry between the left and right rectus femoris muscles during pedaling was associated with improved symmetrical brain activation (Lin, Chen, Lin 2012). In addition, Miyai et al. (2006) demonstrated a relationship between increased sensorimotor cortex activity and gait cadence when body weight support was applied during treadmill walking in stroke survivors. These studies suggested that hemiplegic locomotion might be attributed to the alterations in brain activity in people post-stroke.

1.6 SPECIFIC AIMS

The purpose of this dissertation is to determine whether supraspinal control of locomotor movements is altered by stroke. We used fMRI to examine brain activity during pedaling in people post-stroke and, for comparison, control subjects. The general hypothesis was that stroke-induced brain activation during locomotion would be different from that of control subjects, and the difference would be responsible for locomotor impairments.

1.6.1 Aim 1: Changes in hemodynamic response in chronic stroke survivors do not affect fMRI signal detection in a block experimental design

The goal of this first aim (Chapter 2) was to determine whether the spatiotemporal characteristics of hemodynamic responses obtained from stroke subjects during an event-related paradigm would be different from that of control subjects; and whether the different hemodynamic response could be used to develop individualized hemodynamic response functions that could be used to enhance BOLD-fMRI signal detection in block experiments. To test this aim, estimated hemodynamic responses were obtained from stroke and control subjects while they performed a unilateral, event-related foot-tapping or knee flexion and extension task. This information was then used to create individualized hemodynamic response functions for foot tapping data obtained in block-designed experiments. Comparisons were made for the brain activation during a block-designed experiment between two analysis models: a canonical versus an individualized function. We proposed that the spatiotemporal profile of hemodynamic responses

measured from stroke subjects would be abnormal, resulting in poor detection of movement-related brain activation when a canonical hemodynamic response function was used. We further hypothesized that using individualized hemodynamic responses would enhance the detection of brain activation.

1.6.2 Aim 2: Decreased brain activity in stroke survivors during pedaling: an fMRI study

In the second aim (Chapter 3) we examined if the supraspinal control of locomotor movements, which involves rhythmic, reciprocal, flexion and extension movements of multiple joints in both legs, would be different after stroke. To address our objective, we used fMRI to examine brain activity during pedaling. We hypothesized that if asymmetrical brain activity is responsible for locomotor impairments, then stroke-induced asymmetry of brain activation would exist during pedaling. We also hypothesized that if motor-related brain areas, such as premotor and pre-supplementary motor area, are extraneous regions in control of locomotion post-stroke, then these areas would be active in individuals with stroke, but not in control subjects, which would be represented as increased volume of activation or larger active areas in the cortex in the individuals with stroke compared to the control subjects. We also recorded brain activity with fMRI during unilateral, single joint flexion and extension movements of the lower limbs in order to compare supraspinal control mechanisms across locomotor and non-locomotor tasks.

1.6.3 Aim 3: Relationship between locomotor impairment and pedaling-related brain activity post-stroke

The last aim (Chapter 4) was designed to investigate the relationship between locomotor impairments, i.e. pedaling and walking, and the pedaling-related brain activity in stroke subjects. We emphasized abnormal locomotor velocity and symmetry as impairments since both are the main locomotor deficits for stroke subjects. To address our objective, locomotor symmetry and velocity were measured using a modified cycling ergometer (pedaling), and a motion analysis system, and force plates (walking). The results from Aim 2 demonstrated that stroke subjects had reduced volume of activation, but not intensity of activation, when compared to control subjects. The results also demonstrated symmetrical sensorimotor cortex activation between the damaged and undamaged hemispheres, while the activation of the cerebellum was shifted to the damaged hemisphere in the stroke group. Therefore, we developed three hypotheses. First, if reduced volume of activation is responsible for impaired locomotor velocity, then volume of activation would be directly correlated to locomotor velocity. Second, if the symmetrical cortical activity in the stroke subjects is directly related to the locomotor symmetry, then stroke subjects would demonstrate symmetrical locomotion. Third, if increased cerebellar activation on the damaged hemisphere is responsible for the greater activity of the non-paretic leg as compensation for the paretic leg, then locomotor symmetry (non-paretic>paretic leg) would be directly related to the cerebellar activation symmetry (damaged>undamaged hemisphere).

CHAPTER 2: CHANGES IN HEMODYNAMIC RESPONSES IN CHRONIC STROKE SURVIVORS DO NOT AFFECT FMRI SIGNAL DETECTION IN A BLOCK EXPERIMENTAL DESIGN

2.1 INTRODUCTION

Blood oxygen level-dependent (BOLD) contrast functional magnetic resonance imaging (fMRI) has been used extensively to examine movement-related brain activity in people post-stroke. BOLD-fMRI is an indirect measure of brain activity that depends on coupling between neuronal activation and vascular responses triggered by changes in the ratio of oxygenated to deoxygenated hemoglobin (Kwong et al., 1992; Ogawa et al., 1992). Many studies use canonical functions to model task-related changes in brain activity measured with BOLD-fMRI. This approach assumes normal neurovascular coupling and normal hemodynamic responses to local neuronal activity. However, these assumptions may not be correct for people post-stroke because stroke is a condition affecting cerebral blood vessels. Hence, the appropriate function for modeling hemodynamic responses after stroke may differ from the canonical functions used for the normal brain. The use of an inappropriate model may lead to inaccurate descriptions of task-related brain activity.

There is considerable evidence to suggest that the spatiotemporal characteristics of hemodynamic responses are abnormal after stroke and that these abnormalities result in inaccurate representations of brain activity as measured by BOLD-fMRI. Several investigators have reported delayed time to peak, decreased amplitude, and prolonged initial dip of hemodynamic responses measured from stroke survivors (Altamura et al.,

2009; Bonakdarpour, Parrish, Thompson 2007; Newton et al., 2002; Pineiro et al., 2002; Roc et al., 2006). Others have shown that hemodynamic responses in this population are negative instead of positive for the entire duration of task performance (Fridriksson et al., 2006; Roc et al., 2006) or attenuated in amplitude with task repetition (Mazzetto-Betti et al., 2010). When canonical functions developed for the normal brain are used to model stroke-related hemodynamic responses, either little or no brain activation is detected with BOLD-fMRI despite normal task performance, or unambiguous brain activation measured with magnetoencephalography is detected (Murata et al., 2006; Roc et al., 2006; Rossini et al., 2004). Magnetoencephalography measures magnetic fields produced by the brain, and it does not rely on vascular adaptations to neuronal activity. These results suggest that altered hemodynamic responses contribute to poor signal detection with BOLD-fMRI. Further support for this idea comes from observations wherein detection of brain activity with BOLD-fMRI is improved after canonical functions are modified to account for stroke-related changes in hemodynamic responses (Altamura et al., 2009).

There are several possible approaches to enhancing the accuracy with which BOLD-fMRI can detect task-related brain activity after stroke. One option is to exclude stroke survivors with known compromises of cerebral blood flow, as abnormalities in hemodynamic responses are extensively documented in stroke survivors with cerebral artery occlusive disease (Fridriksson et al., 2006; Newton et al., 2002; Roc et al., 2006; Rossini et al., 2004) and in people without stroke who have complete or partial occlusion of cerebral vasculature (Carusone et al., 2002; Hamzei et al., 2003; Murata et al., 2006; Rother et al., 2002). A disadvantage of this approach is a smaller pool of stroke survivors

from which to sample. Moreover, changes in the spatiotemporal profile of hemodynamic responses have also been observed in survivors of hemorrhagic and thromboembolic stroke (Bonakdarpour, Parrish, Thompson 2007) and strokes with no demonstrable cerebrovascular occlusion (Altamura et al., 2009; Mazzetto-Betti et al., 2010; Newton et al., 2002; Pineiro et al., 2002). These results suggest changes in the vascular physiology that lead to stroke as well as those that result from stroke may contribute to abnormal hemodynamic responses (reviewed in (Marshall 2004)). Therefore, the exclusion of stroke survivors with known compromise of cerebral blood flow may be inadequate for avoiding misinterpretation of BOLD-fMRI data.

Another possible solution is to analyze BOLD-fMRI data with techniques, such as deconvolution, that make no *a priori* assumptions about the spatiotemporal characteristics of hemodynamic responses. This approach is typically done in the context of event-related experimental designs that examine brief tasks with a clear start and end point. To address this issue for block designs, one might examine the spatiotemporal characteristics of hemodynamic responses during event-related experiments and use this information to develop individualized functions to model the hemodynamic responses obtained during block designs. To our knowledge, this approach has not been attempted previously, and it is the focus of the present investigation. However, even this approach has practical limitations because it requires additional scanning time which could become problematic, particularly if an event-related protocol had to be added to every experimental session involving a block paradigm.

The purpose of this study was to determine whether the spatiotemporal characteristics of hemodynamic responses obtained from stroke survivors during an

event-related paradigm could be used to develop individualized hemodynamic response functions that could be used to enhance BOLD-fMRI signal detection in block experiments. Our long-term goal was to use this information to develop individualized hemodynamic response functions for stroke survivors that could be used to analyze brain activity associated with locomotor-like movements of the lower limbs. However, because locomotion is a continuous behavior, there is no event-related task from which to obtain the spatiotemporal profile of hemodynamic responses. Therefore, subjects performed foot tapping or knee flexion and extension, which are lower limb tasks that can be done in a continuous and discrete fashion. We obtained the spatiotemporal profile of hemodynamic responses from event-related lower limb movements and used this information to create individualized hemodynamic response functions for block data. Comparison was made between brain activations obtained when block data were processed with a normal canonical function and with individualized functions. We hypothesized that the spatiotemporal profile of hemodynamic responses measured from stroke survivors would be abnormal, resulting in poor detection of movement-related brain activity with BOLD-fMRI when a normal canonical hemodynamic response function was used. We further predicted that detection of brain activity with BOLD-fMRI would be enhanced when individualized models were used. Finally, we examined the reproducibility of hemodynamic responses obtained across two scan sessions. We reasoned that if the results were reproducible, then data from a single event-related session could be used to analyze block data obtained in subsequent sessions, which would eliminate the need to lengthen every scan session to include an event-related experiment.

2.2 MATERIAL AND METHODS

2.2.1 Methods common to all experiments

Three experiments were performed. In this section, we present methods common to all experiments. Subsequent sections are devoted to methods unique to each experiment.

2.2.1.1 Subject preparation and set-up

All subjects gave written informed consent according to the Declaration of Helsinki and institutional guidelines at Marquette University and the Medical College of Wisconsin. Prior to participating, all subjects underwent MRI safety screening to ensure that they were not claustrophobic or pregnant and that they were free of implants or foreign bodies incompatible with MRI. Before fMRI scans, subjects participated in a familiarization session outside the MRI environment where we explained the experimental procedures and allowed them to practice the desired tasks until we were confident that they were capable of doing them correctly. During practice sessions we also explained the importance of remaining still during fMRI and encouraged subjects to keep their head and trunk stationary during all movement tasks.

During fMRI scanning, subjects lay supine on the bed of a 3T MRI scanner (General Electric Healthcare, Milwaukee, WI). The subject's head was placed in a single channel transmit/receive split head coil assembly (model 2376114, General Electric Healthcare, Milwaukee, WI). To minimize movement, the head was enveloped by a

beaded vacuum pillow. Straps were also used to control head and trunk movement. Each subject wore MRI compatible earphones (model SRM 212, Stax Ltd, Japan) through which audio cues were delivered. An additional set of headphones was used to protect against scanner noise.

The legs were positioned over a foam bolster such that the hips and knees were flexed and the feet were approximately 15 cm above the surface of the scanner table. A circular plastic button (6.35 cm diameter) connected to a switch (Jelly Bean Twist Top Switch, AbleNet, Inc., Roseville, MN) was placed under the foot and was used to record lower limb movements. Each time the button was depressed a pulse was generated. These data were used to calculate movement rate and to ensure that subjects produced desired movements at appropriate times.

During each experiment, subjects' performance was visually monitored. We had access to real time information about head movement. If the subject did not perform the task as instructed or if their head moved more than 2 mm or degrees, we checked the subject for comfort, repeated the instructions to remain still, and restarted the run. A squeeze ball was placed near the subject's hands and could be used at any time to signal a problem. Participants were monitored for safety and comfort and were able to communicate via intercom with the scanner technician throughout the session.

2.2.1.2 Imaging parameters

Functional images (T2*-weighted) were acquired using gradient-echo echoplanar imaging (repetition time (TR): 2000 ms, echo time (TE): 25 ms, flip angle: 77º, 36

contiguous slices in the sagittal plane, 64 x 64 matrix, 4 mm slice thickness, and field of view (FOV): 24 cm). The resolution of the images was 3.75 x 3.75 x 4 mm. Anatomical images (T1-weighted) were obtained approximately half way through the scan session (TR: 9.5 ms, TE: 25 ms, flip angle: 12°, 256 x 244 matrix, resolution: 1 mm^3).

2.2.1.3 Data processing and statistics

Processing of fMRI signals was completed using Analysis of Functional NeuroImages (AFNI) software (Cox 1996). All statistical analyses were completed in SPSS (SPSS Inc, Chicago, IL), and effects were considered significant at $P<0.05$. Quantitative values are reported as mean ±1 standard deviation (SD).

2.2.2 Experiment 1: Hemodynamic responses stroke versus control

2.2.2.1 Subjects

Thirteen individuals with chronic post-stroke hemiparesis (9 females, mean ±SD age 54.8 ±12.8 years) and 9 age-matched control subjects (6 females, mean ±SD age 54.3 ±13.5 years) participated. Stroke participants had sustained a subcortical or cortical stroke at least 1.1 years prior to testing, and the mean ±SD time since stroke was 12.26 ±13.1 years. (See Table 2-1.) There were 6 subjects with right and 6 subjects with left hemiparesis. One subject had stroke-related movement impairments on both sides. The mechanism of stroke was recorded from the medical record. Eight subjects had ischemic stroke. Of these eight, two had cerebrovascular occlusive disease at the time of stroke.

Both had subsequently undergone carotid artery angioplasty. Four subjects had hemorrhagic stroke. In one subject, whose stroke occurred in infancy, we were unable to identify the cause. Individuals with stroke were divided into two groups according to lesion location: subcortical and cortical. The subcortical stroke group (n=7) had brain injuries that involved the internal capsule, corona radiata, basal ganglia, or thalamus. The cortical stroke group (n=6) had injuries affecting one or more of the subcortical structures listed above, and they also had injuries involving a portion of the cerebral cortex outside of the leg area of the primary sensory and motor cortices. (See Figure 2-1.) Control subjects had no signs or history of stroke or other neurological impairment.

Table 2-1. Descriptive characteristics of stroke subjects.

Subject	Age (years)	Sex	Affected limb	Affected brain area	Lesion size (μL)	Time to scan (years)	Mechanism of stroke
S01	60	F	R	Cortical	139120	20.4	I, E
S03	62	F	L	Subcortical	157	8.4	I
S05	56	M	L	Subcortical	51284	51.0	H, AVM
S06	64	F	R	Subcortical	715	6.5	H
S07	20	F	L	Subcortical	7623	19.0	U
S08	73	F	R	Subcortical	156	1.1	I, E
S10	58	F	L	Cortical	40823	6.1	I, CVOD
S11	53	F	R	Subcortical	600	17.4	I
S13	46	M	R>L	Subcortical	1518	4.4	I
S14	52	F	L	Cortical	96263	4.3	H, ICAD
S15	48	M	R	Cortical	74433	8.1	H, ICAD
S17	65	F	L	Cortical	52811	6.2	I
S19	55	M	R	Cortical	136960	6.4	I, CVOD

F=female, M=male, R=right, L=left, Cortical=stroke affecting cerebral cortex, Subcortical=stroke affecting subcortical structures, I=ischemia, E=embolism, H=hemorrhage, AVM=arteriovenous malformation, U=unknown, CVOD=cerebrovascular occlusive disease, ICAD=internal carotid artery dissection.

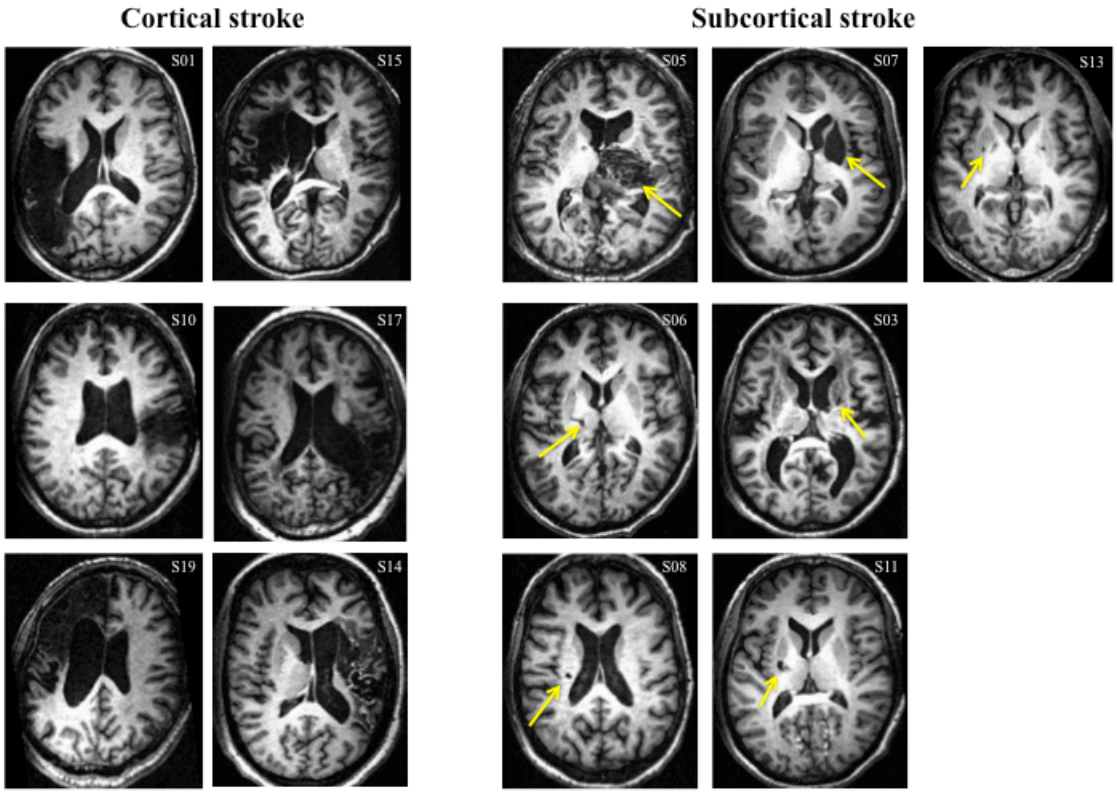

Figure 2-1. T_1-weighted anatomical images displaying brain lesions of stroke subjects. Arrows are positioned to indicate lesion location. The images are shown in the neurological convention (left is left).

2.2.2.2 Experimental protocol

Subjects were asked to tap one foot at a time on the button at a comfortable rate by dorsiflexing and plantarflexing the ankle. The left and right limbs were examined. A static tone indicated when to tap, and silence indicated rest. Knee flexion and extension was allowed in stroke participants (n=7) who could not perform ankle movements.

An event-related design consisting of 3 runs was utilized. A single run included 20 moving events and 40 resting events, 2s per event, presented in random order. This task was assumed to produce a brief burst of neuronal activity within the sensorimotor

cortex. This design was created by AFNI sub-routine functions called *RSFgen* and *nodata*. *RSFgen* was used to generate the randomized event-related model for a given hemodynamic response duration and number of input stimuli by generating an 'original' array for given sets of parameters. Then, *RSFgen* took the seed number that had been assigned and shuffled the original time-series array, resulting in a randomized stimulus function consisting of a series of 0's and 1's indicating rest and activity, respectively. The *RSFgen* parameters for this study included length with the time series = 60 TRs, number of input stimuli = 1 (tapping), block length for stimuli = 1, random number = 1:10. *Nodata* was used to evaluate the shape of the hemodynamic responses created by the generated model without any input data using deconvolution technique. The parameters for this function included length with the time series = 60 TRs, length of each TR = 2s, degree of polynomial = A (automatic), number of input stimuli = 1 (tapping), minimum time lag of the 1st input stimulus = 0, maximum time lag for the 1st stimulus = 8 TRs (16s) (See Appendix C for more details).

2.2.2.3 Derivation of hemodynamic responses

Digital imaging and communication in medicine (DICOM) files containing fMRI signals were converted into 3-dimensional images [using the *to3d* command with parameter settings time = zt (means that the slices are input in the order z-axis first, then t- axis), number of points in the z-direction = 36 slices, number of points in the t-direction = 98 TRs, length of each TR = 2000ms, alt+z]. A time-series of each individual voxel was aligned to the same temporal origin within each TR using heptic (7th order)

Lagrange polynomial interpolation technique [using *3dTshift* command with paramter settings align each slice to time offset (tzero)= 0, ignore the first 4 TRs (ignore)= 4, heptic]. The first 4 TRs within each run were removed to eliminate non-steady state magnetization artifact [using *3dTcat* command]. Multiple runs were concatenated [using *3dTcat* command]. The concatenated data was registered to the functional scan obtained closest in time to the anatomical scan using iterated a linearized weighted least squares technique to make each sub-brick as like as possible to the base brick [*3dvolreg* with parameter settings heptic, base '[0]']. To derive voxel-wise estimates of hemodynamic responses, deconvolution technique between the input stimulus function and the measured time-series fMRI data was used. Separate baseline estimates were defined for each run. Estimated hemodynamic responses comprised 16 points, representing the response from 0 to 30s after stimulus onset. The estimates of hemodynamic response were then convolved with time stimulus function, resulting in a voxel-wise hemodynamic response function. To identify voxels containing BOLD signals associated with the movement task, multiple linear regression technique using *3dDeconvolve* was performed using the voxel-wise hemodynamic response function with head position as a variable of no interest. The time-series was modeled by $y = \beta_0 + \beta_1 x_1 + \beta_2 x_2 + ... + \beta_7 x_7 + \varepsilon$, where x_1 was the delayed non-movement model; x_2 - x_7 were head movement in 6 directions, acting as variables of no interest.

To identify significantly active voxels at a familywise error rate of $P<0.05$, we used a Monte Carlo simulation to set an appropriate cluster size for a given individual voxel P-value [using *AlphaSim* command]. The Monte Carlo simulation is a simulation of the process of image generation, spatial correlation of voxels, voxel intensity

thresholding, masking, and cluster identification. The combination of individual voxel probability thresholding and minimum cluster size thresholding provides an estimate of the probability of a false positive detection per image, which is determined from the frequency count of cluster sizes. The parameters used for this function included voxel dimensions=3.5x3.5x4 mm [to generate a random image], fwhmx= 5.14, fwhmy=4.10, fwhmz= 2.98 [to simulate the effect of spatial correlation of voxels by convolving the generated random image with a Gaussian function]. Specifically, this process was performed by taking the 3D fast Fourier transform of the random image, multiplying this transform by the transform of the Gaussian function, and taking the inverse of the Fourier transform, yielding the result. To set the voxel intensity thresholding, power calculations was performed to define Zthr. Once Zthr had been set, then all voxels inside the entire volume or inside the true activation region were compared against Zthr. The thresholding was set such that those voxels with an intensity greater than Zthr to 1 were considered active and those voxels with intensity less than Zthr were set to 0. To simulate masks, the brain mask dataset from each individual subject was used. The last step for this simulation was to identify which activated voxels (the voxels with a magnitude of 1 from the voxel thresholding step) belonged to clusters. A parameter of rmm=6.6 was used to defined whether two voxels are in the same cluster. Every activated voxel was a member of one, and only one, cluster. Once all clusters have been found, the size (in number of voxels) of each cluster was recorded in a frequency table.

Percent signal change was calculated as the change in amplitude of the BOLD signal from baseline [expression: "100 *(d/((a+b+c)/3))*step(1-abs((d/((a+b+c)/3))))" \, where a, b and c were baseline constants of each run, d was a sub-brick containing the

regression coefficient, and step function controls outflow if baseline is close to 0] . Significantly correlated voxels outside of the brain and negatively correlated voxels were ignored. Any voxels with percent signal change >10 were also ignored, as these large changes were likely due to edge effects (See Appendix C for more details).

For each subject, estimates of hemodynamic responses were obtained from the sensorimotor cortex contralateral to and ipsilateral to the moving limb. Because we tested the right and left limbs, a total of 4 hemodynamic responses were obtained. Each estimate was the average of the hemodynamic responses across all active voxels in the sensorimotor cortex, which included primary motor cortex (M1), primary somatosensory cortex (S1), and Brodmann's area 6 (BA6). The anatomical boundaries for the sensorimotor cortex were defined from the T_1-weighted images as previously described (Wexler et al., 1997). In the axial plane, the sensorimotor cortex extended anteriorly from the postcentral sulcus to cover approximately the posterior half of the superior frontal gyrus, and from the medial border of each hemisphere spanning laterally over the dorsolateral frontal lobe. In the sagittal plane, the sensorimotor cortex was bordered inferiorly by the cingulate sulcus, extending superiorly to the top of the hemisphere. Each subject's data were analyzed individually in its original coordinate system to avoid distortion arising from transformation to a standardized coordinate system.

2.2.2.4 Data analysis and statistics

Peak amplitude, time-to-peak amplitude, and rate of change of amplitude (ROC) were measured from each estimated hemodynamic response for each subject. Peak

amplitude was defined as the maximum value of the hemodynamic response. Time-to-peak was defined as the length of time from the movement cue to the peak amplitude. Rate of change was defined as the change in amplitude of the normalized hemodynamic response per repetition time (TR=2s), where normalization was accomplished by dividing the hemodynamic response by its amplitude at 6s after stimulus onset. Rate of change was calculated for each of six different TRs beginning with the second TR after stimulus onset (ROC1: 2-4s, ROC2: 4-6s, ROC3: 6-8s, ROC4: 8-10s, ROC5: 10-12s, ROC6: 12-14s). The rising portion of the hemodynamic response was represented in ROC1 and ROC2, and the declining portion was represented by ROC3 to ROC6. See Figure 2-2A.

Multivariate analysis of variance (MANOVA) with repeated measures of the dependent variables was used to determine whether the estimates of the hemodynamic response in the control group were affected by moving limb (left versus right) or active hemisphere (ipsi- versus contralateral). No significant effect was identified (P=0.350). Subsequently, we took the average across the four hemodynamic responses for each subject for each variable.

To test whether the hemodynamic responses recorded from the stroke group were different from the control group, differences between each stroke data point and the mean of the control group were calculated for each variable. These computations were completed for the subcortical and cortical stroke groups and for all stroke subjects. MANOVA with repeated measures of the dependent variables was used to identify significant differences between each stroke group and the control group and any interaction effects between the subcortical and cortical stroke groups.

To understand the effect of active hemisphere, we split the data within each stroke group into the hemodynamic responses associated with the undamaged and damaged hemispheres, regardless of moving limb. To understand the effect of the moving limb on the hemodynamic responses, we regrouped the data into the hemodynamic responses associated with the non-paretic and paretic limb movement, regardless of the active hemisphere. MANOVA with repeated measures of the dependent variables was used to identify differences between the undamaged and damaged hemispheres and differences between paretic and non-paretic limb movement.

We computed each subject's average movement rate across all trials and their average delay-to-stop moving. The latter was defined as the amount of time spent performing the movement task after the audio cue ended. Pearson correlation coefficients were calculated to examine the association between the characteristics of the hemodynamic responses and task performance.

2.2.3 Experiment 2: Canonical versus individualized hemodynamic response functions

2.2.3.1 Subjects

Six individuals with cortical stroke (4 females; age 56.3±6 years) and 9 age-matched control subjects (6 females; age 54.3±13.5 years), all of whom completed Experiment 1, participated. Only individuals with cortical stroke were examined here because the spatiotemporal profile of hemodynamic responses obtained from this subset of stroke subjects was different from control subjects.

2.2.3.2 Preparation, set-up, and experimental protocol

The experimental set-up and protocol were the same as in Experiment 1, except that we utilized a block design instead of an event-related design. The task comprised a single run of an ABABABABABABA pattern, where A represented a 16s block of rest and B represented a 16s block of movement. During the movement blocks, subjects were asked to tap their foot at a comfortable pace. Subjects who performed knee flexion and extension (n=3) in Experiment 1 were allowed to perform the same movement here. A static tone indicated when to move; silence indicated rest. The left and right legs were examined separately.

2.2.3.3 Derivation of individualized hemodynamic response functions, data analysis, and statistics

To derive an individualized hemodynamic response function for each subject, the four different hemodynamic responses, which were obtained from sensorimotor cortex contralateral to and ipsilateral to the moving limb during right and left foot-tapping, for each subject in Experiment 1 were averaged. This resulted in a single hemodynamic response for each subject. We then convolved each subject's average hemodynamic response with the block function used in this experiment. The result was an individualized hemodynamic response function for each subject.

To identify voxels containing movement-related brain activity, each subject's individualized hemodynamic response function was fit with the measured BOLD signal. Head position was used as a variable of no interest. As described previously (Mehta et

al., 2009), only the portion of the BOLD time-series after movement stopped was used. This data processing was performed using multiple linear regression analysis of 3dDeconvolve command. To compare detection power with the normal canonical model, identical analysis with a canonical hemodynamic response function was performed.

The volume, intensity, and center of activation were used to assess detection power. For each subject, each variable was computed from bilateral sensorimotor cortex which was an area where we observed consistent activity across subjects. Volume of activation was defined as the number of significantly active voxels in the sensorimotor cortex multiplied by voxel volume in microliters (μL). Intensity of activation was defined as the average percent signal change from baseline in the active portion of the sensorimotor cortex. Center of activation for activated clusters was reported as x, y, and z coordinates in original space.

MANOVA with repeated measures of volume, intensity, and x, y, z coordinates of center of activation was used to compare canonical and individualized hemodynamic response functions with respect to signal detection power. This procedure was completed for left and right limb movement.

2.2.4 Experiment 3: Reproducibility

Eleven stroke (7 females; age 53±13.2 years, 5 subjects with cortical stroke, 6 subjects with subcortical stroke) and 9 age-matched controls (6 females, age 54.3 ±13.5 years) subjects who participated in Experiment 1 repeated the procedures from that experiment for the purpose of examining the reproducibility of the spatiotemporal

characteristics of hemodynamic responses. The time elapsed between the first and the second session was 33.17 days (±66.85) and 9.33 days (±6.0) in the stroke and control groups, respectively. The experimental set-up, protocol, data analysis and statistics were identical to Experiment 1. MANOVA with repeated measures of the dependent variables was used to identify between-day differences in peak amplitude, time-to-peak, and rate of change.

2.3 RESULTS

2.3.1 Experiment 1: Hemodynamic responses stroke versus control

Contrary to expectations, there was no difference between the control and stroke groups with respect to the peak amplitude or time-to-peak of the hemodynamic response. There was also no difference between these groups for rate of rise of the hemodynamic response as represented by ROC1 and ROC2. The only differences in the hemodynamic response between the stroke and control groups occurred in the declining phase of the response where the initial portion of the decline (ROC3) occurred more gradually and the late portion of the decline (ROC5) happened more rapidly in the stroke as compared to the control group. See Figure 2-2 A and B for graphical representation and Table 2-2 for group means (±SD) and P-values.

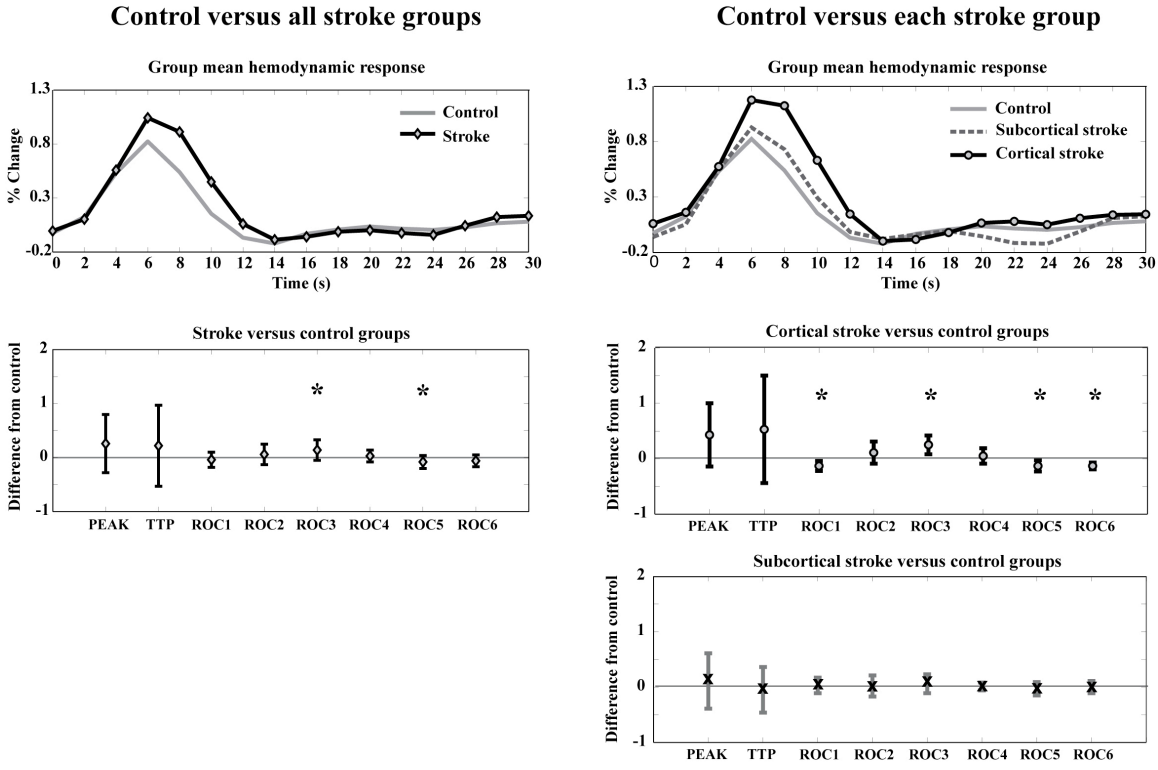

Figure 2-2. Graphical representations comparing the spatiotemporal characteristics of hemomdynamic responses in individuals with and without stroke. A and C display the group mean time course of the hemodynamic responses observed in each group. B, D, and E represent mean (±SD) between-group differences for each dependent variable. PEAK=peak amplitude of the hemodynamic response, TTP=time to peak amplitude of the hemodynamic response, ROC=rate of change of amplitude of the hemodynamic response (ROC1: 2-4s, ROC2: 4-6s, ROC3: 6-8s, ROC4: 8-10s, ROC5: 10-12s, ROC6: 12-14s). Asterisks indicate significance at $P<0.05$.

The spatiotemporal characteristics of hemodynamic responses were affected by stroke location. When we split the stroke group into the subcortical and cortical stroke groups, we found that the cortical stroke group had a slower rate of rise in ROC1, a slower rate of decline in ROC3, and a faster rate of decline in ROC5-ROC6, as compared to the control group. In contrast, we found that the subcortical stroke group was not significantly different from the control group with respect to any characteristics of the

hemodynamic response. MANOVA with repeated measures revealed no interaction between the subcortical and cortical stroke groups. This observation suggests that that both stroke groups were different from the control group in a similar fashion but that a cortical stroke may cause a more distinctive change in the hemodynamic response as compared to a subcortical stroke. See Figure 2-2 C, D, and E and Table 2-2.

Table 2-2. Group mean (±SD) values for peak amplitude, time to peak amplitude, and rate of change of amplitude of hemodynamic responses in all four groups examined.

			Control group	Stroke group	*P-value (control vs stroke)*	Cortical stroke group	*P-value (control vs cortical stroke)*	Subcortical stroke group	*P-value (control vs subcortical stroke)*
Peak amplitude		Mean (±SD)	0.82 (±0.3)	1.09 (±0.5)		1.26 (±0.6)		0.94 (±0.5)	
		Diff from control		0.26 (±0.5)	0.105	0.43 (±0.6)	0.124	0.11 (±0.5)	0.567
Time-to-peak		Mean (±SD)	6.06 (±0.2)	6.26 (±0.8)		6.58 (±1.0)		6.00 (±0.4)	
		Diff from control		0.22 (±0.8)	0.315	0.53(±1.0)	0.236	-0.05 (±0.4)	0.757
Rate of change of amplitude	ROC1	Mean (±SD)	0.54 (±0.1)	0.48 (±0.1)		0.40 (±0.1)		0.56 (±0.1)	
		Diff from control		-0.04 (±0.1)	0.292	-0.13 (±0.1)	***0.020***	0.03 (±0.1)	0.619
	ROC2	Mean (±SD)	0.34 (±0.1)	0.40 (±0.2)		0.45 (±0.2)		0.36 (±0.2)	
		Diff from control		0.06 (±0.2)	0.277	0.11 (±0.2)	0.257	0.02 (±0.2)	0.770
	ROC3	Mean (±SD)	-0.34 (±0.1)	0.19 (±0.2)		-0.09 (±0.2)		-0.28 (±0.2)	
		Diff from control		0.14 (±0.2)	***0.018***	0.25 (±0.2)	***0.017***	0.06 (±0.2)	0.408
	ROC4	Mean (±SD)	-0.45 (±0.1)	-0.42 (±0.1)		-0.40 (±0.1)		-0.44 (±0.1)	
		Diff from control		0.03 (±0. 1)	0.371	0.05 (±0.1)	0.402	0.01 (±0.1)	0.824
	ROC5	Mean (±SD)	-0.25 (±0.1)	-0.33 (±0.1)		-0.38 (±0.1)		-0.28 (±0.1)	
		Diff from control		-0.08 (±0.1)	***0.045***	-0.13 (±0.1)	***0.031***	-0.03 (±0.1)	0.535
	ROC6	Mean (±SD)	-0.06 (±0.1)	-0.11 (±0.1)		-0.19 (±0.1)		-0.05 (±0.1)	
		Diff from control		-0.06 (±0.1)	0.084	-0.13 (±0.1)	***0.003***	0.00 (±0.1)	0.898

ROC=rate of change (ROC1: 2-4s, ROC2: 4-6s, ROC3: 6-8s, ROC4: 8-10s, ROC5: 10-12s, ROC6: 12-14s), SD=standard deviation, Diff from control=difference from control. Significant between-group differences (P<0.05) are represented in bold.

The spatiotemporal profile of the hemodynamic response was not affected by active hemisphere (undamaged versus damaged, P=0.208) nor by the limb that was moving (non-paretic versus paretic, P=0.478). See Figure 2-3.

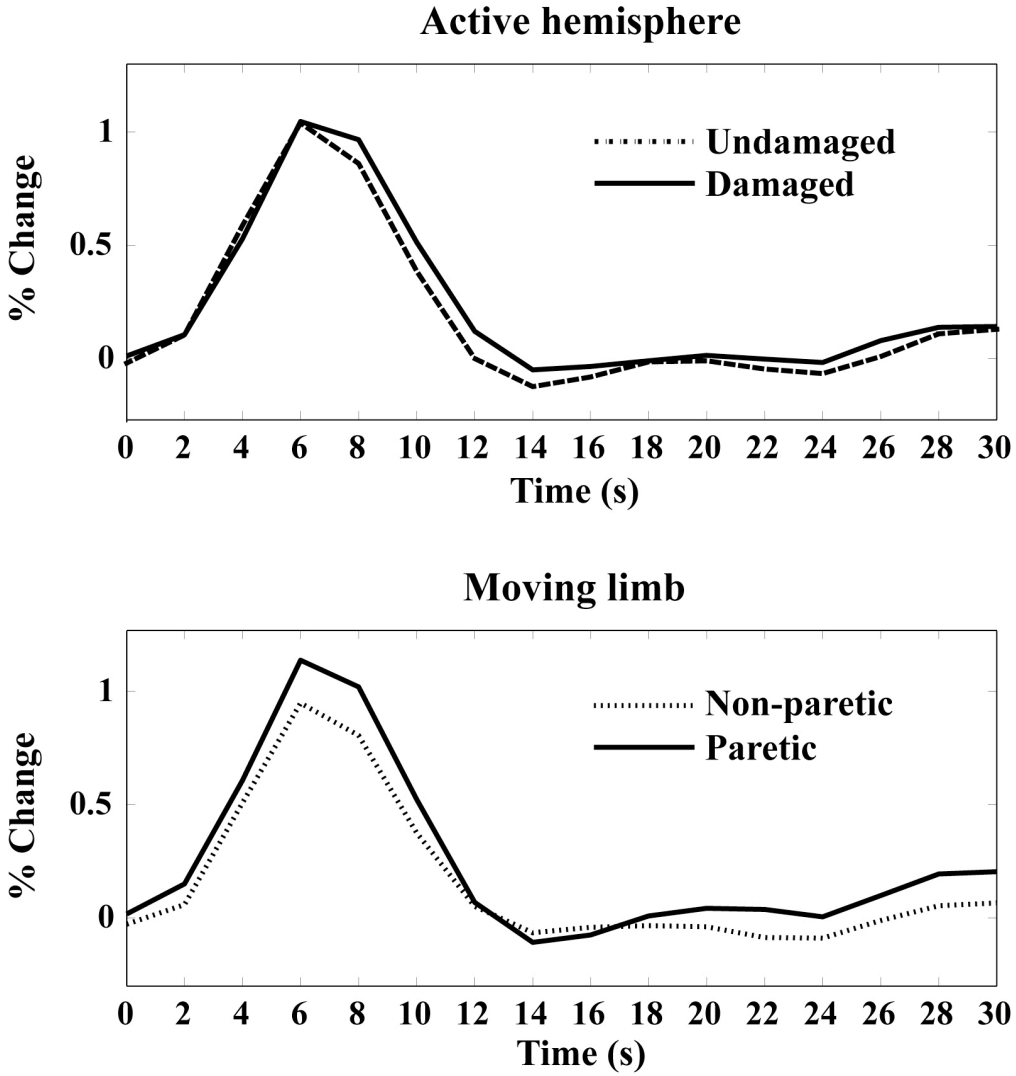

Figure 2-3. Graphical representations comparing the spatiotemporal characteristics of hemomdynamic responses in individuals with stroke. Top figure compares the group mean time courses of the hemomdynamic responses observed in the damaged and undamaged cortex. Bottom figure compares the group mean time courses of the hemomdynamic responses observed during paretic and non-paretic limb movement.

It is possible that differences between the stroke and control groups resulted from differences in task performance. Indeed, the stroke group moved at a slower rate than the control group (control group=1.92±0.6 Hz, stroke group=1.57±0.4 Hz, P=0.009), and within the stroke group, the paretic limb moved more slowly than the non-paretic limb (non-paretic=1.69±0.4 Hz, paretic=1.42±0.4 Hz, P=0.007). Delay-to-stop moving in the stroke group was not different from the control group (control group=0.66±0.3 s, stroke group=0.76±0.4 s, P=0.405), but in the stroke group, the paretic leg took longer to stop moving compared to the non-paretic leg (non-paretic =0.63±0.4 s, paretic=0.91±0.3 s, P=0.009). However, there was no significant correlation between movement rate and rate of rise in ROC1 (R=0.208, P=0.693). There was also no significant correlation between delay-to-stop and rate of decline in ROC3, ROC5, or ROC6 (R=0.228, P=0.664 for ROC3; R=-0.275, P=0.597 for ROC5; R=0.273,P=0.600 for ROC6).

2.3.2 Experiment 2: Individualized versus canonical hemodynamic response functions

The hemomdynamic response function used to fit the data (canonical versus individualized) had no effect on signal detection in the control or cortical stroke group. As shown in Figure 2-4, there were no visually apparent differences between methods with respect to the size, shape, or location of brain activity observed in the sensorimotor cortex. Indeed, MANOVA results showed that there was no significant difference between methods with respect to volume, intensity, or x, y, z coordinates of brain activity in the sensorimotor cortex. This observation was consistent for left and right limb movement in control subjects as well as paretic and non-paretic limb movement in the

cortical stroke group (Cortical stroke group: P=0.128 for non-paretic and P=0.277 for paretic; control group: P=0.623 for left and P=0.072 for right). See Figure 2-5.

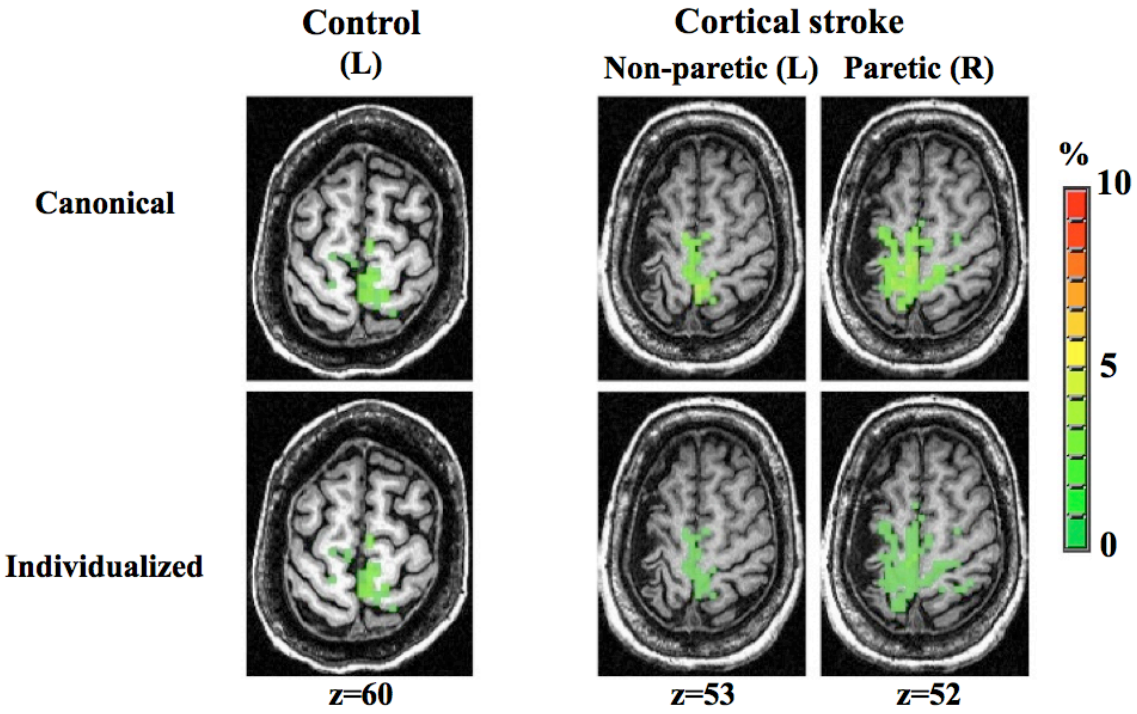

Figure 2-4. Representative examples of brain activation maps derived from data processed with canonical and individualized models of hemodynamic responses. The color bar represents percent signal change (0-10%). Control (L) is a map from a single representative control subject tapping his left foot. Cortical stroke Non-paretic (L) is a map from a representative subject with cortical stroke tapping with his non-paretic foot, which in this case is the left foot. Cortical stroke Paretic (R) is a map from the same representative subject tapping with his paretic foot, which is his right foot.

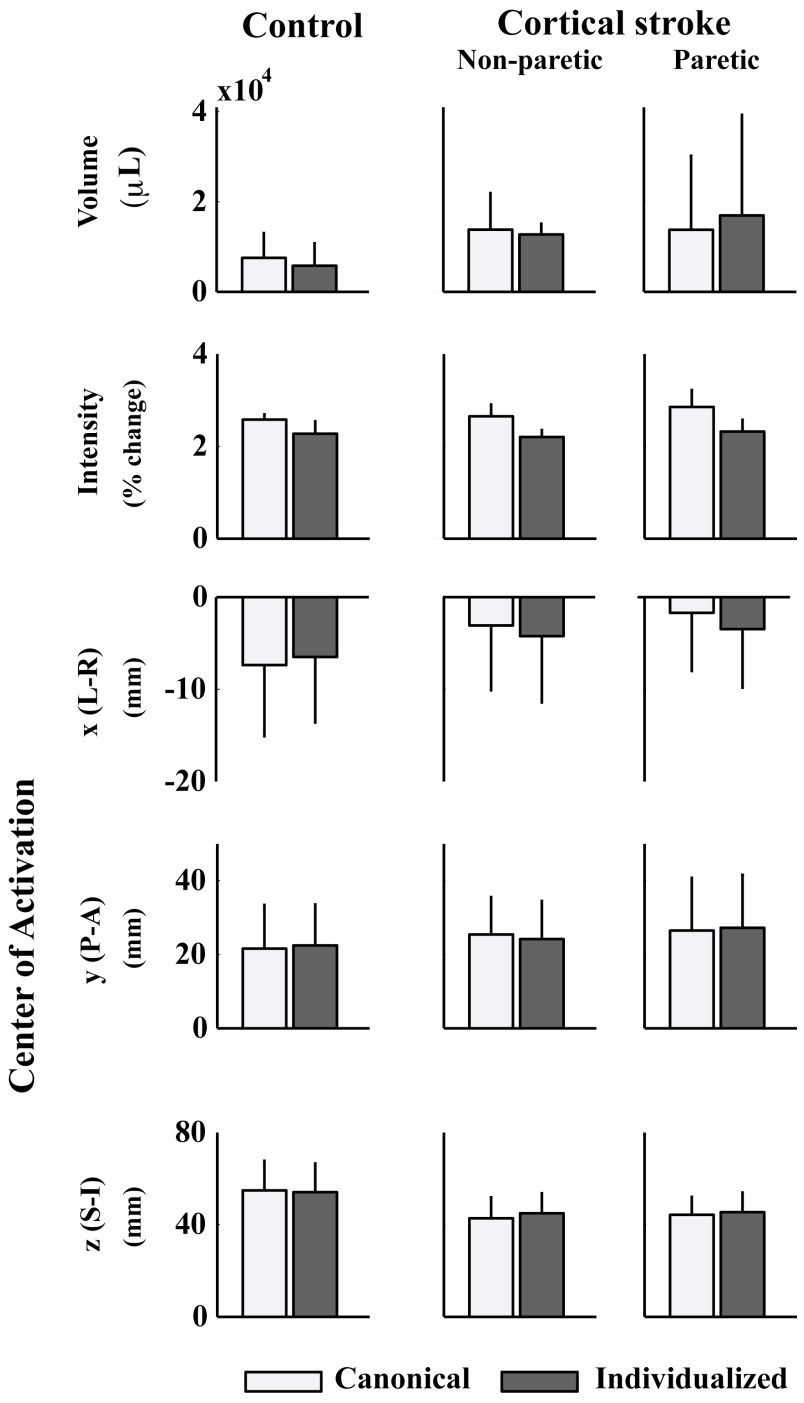

Figure 2-5. Bar plots representing the volume, intensity, and center of activation (x, y, z) of brain activity obtained with canonical and individualized methods for processing BOLD-fMRI data. Values are group means (±SD). L-R=left-right, P-A=posterior-anterior, S-I=superior-inferior.

2.3.3 Experiment 3: Reproducibility

As shown in Figure 2-6, the spatiotemporal profiles of the hemodynamic responses recorded from stroke and control subjects were repeatable across days. MANOVA with repeated measures revealed no between-day difference in the volume, intensity, or x, y, z coordinates of brain activity during movement (P=0.811 for control group, P=0.250 for stroke group, P=0.718 for cortical stroke group, and P=0.491 for subcortical stroke group). See Table 2-3 for mean (±SD) and P-values.

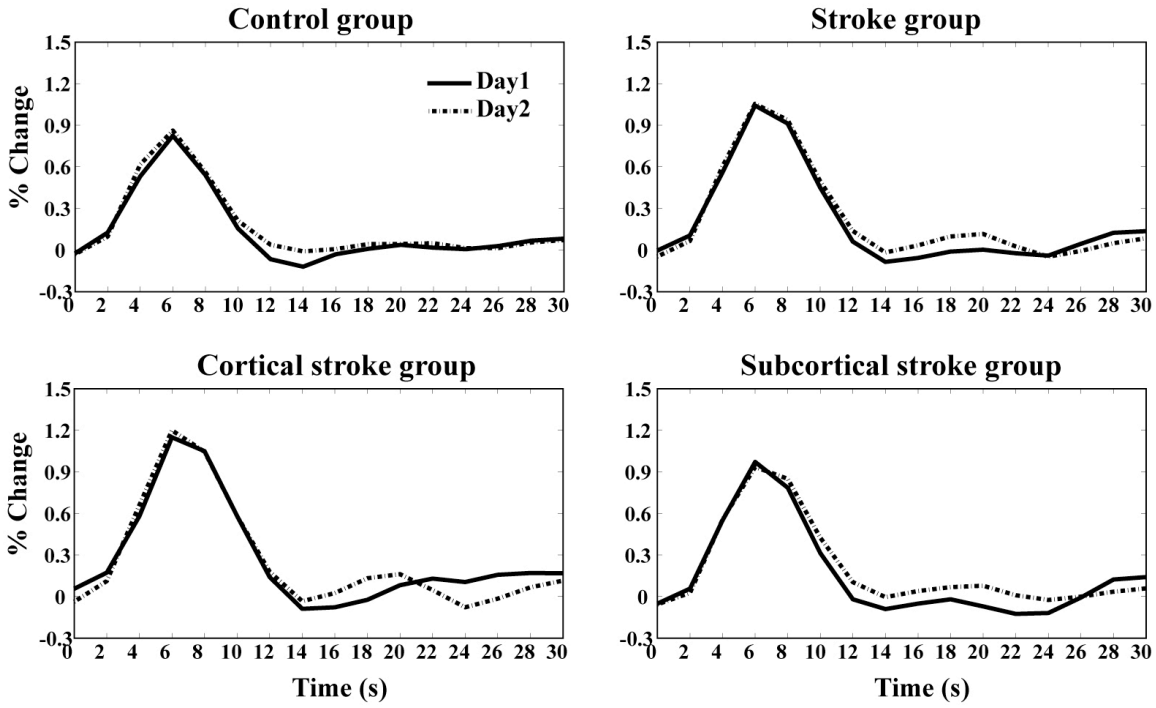

Figure 2-6. Graphical representations comparing the group mean time courses of hemodynamic responses obtained on two different days.

Table 2-3. Group mean (±SD) values for peak amplitude, time to peak amplitude, and rate of change of amplitude (ROC) of hemodynamic responses obtained on two different days.

		Control group		Stroke group		Cortical stroke group		Subcortical stroke group	
		Day1	Day2	Day1	Day2	Day1	Day2	Day1	Day2
Peak amplitude		0.82 (±0.3)	0.91 (±0.5)	1.08 (±0.6)	1.10 (±0.5)	1.21 (±0.6)	1.23 (±0.6)	0.98 (±0.5)	0.99 (±0.4)
Time-to-peak amplitude		6.06 (±0.2)	5.91 (±0.8)	6.14 (±0.6)	6.32 (±0.6)	6.30 (±0.8)	6.30 (±0.3)	6.00 (±0.5)	6.33 (±0.8)
Rate of change of amplitude	ROC1	0.54 (±0.1)	0.63 (±0.2)	0.48 (±0.1)	0.55 (±0.1)	0.41 (±0.1)	0.51 (±0.2)	0.54 (±0.1)	0.59 (±0.1)
	ROC 2	0.34 (±0.1)	0.25 (±0.2)	0.40 (±0.2)	0.41 (±0.2)	0.42 (±0.2)	0.41 (±0.1)	0.38 (±0.2)	0.40 (±0.3)
	ROC 3	-0.34 (±0.1)	-0.30 (±0.2)	-0.21 (±0.2)	-0.14 (±0.2)	-0.14 (±0.1)	-0.15 (±0.1)	-0.27 (±0.2)	-0.13 (±0.2)
	ROC 4	-0.45 (±0.1)	-0.40 (±0.1)	-0.43 (±0.1)	-0.40 (±0.1)	-0.38 (±0.2)	-0.35 (±0.1)	-0.46 (±0.1)	-0.45 (±0.1)
	ROC 5	-0.25 (±0.1)	-0.21 (±0.1)	-0.31 (±0.1)	-0.31 (±0.1)	-0.35 (±0.1)	-0.31 (±0.1)	-0.29 (±0.1)	-0.32 (±0.1)
	ROC 6	-0.05 (±0.1)	-0.08 (±0.1)	-0.11 (±0.1)	-0.13 (±0.1)	-0.18 (±0.1)	-0.17 (±0.1)	-0.05 (±0.1)	-0.10 (±0.1)
P-value		0.811		0.250		0.718		0.491	

P-values represent within-group comparisons for Day 1 versus Day 2.

2.4 DISCUSSION

Consistent with our hypothesis, this study showed that the spatiotemporal profile of hemodynamic responses measured with BOLD-fMRI in stroke survivors was not the same as that observed in individuals without stroke. However, these differences were not as substantial as expected from previous reports and were not large enough to necessitate the use of individualized hemodynamic response functions to obtain valid measures of movement-related brain activity. Specifically, we observed small between-group differences in the rates of rise and decline of hemodynamic responses that were more apparent in individuals with cortical as compared to subcortical stroke. There were no differences in the peak amplitude or time-to-peak amplitude of hemodynamic responses in people with and without stroke. We conclude that all strokes do not affect the spatiotemporal characteristics of hemodynamic responses in such a way as to produce inaccurate representations of brain activity as measured by BOLD-fMRI. Nevertheless, care should be taken to identify individuals whose BOLD-fMRI data may not provide an accurate representation of underlying brain activation when canonical models are used for data processing. One approach for identifying these individuals is to use an event-related paradigm and deconvolution algorithms to examine the spatiotemporal characteristics of hemodynamic responses, as we did here. Examination of hemodynamic responses need not be done for each scan session, as our data suggest that the characteristics of hemodynamic responses in stroke survivors are reproducible across days.

2.4.1 Similarities in hemodynamic responses in people with and without stroke

The most striking finding of this study was the absence of major changes in the spatiotemporal profile of hemodynamic responses that interfered with detection of task-related brain activity as measured with BOLD-fMRI in people post stroke. This observation is different from other studies reporting poor detection of brain activity with BOLD-fMRI when data was processed with canonical hemodynamic response functions developed for the normal brain (Hamzei et al., 2003; Mazzetto-Betti et al., 2010; Murata et al., 2006; Rossini et al., 2004). Impaired detection of task-related brain activity with BOLD-fMRI in people post-stroke has been attributed to abnormal spatiotemporal characteristics of hemodynamic responses (Hamzei et al., 2003; Murata et al., 2006; Rossini et al., 2004). Indeed, previous studies have reported markedly abnormal hemodynamic responses in stroke survivors that were characterized by delayed time-to-peak, decreased peak amplitude, prolonged initial dip, and completely negative responses (Altamura et al., 2009; Bonakdarpour, Parrish, Thompson 2007; Fridriksson et al., 2006; Mazzetto-Betti et al., 2010; Newton et al., 2002; Pineiro et al., 2002; Roc et al., 2006). These abnormalities have been attributed to changes in neurovascular coupling which is the process by which neural activity triggers blood flow changes that decrease the ratio of deoxygenated to oxygenated hemoglobin in local vasculature. These processes result in an increase in the BOLD-fMRI signal. Hence, our observations suggest that the stroke survivors examined here had more normal neurovascular coupling than many stroke survivors examined previously and that stroke is not always associated with impaired neurovascular coupling that leads to poor detection of brain activity with BOLD-fMRI.

Abnormal neurovascular coupling post-stroke has been attributed to poor cerebrovascular autoregulation caused by cerebrovascular occlusive disease. Unlike the present study, many previous studies have examined hemodynamic responses in individuals with cerebrovascular occlusive disease characterized by high grade stenosis or occlusion of the internal carotid or middle cerebral arteries (Altamura et al., 2009; Carusone et al., 2002; Hamzei et al., 2003; Murata et al., 2006; Newton et al., 2002; Roc et al., 2006; Rossini et al., 2004). In these studies, impaired autoregulation of cerebral vasculature can explain the observed changes in the spatiotemporal profile of hemodynamic responses and subsequent poor detection of brain activity with BOLD-fMRI. Autoregulation is the process whereby cerebral blood vessels alter blood flow by altering vessel diameter. In the presence of cerebrovascular occlusive disease, the brain is in a state of chronic hypoperfusion resulting in compensatory vasodilation. Autoregulation to task-related neural activity may be diminished because cerebral blood vessels are already maximally dilated. Moreover, even if cerebral blood vessels are not maximally dilated, their response to neural activity may be sluggish because of structural changes affecting the elasticity of vessel walls such as thickening of the basement membrane, thinning of the endothelium, or plaque formation (reviewed in (Marshall 2004)). Further support for impaired autoregulation as an explanation for abnormal hemodynamic responses comes from studies demonstrating that stroke survivors with abnormal vasomotor reactivity are more likely than those with normal vasomotor reactivity to have abnormal hemodynamic responses (Rossini et al., 2004). Similar results have been observed in individuals with cerebrovascular occlusive disease who have *not* experienced a stroke (Carusone et al., 2002; Hamzei et al., 2003; Rother et al.,

2002), which further suggests that cerebrovascular occlusive disease is an important contributor to abnormal hemodynamic responses.

Unlike many existing publications on hemodynamic responses post-stroke, the subjects in the present study displayed scant evidence of cerebrovascular occlusive disease. This observation likely explains differences between our results and those reported previously. As shown in Table 2-1, four subjects had hemorrhagic strokes that were caused by arterial venous malformation or internal carotid artery dissection. Eight subjects experienced ischemic strokes. Of those eight, two had significant cerebrovascular stenosis at the time of stroke. Both of these subjects had subsequently undergone carotid artery angioplasty to improve cerebral perfusion. In the remaining subjects with ischemic stroke, cerebrovascular stenosis ranged from zero to <50% occlusion. Significant occlusion is typically defined as ≥70% occlusion. We were unable to identify the cause of stroke in 1 subject, but it occurred in infancy, and the subject was only 21 years of age when we studied her. Thus, it seems unlikely that she had cerebrovascular occlusive disease. Hence, we conclude that the absence of substantial changes in hemodynamic responses that affect signal detection in the subjects examined here can be explained by the absence of cerebrovascular occlusive disease and normal autoregulation.

2.4.2 Differences in hemodynamic responses in people with and without stroke

Having ruled out cerebrovascular occlusive disease as an important contributor to the spatiotemporal characteristics of the hemodynamic responses observed here, tissue damage caused by stroke is a plausible explanation for between-group differences.

Bonakdapur et al. reported altered hemodynamic responses post-stroke in the absence of significant cerebrovascular stenosis. This group reported that abnormal hemodynamic responses in stroke survivors were observed predominantly in damaged regions of the brain. They suggested that lesion-related damage to the vascular bed supplying the cortex may have caused these changes. Of interest, there was one subject (also free of cerebrovascular occlusive disease) who had abnormal hemodynamic responses on the damaged *and* intact sides of the brain. This individual had the most extensive stroke-related brain damage of all the subjects examined, and he had a closed head injury prior to a stroke (Bonakdarpour, Parrish, Thompson 2007). In light of this observation, Bonakdarpour's group suggested that the extensiveness of his brain injury may have resulted in extensive and diffuse damage to the vascular bed. In turn, this damage may have led to abnormal neurovascular coupling and abnormal hemodynamic responses across the entire brain.

Lesion-induced changes in the vascular bed may also explain why the hemodynamic responses seen here differed with lesion location (cortical versus subcortical). If brain damage disrupts the vascular bed and changes neurovascular coupling, then one can reason that the more extensive the tissue damage, the more abnormal the hemodynamic response. The subjects with cortical stroke tested in the present study had more extensive brain damage than subjects in the subcortical stroke group (Table 2-1). The cortical stroke group also showed more distinctive changes in the hemodynamic response as compared to the subcortical stroke group. Consistent with the observations of Bonakdarpour *et al*., vascular bed damage may account for these changes. In subcortical stroke, vascular changes in the brain may be distant from the

gray matter where the BOLD-fMRI signal is recorded. Consequently, these changes may have only a minimal effect on the signal. This conclusion is further supported by literature suggesting that altered hemodynamic responses are not observed in diaschisis (Fair et al., 2009), which is a condition characterized by loss of function in a portion of the brain that is distant from the lesion.

Behavioral explanations for between-group differences are unlikely. Indeed, the stroke group moved more slowly than the control group. However, slow movement would likely be associated with a lower than normal peak amplitude because the amplitude of hemodynamic responses increases with movement rate (Lutz et al., 2005; Rao et al., 1996). In our results, we saw larger values for peak amplitude in the stroke group as compared to the control group. It is also unlikely that behavior explains the slower rate of decline in the stroke group as compared to the control group, as stroke survivors did not have a longer delay-to-stop moving than the control subjects.

2.4.3 Canonical versus individualized models

Contrary to our prediction, detection of brain activity with BOLD-fMRI was not enhanced when individualized models of hemodynamic responses were used in place of normal canonical functions. This result differs from previous observations (Bonakdarpour, Parrish, Thompson 2007; Mazzetto-Betti et al., 2010; Newton et al., 2002) but is not surprising in light of knowledge that the spatiotemporal profile of hemodynamic responses was not dramatically different in the stroke and control subjects examined here. These data suggest that the use of a normal canonical model is appropriate for processing movement-related brain activity in people with stroke,

provided that changes in the characteristics of hemodynamic responses are within the range of values observed here. This conclusion is not in conflict with prior reports of enhanced sensitivity of BOLD-fMRI with individualized models where substantial changes in the characteristics of hemodynamic responses were observed. Indeed, there is likely a threshold beyond which canonical functions do not accurately model hemodynamic responses in people post-stroke. Unfortunately, we cannot determine when individualized models become necessary because there was a limited range of variability in the characteristics of the hemodynamic responses observed here, and no subject's functional brain activity was substantially changed by the individualized model. Future studies should make an effort to identify individuals with a variety of altered hemodynamic responses to determine under what circumstances individualized models are needed. Meanwhile, the prudent investigator should use caution in applying canonical functions to BOLD-fMRI data recorded from stroke survivors with cerebrovascular occlusive disease, as the literature has repeatedly shown abnormal hemodynamic responses in this population. Moreover, even in the absence of significant cerebrovascular occlusive disease, investigators should examine the spatiotemporal profile of hemodynamic responses recorded from stroke survivors to confirm that changes are qualitatively and quantitatively similar to those observed here before applying a canonical function.

Also because hemodynamic responses were not dramatically different between stroke and control subjects, this study was unable to assess the effectiveness of individualized models for enhancing BOLD-fMRI signal detection in stroke survivors with abnormal hemodynamic responses. We consider that the similarity of results

obtained from the canonical and individualized approaches was due to the lack of substantial changes in the hemodynamic responses recorded from stroke survivors. We still do not know whether our approach, whereby the characteristics of hemodynamic responses derived from an event-related task were used to create a function for modeling block data, enhances BOLD-fMRI signal detection. Additional studies that identify stroke survivors with abnormal hemodynamic responses are needed to examine the usefulness of this approach.

2.4.4 Reproducibility

Our data suggests that examination of the spatiotemporal profile of hemodynamic responses are not necessary for each scan session, as our data demonstrates that the characteristics of hemodynamic responses in stroke survivors are reproducible across days. One other study has demonstrated reproducibility of hemodynamic responses across days in control subjects (Aguirre, Zarahn, D'esposito 1998), but to our knowledge, this is the first such demonstration in stroke survivors. This observation has practical utility because it suggests that an event-related protocol to examine the spatiotemporal characteristics of hemodynamic responses is not necessary each time an fMRI study is completed. Instead, the results of a single experiment can be applied for subsequent experiments provided that the two sessions are within approximately one month of each other and stroke survivors are in the chronic stage of recovery. However, the reproducibility of the hemodynamic responses across days in acute and sub-acute stroke survivors may not be as robust, because vascular events associated with acute stroke and

the early stages of recovery cause transient changes in neurovascular coupling (reviewed in (Marshall 2004)).

2.5 CONCLUSION

This paper demonstrates that, in the context of a block design fMRI experiment, canonical models developed for the normal brain can be as effective as individualized models for accurate representation of task-related brain activity in stroke survivors. This finding can be attributed to the absence of dramatic abnormalities in the spatiotemporal profiles of the hemodynamic responses in stroke survivors without cerebrovascular occlusive disease. However, before applying canonical functions to stroke data, one should verify that hemodynamic responses in the sample of interest are no more abnormal than those seen here. Examination of hemodynamic responses need not be performed on the same day as the block design, since the spatiotemporal profile of hemodynamic responses is reproducible across days.

CHAPTER 3: DECREASED BRAIN ACTIVITY IN STROKE SURVIVORS DURING PEDALING: AN FMRI STUDY

3.1 INTRODUCTION

Advances in functional imaging and electrophysiological technologies such as functional magnetic resonance imaging (fMRI) (Mehta et al., 2012), near infrared spectroscopy (NIRS) (Miyai et al., 2001; Suzuki et al., 2004; Suzuki et al., 2008), transcranial magnetic stimulation (TMS) (Capaday et al., 1999; Petersen, Christensen, Nielsen 1998; Petersen et al., 2001; Pyndt and Nielsen 2003; Schubert et al., 1999), and electroencephalography (EEG) (Gwin et al., 2011; Sakamoto et al., 2004) have made it possible to examine human brain activity during locomotor behaviors such as walking, running, and pedaling. Consequently, there is now a substantial body of literature demonstrating that several areas of the brain, including the primary somatosensory (S1) and motor cortices (M1), supplemental motor area (SMA), premotor area (PMA), and cerebellum contribute to human locomotion (Christensen et al., 2000; Fukuyama et al., 1997; Harada et al., 2009; Mehta et al., 2012; Mihara et al., 2007; Miyai et al., 2001; Suzuki et al., 2004; Suzuki et al., 2008; Williamson et al., 1997). However, little is known about the way in which the brain contributes to locomotor control and recovery after stroke, which is the focus of this paper.

Previous work suggests that impaired locomotion in stroke survivors is associated with the asymmetrical activation of the S1 and M1 area (Lin, Chen, Lin 2012; Miyai et al., 2002; Miyai et al., 2003; Miyai et al., 2006), and recruitment of brain areas that are not normally involved in locomotor tasks, such as the PMA, pre-supplementary motor area (pre-SMA), and prefrontal area (Miyai et al., 2002; Miyai et al., 2006). With

improved locomotor ability caused by increased time post-stroke and/or rehabilitation, S1 and M1 activities become more symmetrical due to a reduction in activity on the undamaged side, an increase in activity on the damaged side (Miyai et al., 2003; Miyai et al., 2006). These observations have led to the conclusion that asymmetrical activity in the S1 and M1 (undamaged>damaged) may contribute to impaired walking performance post-stroke and that restoration of symmetry in this region may be responsible for recovery. Moreover, the abnormally increased activity in the PMA and pre-SMA after stroke, suggests that these regions may be involved in the compensatory mechanism for the cortical damage.

Previous work has provided a useful framework to begin to appreciate the role of the brain in locomotor control and recovery post-stroke. However, the conclusion that recruiting PMA and pre-SMA during hemiparetic locomotion reflects an abnormal activation pattern (Miyai et al., 2002; Miyai et al., 2006) is debatable because these areas have been associated with normal locomotion (Mihara et al., 2007; Suzuki et al., 2004; Suzuki et al., 2008). Previous studies using fMRI have demonstrated that improved non-locomotor functional ability is associated with additional active representations in sensorimotor cortex including supramarginal gyrus, anterior cingulate gyrus, thalamus, secondary somatosensory area (S2), such as PMA, SMA, pre-SMA, and prefrontal area (Dancause 2006; Dobkin et al., 2004; Luft et al., 2005). These findings were particularly prevalent in stroke survivors when lesions involved brain areas that are normally associated with the given task. This suggests that the same adapted control strategies after stroke might be evident across locomotor and non-locomotor tasks. More studies of

brain control of locomotion post-stroke are needed to resolve which brain areas are associated with normal control of movement and which are compensatory.

Unfortunately, the available framework of brain control of locomotion post-stroke is limited to only a few studies (Lin, Chen, Lin 2012; Miyai et al., 2002; Miyai et al., 2003; Miyai et al., 2006). Some of these studies demonstrated a substantial between-subject and between-study variability in active brain areas associated with locomotion, resulting in a lack of consistency in the pattern of brain activation in the control of locomotion post-stroke. Furthermore, the framework is derived mainly from studies of walking where the influence of balance and body weight support confound our understanding of the locomotor component of gait, which involves rhythmic, reciprocal, multi-joint flexion and extension of both lower limbs. Indeed, locomotor movements are deeply integrated with balance and body weight support for successful walking. However, each component is controlled differently in normal walking, and may therefore exhibit independent control and recovery post-stroke.

The purpose of this study was to determine whether supraspinal control of locomotor movements, which involves rhythmic, reciprocal, flexion and extension movements of multiple joints in both legs, would be different after stroke. We also proposed to examine the relationship between locomotor impairments and brain activation measured during pedaling. In this chapter we are focusing on the former objective, and in the next chapter we provide the details for the latter objective.

For this chapter's objective, we used fMRI to examine brain activity during pedaling. Pedaling can be accomplished while lying supine, which lacks the confounding influences of balance and body weight support, and allows the use of fMRI to examine

supraspinal control of locomotion. We hypothesized that if asymmetrical brain activity is responsible for locomotor impairments, then stroke-induced brain activation during pedaling would be asymmetrical. We also hypothesized that if motor-related brain areas, such as PMA and pre-SMA, are abnormally active in the control of locomotion post-stroke, then these areas would be active in stroke survivors but not in healthy individuals, which would be represented as increased volume of activation or larger active areas in the cortex. We also measured fMRI during unilateral, single joint flexion and extension movements of the lower limbs in order to compare supraspinal control mechanisms across locomotor and non-locomotor tasks. To our knowledge, this is the first report describing supraspinal control of a locomotor movement in stroke survivors measured by fMRI.

3.2 METHODS

3.2.1 Subjects

Fourteen individuals with post-stroke hemiparesis and 12 healthy control subjects were recruited. Prior to participating, subjects gave written informed consent according to the Declaration of Helsinki and institutional guidelines at Marquette University and the Medical College of Wisconsin. One stroke and 2 control subjects were unable to complete the study due to claustrophobia or body size incompatibility with the MR scanner. Data from 1 control subject was discarded after an undocumented brain anomaly was identified, and data from a stroke subject was discarded because of excessive head movement. Hence, data from 12 stroke subjects (8 females; age 55.1±13.3 years) and 9 control subjects (6 females; age 53.4±13.1 years) are presented here.

All stroke participants had sustained a stroke at least 1.1 years prior to testing, and the mean (±standard deviation (SD)) time since stroke was 12.91 (±13.47) years. Seven stroke subjects had subcortical lesions involving the internal capsule, corona radiata, basal ganglia, or thalamus. Five stroke subjects had cortical lesions that affected one or more of the subcortical structures listed above and a portion of the cerebral cortex outside of the leg area of the primary sensory and motor cortices. (See Figure 3-1.) There were 6 subjects with right hemiparesis and 5 subjects with left hemiparesis. One subject had stroke-related movement impairments on both sides. Mean (±SD) values for lower extremity Fugl-Meyer score (maximum possible=56) and walking velocity in stroke

subjects were 44.7 (±8.8) and 0.91 (±0.30) m/s, respectively. (See Table 3-1.) Control subjects had no signs or history of stroke or other neurological impairment.

Table 3-1. Descriptive characteristics of stroke subjects.

Subject	Age (years)	Sex	Affected limb	Affected brain area	Time to scan (years)	Fugl-Meyer Score (56)	Walking velocity (m/s)
S01	60	F	R	Cortical	20.4	39	1.10
S03	62	F	L	Subcor	8.4	54	1.11
S05	56	M	L	Subcor	51.0	43	1.04
S06	64	F	R	Subcor	6.5	54	0.82
S07	20	F	L	Subcor	19.0	47	1.13
S08	73	F	R	Subcor	1.1	52	1.04
S10	58	F	L	Cortical	6.1	43	0.48
S11	53	F	R	Subcor	17.4	51	1.05
S13	46	M	R>L	Subcor	4.4	37	0.82
S15	48	M	R	Cortical	8.1	37	0.88
S17	65	F	L	Cortical	6.2	26	0.20
S19	55	M	R	Cortical	6.4	53	1.22

F=female, M=male, R=right, L=left, Cortical=stroke affecting cerebral cortex, Subcortical=stroke affecting subcortical structures.

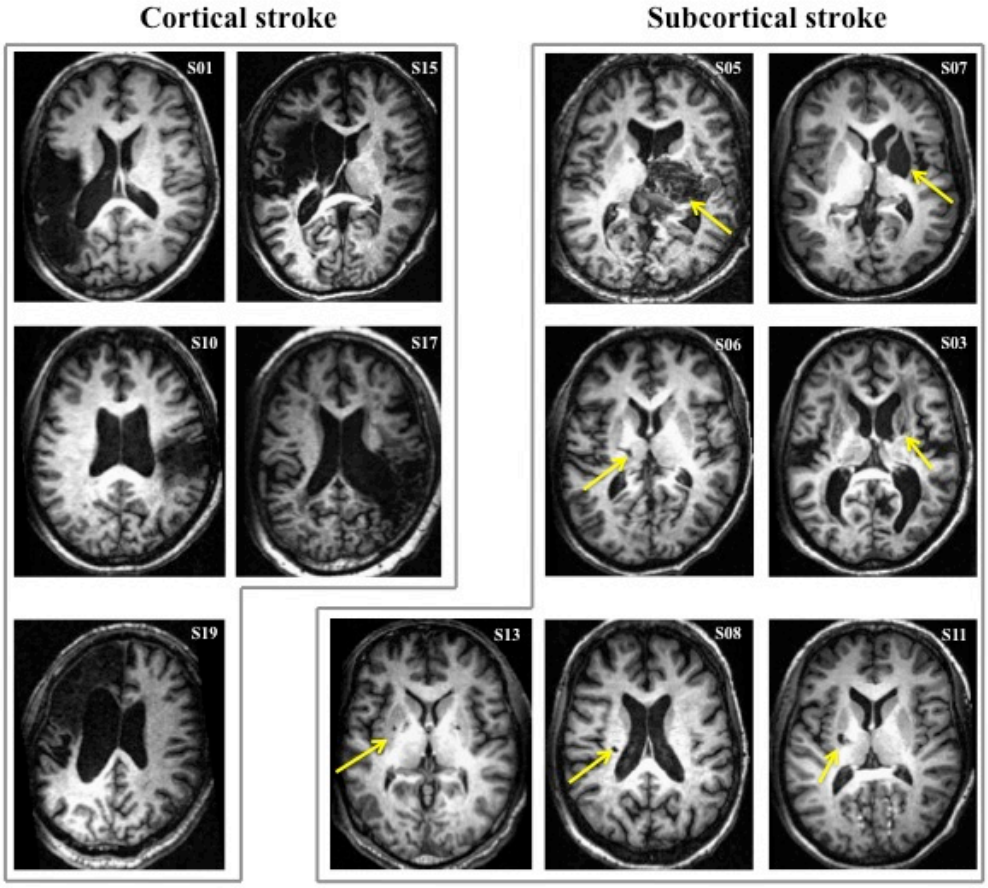

Figure 3-1. T_1-weighted anatomical images displaying brain lesions of stroke subjects. Arrows are positioned to indicate lesion location. The images are shown in neurological convention (left is left).

3.2.2 Instrumentation and data recording

The pedaling device used for this study is a direct drive apparatus fabricated from nonmetallic materials that could be positioned on an MR scanner bed and used to pedal against a light frictional load (Mehta et al., 2012; Mehta et al., 2009). This device was equipped with an MR-compatible optical encoder (model: TD 5207, Micronor Inc., Newbury Park, CA) that was coupled to the crank shaft and used to measure crank position. Signals from the encoder were measured through a fiber optic cable to a

controller unit (model: MR 310, Micronor Inc., Newbury Park, CA) located outside the scanner room. The controller unit converted the optical signals to electrical signals and produced an analog output corresponding to position. Position data were sampled at 2000 Hz using a laptop computer, a 16-bit analog-to-digital converter and data acquisition software (micro 1401 mk II and Spike, Cambridge Electronic Designs, UK). These data were used to compute mean pedaling velocity across subjects.

A circular plastic button (6.35 cm diameter) connected to a switch (Jelly Bean Twist Top Switch, AbleNet, Inc., Roseville, MN) was used to record unilateral, single joint flexion and extension movements of the lower limbs. This button was mounted on a base via a custom-made multi-articular arm so that the button could be oriented beneath the ball of the foot. Each time the button was depressed a pulse was generated, which was recorded using the Presentation program (NeuroBehavioral Systems Inc., Albany, CA). This data was used to calculate movement rate and to ensure that subjects produced desired movements at appropriate times.

A 3.0T GE MR scanner (General Electric Healthcare, Milwaukee, WI) and a GE single channel transmit/receive split head coil assembly (model 2376114, General Electric Healthcare, Milwaukee, WI) were used to acquire image data for the study. Functional images (T2*-weighted) were acquired using echoplanar imaging (repetition time (TR): 2000 ms, echo time (TE): 25 ms, flip angle: 77º, 36 contiguous slices in the sagittal plane, 64 x 64 matrix, 4 mm slice thickness, and field of view (FOV): 24 cm). The resolution of the images was 3.75 x 3.75 x 4 mm. Anatomical images (T1-weighted) were obtained approximately half way through the scan session (TR: 9.5 ms, TE: 25 ms, flip angle: 12°, 256 x 244 matrix, resolution: 1 mm^3).

Presentation software was used to synchronize audio cues with MR pulses and to deliver audio cues to the subjects. Audacity (open source software) was used to create the tone used for audio cues prior to the experiment.

Prior to MRI scanning, subjects underwent two safety screenings and were excluded if they were claustrophobic, pregnant, or had any implants or foreign bodies incompatible with fMRI. Each subject also participated in a familiarization session outside the MR environment during which we explained the experimental procedures and allowed subjects to practice the tasks.

During fMRI scanning, subjects lay supine on the MR scanner bed. To minimize movement, the subject's head was enveloped by a beaded vacuum pillow and their trunk was strapped down. Subjects wore MR-compatible earphones (model SRM 212, Stax Ltd, Japan) through which audio cues were delivered. An additional set of headphones was used to protect against scanner noise. An emergency squeeze ball, which could be used at any time to signal a problem, was given to the subjects. Participants were observed for safety and comfort and were able to communicate via intercom with the scanner technician throughout the session. We also had access to real time head position information. If the subject did not perform the task as instructed, or if head movement was excessive, we checked the subject for comfort, repeated the instructions to remain still, and restarted the run.

Each subject participated in a pedaling and a unilateral, single joint flexion and extension ("tapping") session in the MR scanner. Pedaling and tapping were performed on two different days. During both sessions a static tone indicated when to move and silence indicated when to rest. During the pedaling session, subjects' feet were fastened

to the pedaling device, and they were asked to pedal at a comfortable rate using both legs. We utilized a block design consisting of 6 runs of pedaling. In a single run, subjects pedaled for 30s and rested for 30s. This sequence was repeated 4 times. Each run was preceded by 18s of rest. During the tapping session, subjects' legs were positioned over a foam bolster such that the hip and knees were flexed and the feet were approximately 15 cm above the surface of the scanner table. The circular plastic button was placed under the foot. An event-related design consisting of 3 runs was utilized. A single run included 20 moving events and 40 resting events with 2s per event, presented in random order (Verstynen et al., 2005). Subjects were asked to tap the button by dorsi- and plantar flexing the ankle at a comfortable pace. The task was performed with one foot at a time. Knee flexion and extension was allowed in stroke participants (n=6) who could not perform ankle plantar and dorsiflexion.

3.2.3 fMRI data processing and statistics

Processing of fMRI signals was completed using Analysis of Functional NeuroImages (AFNI) software (Cox 1996). Digital imaging and communication in medicine (DICOM) files containing fMRI signals were converted into 3 dimensional images [using the *to3d* command with parameter settings time = zt (means that the slices are input in the order z-axis first, then t-axis), number of points in the z-direction = 36 slices, number of points in the t-direction = 128 TRs, length of each TR = 2000ms, alt+z]. A time series of each individual voxel was aligned to the same temporal origin within each TR using heptic (7^{th} order) Lagrange polynomial interpolation technique [using *3dTshift* command with paramter settings align each slice to time offset (tzero) = 0,

ignore the first 4 TRs (ignore)= 4, heptic]. The first 4 TRs within each run were removed to eliminate non-teady state magnetization artifact [using *3dTcat* command]. Multiple runs were concatenated [using *3dTcat* command]. The concatenated data was registered to the functional scan obtained closest in time to the anatomical scan using iterated a linearized weighted least squares technique to make each sub-brick as like as possible to the base brick [*3dvolreg* with parameter settings heptic, base '[0]']. To identify voxels containing pedaling-related brain activity, multiple linear regression technique using *3dDeconvolve* was performed using the voxel-wise hemodynamic response function with head position as a variable of no interest. The time-series was modeled by $y = \beta_0 + \beta_1 x_1 + \beta_2 x_2 + ... + \beta_7 x_7 + \varepsilon$, where x_1 was the delayed non-movement model; x_2 - x_7 were head movement in 6 directions, acting as variables of no interest. As described previously (Mehta et al., 2009), only the portion of the BOLD time-series after movement stopped was used. To identify voxels containing tapping related brain activity, voxel-wise hemodynamic response functions were used instead of a canonical function. Head position was used as a variable of no interest. Functional data were blurred using a 4 mm full width half maximum Gaussian filter [using *3dFWHMx* command].

To identify significantly active voxels at a familywise error rate of $P<0.05$, we used a Monte Carlo simulation to set an appropriate cluster size for a given individual voxel P-value [using *AlphaSim* command]. The Monte Carlo simulation is a simulation of the process of image generation, spatial correlation of voxels, voxel intensity thresholding, masking, and cluster identification. The combination of individual voxel probability thresholding and minimum cluster size thresholding provides an estimate of

the probability of a false positive detection per image, which is determined from the frequency count of cluster sizes. The parameters used for this function included voxel dimensions=3.5x3.5x4 mm [to generate a random image], fwhmx= 5.14, fwhmy=4.10, fwhmz= 2.98 [to simulate the effect of spatial correlation of voxels by convolving the generated random image with a Gaussian function]. Specifically, this process was performed by taking the 3D fast Fourier transform of the random image, multiplying this transform by the transform of the Gaussian function and taking the inverse of the Fourier transform, yielding the result. To set the voxel intensity thresholding, power calculations was performed to define Zthr. Once Zthr had been set, then all voxels inside the entire volume or inside the true activation region were compared against Zthr. The thresholding was set such that those voxels with an intensity greater than Zthr to 1 were considered active and those voxels with intensity less than Zthr were set to 0. To simulate masks, the brain mask dataset from each individual subject was used. The last step for this simulation was to identify which activated voxels (the voxels with a magnitude of 1 from the voxel thresholding step) belonged to clusters. A parameter of rmm=6.6 was used to defined whether two voxels are in the same cluster. Every activated voxel was a member of one, and only one, cluster. Once all clusters have been found, the size (in number of voxels) of each cluster was recorded in a frequency table.

Percent signal change was calculated as the change in amplitude of the BOLD signal from baseline [expression: "100 *(g/((a+b+c+d+e+f)/6))*step (1abs((g/((a+b+c+d+e+f)/6))))" , where a-f are the baseline constant of each pedaling run, g is a sub-brick containing the regression coefficient, and step function controls outflow if baseline is close to 0]. Significantly correlated voxels outside of the brain and negatively

correlated voxels were ignored. Any voxels with percent signal change >10 were also ignored, as these large changes were likely due to edge effects (See Appendix C for more details).

Each subject's data was analyzed individually in the original coordinate system to avoid distortion arising from transformation to a standardized coordinate system. Measures of pedaling and tapping related brain activity were extracted from the sensorimotor cortex and the cerebellum, as these regions were consistently active across stroke and control subjects. The sensorimotor cortex included the primary motor cortex (M1), primary somatosensory cortex (S1), and Brodmann's area 6 (BA6). The cerebellum included cerebellar lobules IV, V, and VIII. The anatomical boundaries for the sensorimotor cortex and cerebellum were defined from the T_1 weighted images as previously described (Schmahmann et al., 1999; Wexler et al., 1997). In the axial plane, the sensorimotor cortex extended anteriorly from the postcentral sulcus to cover approximately the posterior half of the superior frontal gyrus and from the medial border of each hemisphere spanning laterally over the dorsolateral frontal lobe. In the sagittal plane, the sensorimotor cortex was bordered inferiorly by the cingulate sulcus, extending superiorly to the top of the hemisphere. Cerebellar lobules IV and V were located in the anterior lobe of the cerebellum between the preculminate fissure and the primary fissure. Cerebellar lobule VIII was located in the posterior lobe of the cerebellum between the prepyramidal (prebiventer) fissure and the secondary fissure.

3.2.4 Dependent variables and statistical analysis

Volume, intensity, and laterality index (LI) of brain activation were used to describe pedaling- and tapping-related brain activity. Volume and intensity of brain activation were computed individually for each subject for bilateral sensorimotor cortex, bilateral cerebellum, and for these two regions combined (SMC-Cb). Volume of activation was defined as the number of significantly active voxels in each brain region multiplied by voxel volume in microliters (μL). Intensity of activation was defined as the average percent signal change from baseline in the active portion of the region of interest. Laterality index was computed separately for the sensorimotor cortex and cerebellum. Laterality index in stroke subjects was defined as the difference in volume of activation between the damaged and undamaged sides of the brain as a proportion of total volume of activation on both sides of the brain. Laterality index for control subjects was the difference in volume of activation between the left and right sides of the brain as a proportion of total volume. (See Eq. 1 and 2).

$$LI = \frac{(\text{Damaged} - \text{Undamaged})}{(\text{Damaged} + \text{Undamaged})}$$ Eq. 1. Laterality index (LI) for stroke subjects.

$$LI = \frac{(\text{Left} - \text{Right})}{(\text{Left} + \text{Right})}$$ Eq. 2. Laterality index (LI) for control subjects.

Laterality index could assume any value between -1 and 1. A value of -1 would indicate that all active voxels were on the undamaged (stroke subjects) or right (control subjects) side of the brain, and 1 would indicate that all active voxels were on the damaged (stroke subjects) or left (control subjects) side. Zero would indicate perfectly symmetrical brain

activity in the region of interest.

For the pedaling data, group means (±SD) for volume and intensity of activation in the sensorimotor cortex, cerebellum, and for these two regions combined (SMC-Cb) were computed for 4 different groups: all control subjects, all stroke subjects, stroke subjects with cortical lesions, and stroke subjects with subcortical lesions. In the same four groups, group means (±SD) for LI were computed separately for sensorimotor cortex and cerebellum. Independent t-tests were used to test for between-group differences (control versus stroke subjects) in volume and intensity of activation in the sensorimotor cortex, cerebellum, and for these two regions combined (SMC-Cb). Also, multivariate general linear model was used to test between-group differences (control versus stroke subjects) in volume and intensity of activation in the primary sensorimotor area (M1/S1), Brodmann's area 6, and cerebellum. Independent t-tests were also used to test for effects of lesion location (subcortical versus subcortical group) on volume and intensity of activation in the two regions combined (SMC-Cb). For each of the 4 groups, one-sample t-tests were used to determine whether LI was different from zero in the sensorimotor cortex and cerebellum.

For the tapping data, group means (±SD) were computed for volume, intensity, and LI of activation in the sensorimotor cortex; volume and intensity of activation in the cerebellum and the two regions combined (SMC-Cb) associated with left and right (control group) or paretic and non-paretic (stroke group) limb movements. Average values from the left and right limbs in the control group were used in subsequent analysis. One-way analysis of variance (ANOVA) was used to identify differences among the control group and paretic and non-paretic limb in the stroke group with respect to

volume, and intensity of activation in sensorimotor cortex, cerebellum, and the two regions combined (SMC-Cb) during tapping. Also, multivariate general linear model was used to test differences among the control group and paretic and non-paretic limb in the stroke group with respect to volume, and intensity of activation in the primary sensorimotor area (M1/S1), Brodmann's area 6, and cerebellum. If needed, an appropriate post-hoc (least significant difference LSD) was used to identify differences between groups. An independent t-test was used to test for differences in the rate of pedaling between the control and stroke group; one-way ANOVA was used to examine differences in tapping rate between the control group and the paretic and non-paretic limb of the stroke group. All tests were considered significant at $P<0.05$.

3.3. RESULTS

All subjects were able to perform pedaling and tapping tasks as instructed while recording brain activity with fMRI. There were no significant between-group differences in the rate of pedaling (P=0.14, control versus stroke group) or tapping (P=0.09, control versus paretic and non-paretic leg of the stroke group). Mean (±SD) pedaling rate for the control and stroke groups was 0.95 (±0.18) Hz and 0.81 (±0.23) Hz, respectively. Mean (±SD) tapping rate was 1.87 (±0.69) Hz in the control group, 1.37 (±0.38) Hz in the paretic foot of the stroke group, and 1.66 (±0.36) Hz in the non-paretic foot of the stroke group. Head movement did not exceed 1.3 mm across subjects and tasks.

The volume of activation of pedaling-related brain activity was reduced in individuals with stroke as compared to control group. As shown in Figures 3-2 and 3-3A, the total volume of activation, as represented by SMC-Cb, was significantly smaller in the stroke group as compared to the control group (stroke group=27,693.8±9,607.5 μL, control group=37,818.8±9,168.5 μL, P=0.03). This observation was likely due to reduced volume of activation in both the sensorimotor cortex and the cerebellum, as Figures 3-3B and C show that the volume of activation in each of these regions was smaller in the stroke as compared to the control group. Reduced volume of activation in the stroke group reached statistical significance in the cerebellum (stroke group=7,697±3,747 μL, control group=11,019±2,096 μL, P=0.02) but not in the sensorimotor cortex (stroke group=19,997±8,434 μL, control group=26,800±7,176 μL, P=0.06). The reduction in total volume of activation associated with pedaling was not affected by lesion location as indicated by no significant difference between stroke groups with cortical and subcortical lesion with respect to volume of activation in the

SMC-Cb (cortical stroke group =24660±9678.5 μL, subcoritcal stroke group =29869±9676.1 μL, P=0.38).

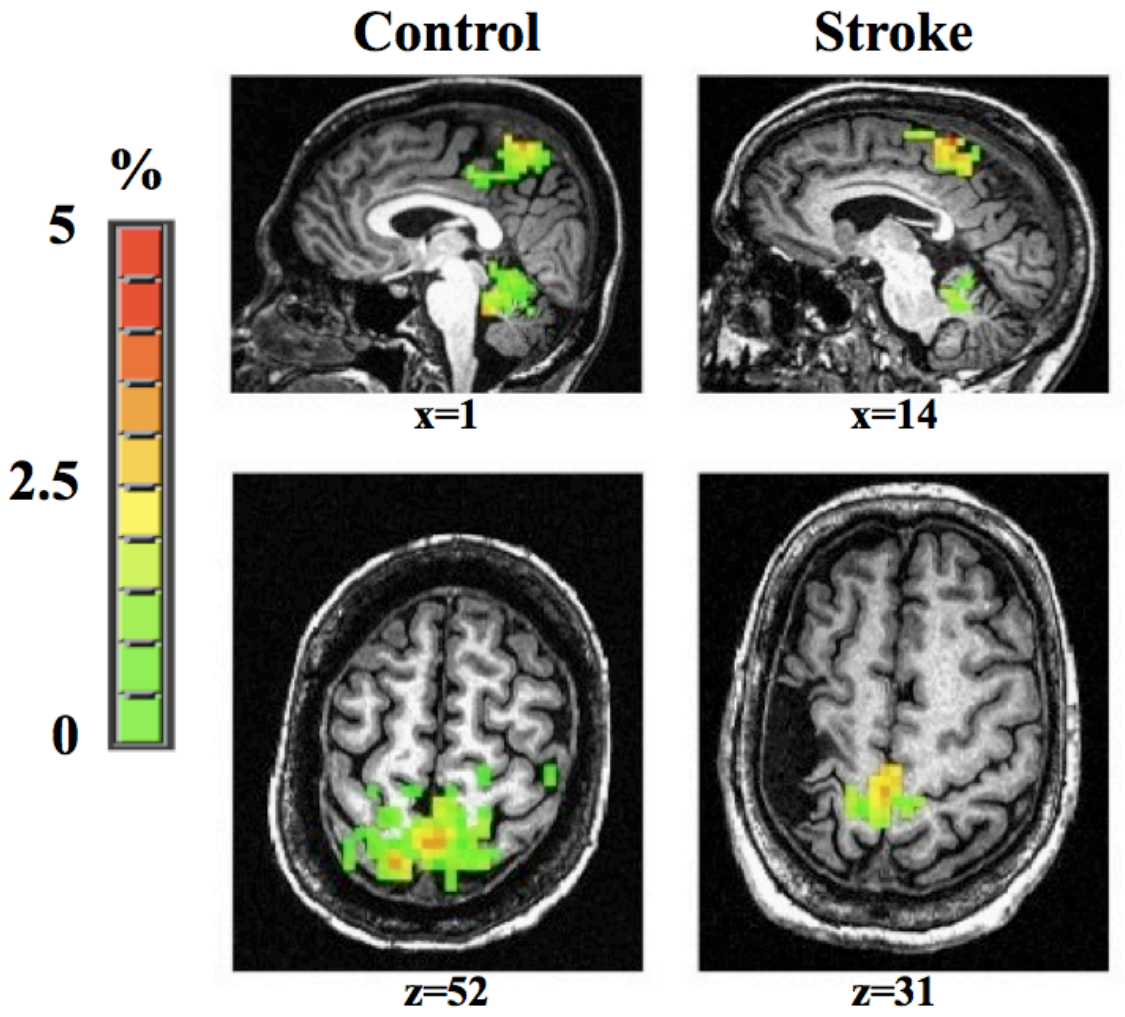

Figure 3-2. Representative examples of brain activation maps from a single subject from each group (control and stroke) associated with the pedaling. The color bar represents percent signal change (0-5%).

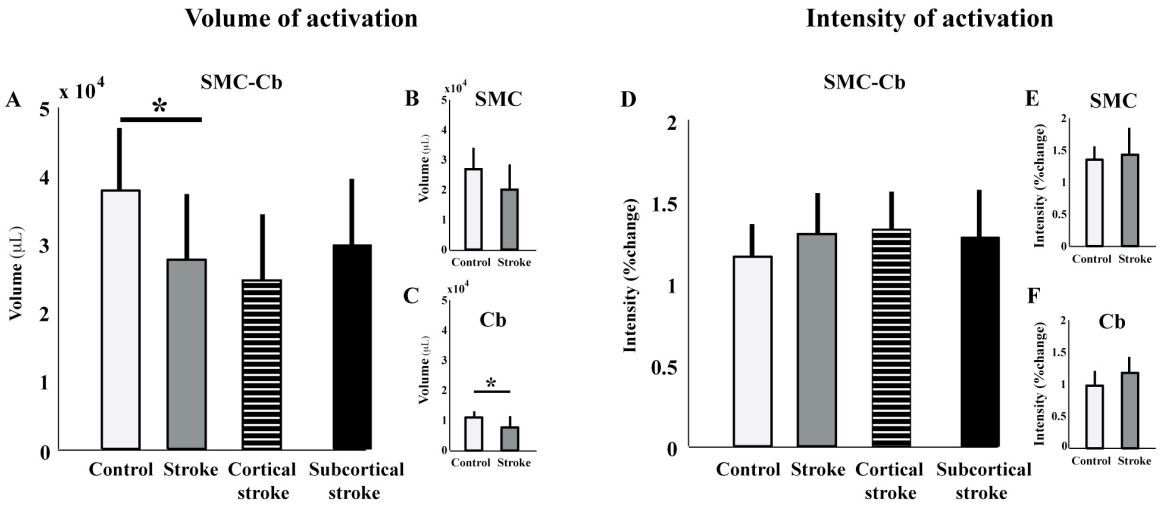

Figure 3-3. Bar plots representing the group mean volume (A-C) and the intensity (D-F) of brain activation during pedaling. SMC=sensorimotor cortex, Cb=cerebellum, SMC-Cb=sensorimotor cortex and cerebellum combined. Values are group means (±SD). Asterisks indicate significance at $p<0.05$.

There were no differences between the stroke and control groups with respect to the intensity of activation of pedaling-related brain activity in any active region. As shown in Figure 3-3D, the intensity of activation in SMC-Cb was 1.16 (±0.20)%, 1.30 (±0.25)%, 1.33 (±0.22)%, and 1.28 ±(0.29)% in the control, all stroke, cortical stroke, and subcortical stroke group, respectively. These differences did not reach statistical significance (P=0.17 for control versus all stroke group, p=0.73 for cortical stroke versus subcortical stroke group). When the sensorimotor cortex was examined alone, mean (±SD) intensity of activation were 1.35 (±0.22)% and 1.43 (±0.42)% for the control and stroke group, respectively (P=0.58). In the cerebellum, intensity of activation was 0.98 (±0.23)% for the control group and 1.18 (±0.25) for the stroke group (P=0.07). See Figures 3-3E and F.

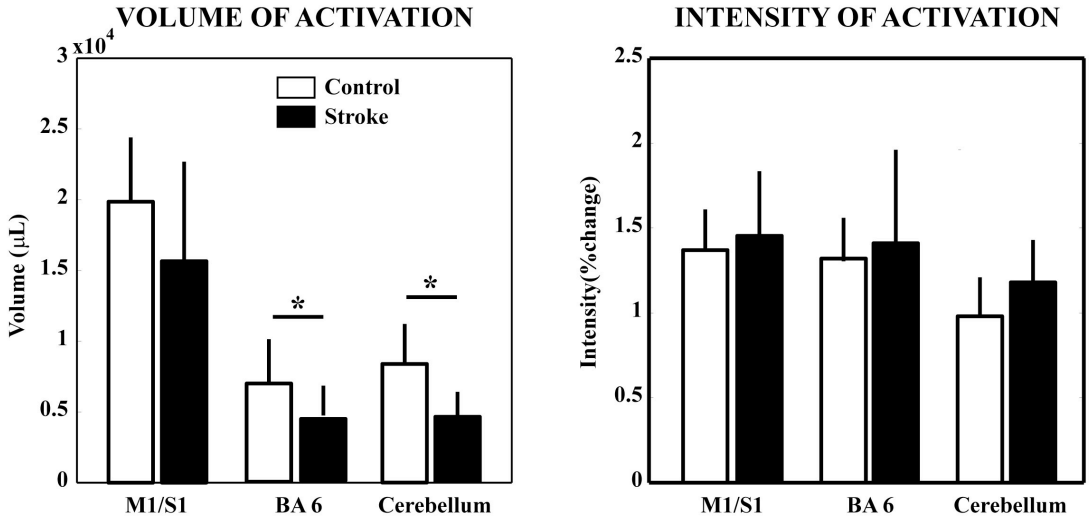

Figure 3-4. Bar plots representing the group mean volume and the intensity of brain activation during pedaling. M1/S1=primary sensorimotor area and BA6=Brodmann's area 6. Values are group means (±SD). Asterisks indicate significance at $p<0.05$.

As shown in Figure 3-4, multivariate general linear model demonstrated significantly decreased volume of activation in the stroke compared to the control group (P=0.018), but there was no difference in the intensity of activation between the two groups (P=0.352). The volume of Brodmann's area 6 (control group=6937.5 ±3133.76 μL, stroke group=4350±2347.39 μL, P=0.043) and cerebellum (control group=8381.25 ±2834.91 μL, stroke group=4591.4±1757.6 μL, P=0.001) were significantly different between the two groups, but not the primary sensorimotor area (control group=19862.5 ±4543.25 μL, stroke group=15646.88±7036.58 μL, P=0.134). Also, multivariate general linear model showed no significant differences of the intensity of activation in the primary sensorimotor area (control group=1.37±0.24%, stroke group=1.44±0.38%), Brodmann's area 6 (control group=1.32±0.24%, stroke group=1.41±0.55%), and cerebellum (control group=0.98±0.23%, stroke group=1.18±0.25%). These findings

were supported by the results of a t-test to test for between- group differences (control versus stroke)

In individuals with stroke, pedaling-related brain activity was symmetrically distributed in the sensorimotor cortex and asymmetrically distributed toward the damaged side of the brain in the cerebellum. (See Figure 3-5.) Specifically, mean (±SD) values for LI in the sensorimotor cortex were -0.06 (±0.20), -0.02 (±0.19), and -0.08 (±0.21) for the all stroke, cortical stroke, and subcortical stroke group, respectively. These values were not significantly different from zero ($P \geq 0.34$). In the cerebellum, mean (±SD) values for LI in the all stroke, cortical stroke, and subcortical stroke group were 0.29 (±0.33), 0.37 (±0.42), and 0.23 (±0.26), respectively. These values were significantly different from zero in the all stroke group ($P=0.01$) but not in the cortical stroke, and subcortical stroke group ($P \geq 0.06$). In the control group, activity in the sensorimotor cortex was lateralized toward the left side of the brain with a mean (±SD) LI value of 0.05 (±0.06) ($P=0.04$). The control group displayed symmetrical activity in the cerebellum as evidenced by a LI of 0.04 (±0.15) that was not significantly different from zero ($P=0.48$).

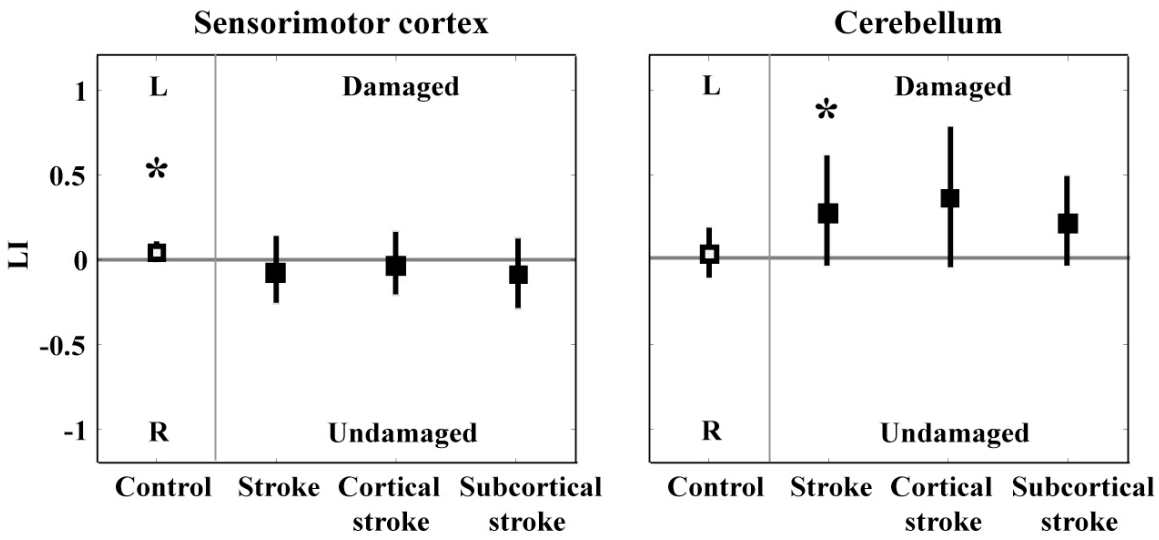

Figure 3-5. Graphical representations showing laterality index (LI) computed from the volume of brain activation associated with pedaling. Values are group means (±SD). L=left hemisphere, R=right hemisphere, Damaged=damaged hemisphere, Undamaged=undamaged hemisphere. Asterisks indicate significance at $p<0.05$.

Stroke-related changes in brain activity during tapping were different from those observed during pedaling. As shown in Figure 3-6, there was no significant volume of activation difference between the control group and the paretic and non-paretic limbs of the stroke group in sensorimotor cortex and cerebellum combined (SMC-Cb), sensorimotor cortex, or cerebellum (P=0.28 for SMC-Cb, P=0.28 for sensoritmotor cortex, P= 0.27 for cerebellum). The intensity of activation in SMC-Cb was reduced in the paretic and non-paretic limbs of the stroke group as compared to control (control=1.87±0.27%, stroke-non-paretic=0.68±0.21%, stroke-paretic=0.77±0.28%, P<0.001). The reduction of intensity of activation was driven by the sensorimotor cortex (control=2.35±0.18%, stroke-non-paretic=0.77±0.31%, stroke-paretic=0.83±0.37%, P<0.001). The intensity of activation in the cerebellum was 0.54±0.12%, 0.55±0.13%, 0.67±0.2% for the control group, the stroke group when moving the non-paretic foot, and the stroke group when moving the paretic foot, respectively (P=0.144).

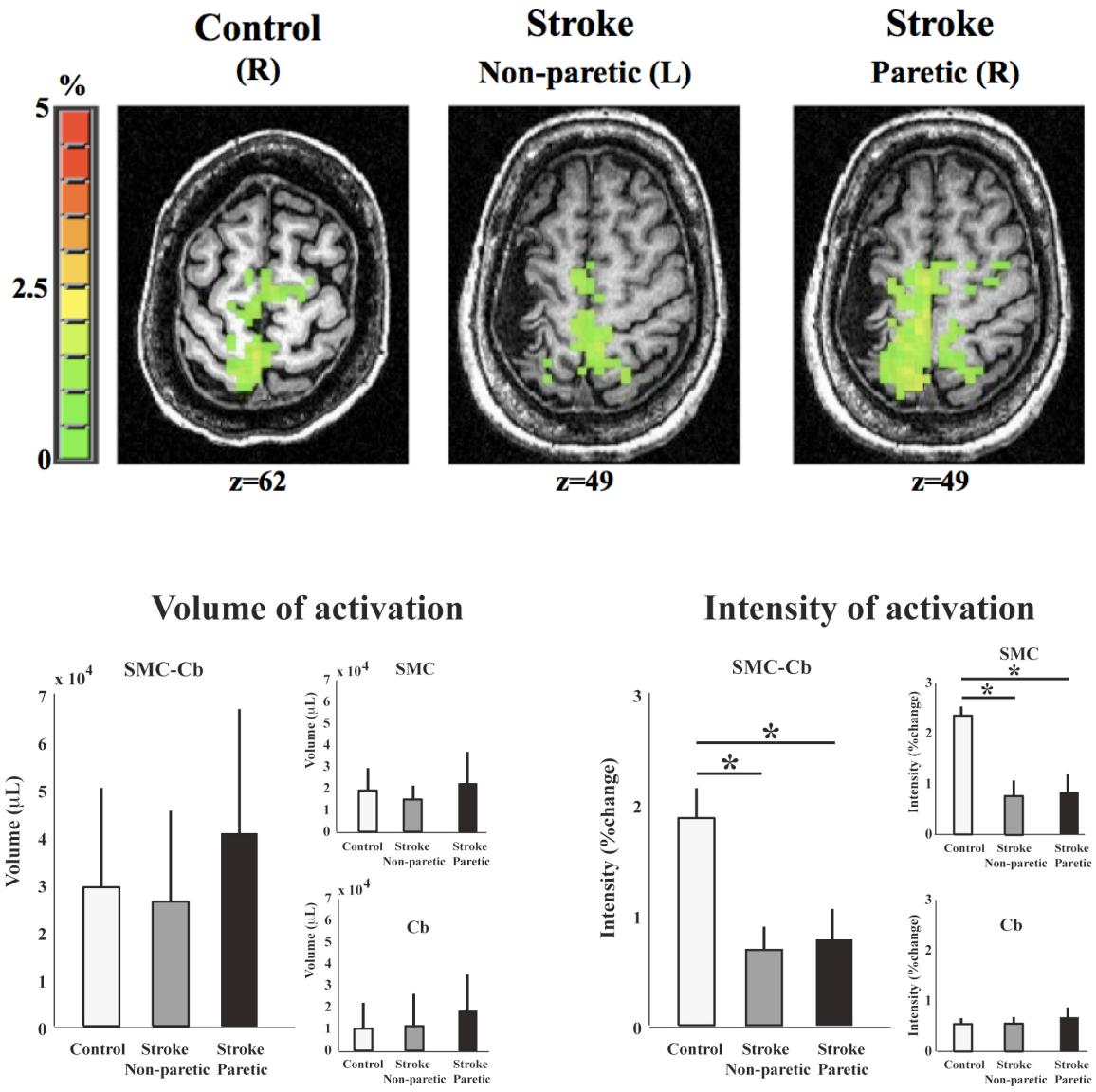

Figure 3-6. Brain activation during foot tapping. Top: Representative examples of brain activation maps. The color bar represents percent signal change (0-5%). Control (R) is a map from a single representative control subject tapping his right foot. Non-paretic (L) limb of stroke subjects is a map from a representative stroke subject tapping with his non-paretic foot, which in this case is the left foot. Paretic (R) limb of a stroke subject is a map from the same representative subject tapping with his paretic foot, which is his right foot. Bottom left: Group mean of volume of activation. Bottom right: Group mean of intensity of activation. SMC=sensorimotor cortex, Cb=cerebellum, SMC-Cb=sensorimotor cortex and cerebellum combined. Values are group means (±SD). Asterisks indicate significance at $p<0.05$.

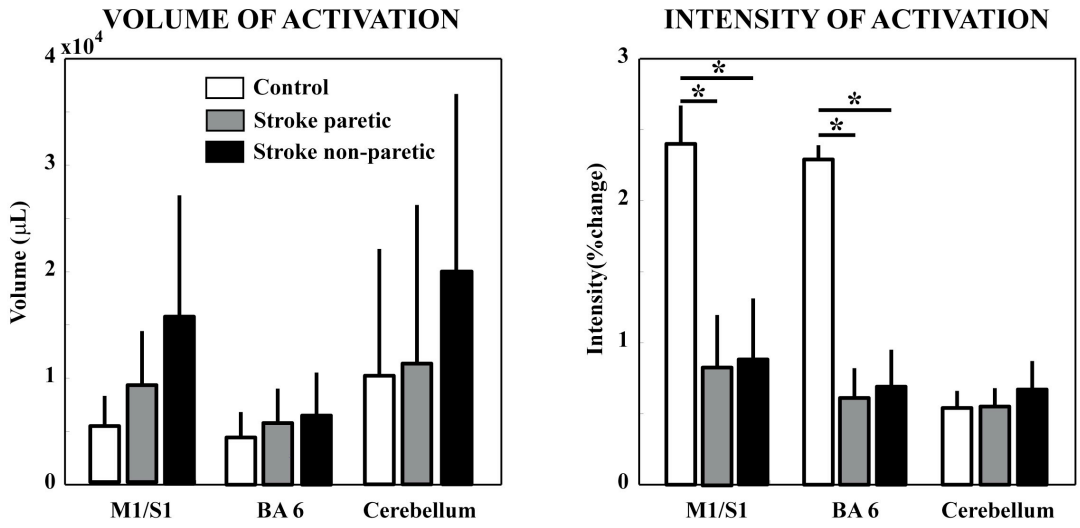

Figure 3-7. Bar plots representing the group mean volume and the intensity of brain activation during foot-tapping. M1/S1=primary sensorimotor area and BA6=Brodmann's area 6. Values are group means (±SD). Asterisks indicate significance at $p<0.05$.

As shown in Figure 3-7, the multivariate general linear model demonstrated significantly decreased intensity of activation in the stroke group as compared to the control group when tapping the paretic and non-paretic side ($P<0.001$). There was was no difference in the volume of activation among the control and stroke groups ($P=0.143$). The intensity of activation in the primary sensorimotor area (control group=2.4±0.27%, stroke group when moving the paretic leg=0.88±0.43%, stroke group when moving the non-paretic leg=0.83±0.37%, $P<0.001$) and in Brodmann's area 6 (control group=2.29±0.1%, stroke group when moving the paretic leg=0.69±0.26%, stroke group when moving the non-paretic leg=0.61±0.21%, $P<0.001$) was significantly different between the two groups. There was no significant between-group diffence in the intensity of cerebellum activation (control group=0.54±0.12%, stroke group when moving the paretic leg=0.67±0.2%, stroke group when moving the non-paretic leg=0.55±0.13%, $P<0.001$). Meanwhile, the volume of activation was not different

among the groups for primary sensorimotor area (control group=5253.13±2838.91 μL, stroke group when moving the paretic leg=15703.13±11392.91 μL, stroke group when moving the non-paretic leg=9093.75±5085.76 μL), Brodmann's area 6 (control group=4425±2387.15 μL, stroke group when moving the paretic leg=6492.19±4028.03 μL, stroke group when moving the non-paretic leg=5779.69±3243.77 μL), or cerebellum (control group=10199.97±11903.40 μL, stroke group when moving the paretic leg=19978.98±16675.67 μL, stroke group when moving the non-paretic leg=11334.38±14893.62 μL).

3.4. DISCUSSION

During locomotor movement, bilateral sensorimotor cortex and cerebellum were activated during pedaling in both stroke and control groups. The main findings were that, in the stroke group, volume of activation of these active areas was reduced, while no intensity of activation difference between groups was observed. The sensorimotor cortex activity was symmetrical, while the cerebellum activity was asymmetrical. This suggests that reduced volume of activation and asymmetrical cerebellum activation might be responsible for locomotor asymmetry. The reduced volume of activation in stroke compared to the control group also suggests that the motor-related brain areas were not abnormally involved in control of locomotion post-stroke. In the non-locomotor task, the volume of activation of the sensorimotor cortex and cerebellum were not different from the control group, whereas the intensity of activation was reduced. This suggests that the brain's functional adaptation after stroke was task-dependent.

3.4.1 Decreased volume of activation could cause impaired locomotion in stroke survivors

We predicted that volume of activation would be increased in stroke subjects, suggesting that motor-related brain areas are abnormally active in control of locomotion post-stroke. Our result was inconsistent with this prediction. We found that volume of activation was decreased, suggesting that (1) the motor-related brain areas are normally involved in controlling locomotion, and (2) the decreased volume of activation of the sensorimotor cortex could contribute to impaired locomotion in stroke subjects. Four mechanisms could account for the reduced volume of activation associated with rhythmic

locomotor movement. First, the reduced volume of activation could be evidence of an increased contribution of spinal centers in controlling locomotion after stroke. It is thought that supraspinal centers in humans normally contribute more to locomotion than the spinal centers (Duysens and Van de Crommert 1998; Yang and Gorassini 2006). However, once a portion of the supraspinal center is injured and cannot function properly, spinal centers may take over some of the supraspinal functions. This idea is supported by previous evidence, which shows that spinal centers can produce simple, immature rhythmic locomotor movements (Duysens and Van de Crommert 1998; Yang, Stephens, Vishram 1998).

Second, the decreased volume of activation of the sensorimotor cortex could reflect low sensory inputs received by sensorimotor cortices. Passive pedaling studies show similar cortical activation during passive and active pedaling (Christensen et al., 2000; Mehta et al., 2012), suggesting that sensory feedback alone (passive pedaling) activates as much of S1 and M1as the sensory feedback plus motor execution (active pedaling). Thus, sensory feedback plays a substantial role in activating locomotor related areas of the brain. A reduction of sensory inputs to the cortex caused by stroke could decrease motor activity. However, one could argue that if the leg representation of the M1 and S1 in the examined subjects is undamaged, then the sensorimotor network should be intact and the reduced volume of activation could not be caused by reduced sensory input to the cortices. One argument is that when the brain is damaged, it results in functional deficits not only in the damaged areas, but also in a portion of the brain connected to, but at a distance from the damaged area, which is referred to as diaschisis

(Feeney and Baron 1986). In this case, the damaged area could be part of the sensory locomotor network.

Third, the reduced volume of activation could reflect the decreased number of neurons in the damaged brain caused by stroke. However, this is unlikely because the same stroke group did not show decreased volume of activation, but rather showed a trend of increased volume of activation when they performed the non-locomotor task. We can potentially conclude that the decreased number of neurons did not cause the observed change in the volume of activation during locomotor movement.

Fourth, the reduced volume of activation could reflect the slower rate of movement. Previous work has shown that the volume of activation (Huda et al., 2008) and intensity of activation (Harada et al., 2009; Mehta et al., 2012) are positively correlated with the rate of movement. However, our stroke subjects pedaled at a non-significantly different rate from the control subjects; therefore the rate of the pedaling cannot account for the volume reduction.

Taken together, we believe that the reduced volume of activation is caused by an increased involvement of spinal locomotor centers and/or a decrease of sensory inputs.

3.4.2 Brain activity symmetry is responsible for locomotor impairments

Symmetrical activity of sensorimotor cortex and cerebellum might be responsible for locomotor impairments. Previous studies have shown that asymmetrical activity in the S1 and M1 (undamaged>damaged) is associated with poor locomotion, and restoration of symmetry in this region is related to improved locomotion (Lin, Chen, Lin 2012; Miyai et al., 2002; Miyai et al., 2003; Miyai et al., 2006). Our result was

inconsistent with the previous findings. We found that the sensorimotor cortex activity was symmetrical, while the cerebellar activity was not symmetrical. One possible mechanism for the symmetrical sensorimotor cortex activity was that the symmetrical activation directly corresponded with the symmetrical locomotion. The stroke subjects recruited in this study were able to perform the pedaling task using both legs equally because the pedaling device was low friction and performed at their own comfortable pace, which is assumed to be easy to perform with minimal effort. Even though this explanation is possible, it is unlikely because one of the main characteristics of the locomotor impairments in stroke group is asymmetry between the two legs (Alexander et al., 2009; Balasubramanian et al., 2007; Bowden et al., 2006; Dettmann, Linder, Sepic 1987; Kautz and Hull 1993; Patterson et al., 2008).

This leads us to the next possible mechanism, which is that the symmetrical sensorimotor cortex activity might be associated with asymmetrical locomotion. Normally, the descending activity of M1 in healthy subjects is a facilitatory signal. In stroke subjects, it is possible that the activation on the undamaged hemisphere was mainly a facilitatory signal, while the activation on the damaged hemisphere was mainly an inhibitory signal, resulting in asymmetrical locomotor pattern. Classen et al. (1997) used TMS to measure the electrical silence period (SP), which reflects cortical inhibitory activity, in stroke subjects. They demonstrated that the SP was abnormally prolonged on the paretic compared to the non-paretic limb, suggesting that the damaged motor cortex is associated with hyperactivity of cortical inhibitory interneurons (Classen et al., 1997). However, fMRI techniques cannot distinguish the type of signals and future studies should be conducted to clarify this issue.

An explanation for the difference between our result and the previous results from Miyai et al. (Miyai et al., 2002; Miyai et al., 2003; Miyai et al., 2006) that shows reduced symmetry of brain activation is that the previous experiments studied the brain activation associated with walking while our study focused on rhythmic locomotor components of walking. Their asymmetrical sensorimotor cortex activation results might be associated not only with the locomotor movement, but also with balance or body weight support components.

Our study is the first study that examined the activation of the cerebellum associated with a locomotor task in stroke subjects. Cerebellum is thought to be involved in walking in the generation of appropriate patterns of limb movement (coordination), dynamic regulation of balance, and adaptation of posture and locomotion through practice (Jayaram et al., 2011; Morton and Bastian 2004). A recent locomotor adaptive learning study using TMS has shown a reduction of cerebellar inhibition to the contralateral M1 after healthy subjects learned a new locomotor pattern on a split-belt treadmill, suggesting that the cerebellum plays a role in an adaptation of locomotion via the cerebellocortical loop of the sensorimotor network (Jayaram et al., 2011). Our result demonstrated that pedaling-related cerebellar activation was greater on the damaged than the undamaged hemisphere, suggesting that the imbalanced activity of cerebellum in the stroke subjects could be compensating for the cortical damage in controlling locomotion. This could be occurring via the cerebellocortical loop of the sensorimotor network (Jayaram et al., 2011; Kelly and Strick 2003; Molinari, Filippini, Leggio 2002), which connects between the cerebellum and the contralateral motor cortex. Therefore, the increased activation of the cerebellum on the damaged hemisphere could facilitate

contralateral (undamaged) cortical activation, which subsequently increases descending motor control to the non-paretic leg. As a result, the performance of the non-paretic leg is enhanced to compensate the performance of the paretic leg during rhythmic locomotor movement, resulting in reduced symmetrical locomotor movement in stroke survivors.

3.4.3 Brain reorganization is task-dependent

Stroke-induced supraspinal adaptations associated with locomotor and non-locomotor tasks were different, suggesting that the brain reorganization is task-dependent. To the best of our knowledge, our study is the first to examine within-subject brain adaptation across tasks in stroke subjects.

Our results demonstrated that volume of activation of the sensorimotor cortex associated with non-locomotor movement was not different between the stroke and control subjects, unlike the locomotor task where the volume of activation was decreased in the stroke compared to the control group. We also found that the intensity of activation of the sensorimotor cortex associated with paretic foot-tapping was decreased in stroke subjects, which again is unlike the locomotor task where the intensity of activation was not different between the groups. An explanation that could account for the different adaptations of the two tasks is that the locomotor and non-locomotor movement is controlled by different underlying mechanisms. Locomotor movement is an automatic action, which is mainly controlled by spinal centers, but requires constant supraspinal inputs for maintaining the ongoing movement (Jain et al., 2012; Petersen et al., 2001). However, non-locomotor movement, which is not an automatic movement, might require higher levels of involvement from the supraspinal centers than automatic

movement. Different participation in the supraspinal control between the two tasks might cause different brain adaptations after stroke.

3.4.4 Brain hemisphere dominance could influence the asymmetry of the brain activation in control subjects

Brain hemisphere dominance could have an impact on the lateralization of the brain activation. Previous work using fMRI and NIRS has shown greater activity in the dominant hemisphere than the non-dominant hemisphere regardless of unilateral or bilateral movement tasks (Hamzei et al., 2003; Huda et al., 2008; Miyai et al., 2001). The asymmetry in these studies was thought to be an effect of hemisphere dominance (Hamzei et al., 2003; Huda et al., 2008; Kapreli et al., 2006; Nirkko et al., 2001). Consistent with the previous findings, our results showed lateralized brain activations in the sensorimotor cortex for the control group toward the dominant hemisphere [eight out of our nine control subjects were right-handed]. Although as a group the laterality index was significantly different from zero, the mean value was very small (LI=0.05), and subsequently the activation could be considered symmetrical (Springer et al., 1999). In the stroke subjects, the symmetrical ratio measured by LI was computed as the amount of activation in the damaged compared to the undamaged hemisphere. Dominance in stroke subjects was equally mixed with 6 subjects having left and 6 subjects having right-dominant hemispheres, unlike the control group who had more left compared to right hemisphere dominant subjects. Therefore, it is possible that the effect of the brain dominance was suppressed in the stroke group.

3.5 LIMITATION

In this study, the intensity of brain activation was measured as the mean signal change of all the active voxels within each region of interest. The intensity of the voxels located in the middle of the region tends to be greater than the surrounding voxels. Therefore, the mean taken from large clusters might be smaller than the mean from smaller clusters. As a result, it is possible that the different intensity of activation for a given task may not be real if it is not measured from the same cluster size located in the same area. As observed in our results, the mean intensity of activation during foot-tapping taken from a smaller cluster in the control group was significantly greater than the mean signal measured from a larger cluster in the stroke group.

One way that we can solve this problem is to measure maximal or peak signal intensity. However, maximal signal intensity is measured from one voxel, which for our data is likely located close to the edge of the brain, and as a result could be contaminated with edge artifacts. Moreover, any single voxel, regardless of its location, may not be representative of typical activation intensity across the entire region. Therefore, mean signal intensity provides a more representative measure of signal intensity than the maximally activated voxel. Another possible approach is to measure the mean intensity of activation in a cluster of a predetermined size that contains (at is center) the maximally activated voxel. However, because we analyzed the fMRI data for each subject individually, variation in the location of the "center" voxel was high. For example, a subject might have more than one "center" voxel. Alternatively, in different subjects, the "center" voxel might be located in a different sub-area of a brain region. Different sub-regions might have different functions. As a result, "center" voxels in different subjects

could represent functionally different brain regions. In light of the limitations of each approach, we concluded that mean percent signal change across the entire region provided the most appropriate representation of activation intensity.

3.6 CONCLUSION

Rhythmic locomotor movement is one of the main features of walking. The two compensatory brain mechanisms in the stroke group that may contribute to impaired locomotor movement are the lateralized cerebellar activation and the reduced volume of activation. The brain adaptations involved in controlling the pedaling and foot-tapping were different, which could be due to the different underlying levels of brain involvement in the two tasks.

In the next chapter, we examine the relationship between the patterns of brain activity associated with pedaling established in this chapter and stroke-related impairments in locomotor movement.

CHAPTER 4: RELATIONSHIP BETWEEN LOCOMOTOR IMPAIRMENT AND PEDALING-RELATED BRAIN ACTIVITY POST-STROKE

4.1 INTRODUCTION

Understanding the relationship between locomotor-related brain activity and locomotor impairment in stroke survivors could provide insights into the plasticity of the neural control of locomotion. Little is known about the relationship between brain activity and locomotor impairment because of a limited number of locomotor-related brain activation studies. This has been due to technical challenges in measuring brain activation during locomotion. One challenge is that the physical constraints of available brain imaging modalities do not easily accommodate walking. In addition, imaging modalities are generally sensitive to movement, especially head movement, which is difficult to control during motor tasks involving several joints and muscles, such as walking and pedaling.

In our laboratory, we successfully used a pedaling paradigm and functional magnetic resonance imaging (fMRI) to study brain activation associated with rhythmic locomotor movement in stroke survivors. Our results, as shown in Chapter 3 of this dissertation, demonstrated that compared to controls, stroke subjects had reduced volume of activation but no difference in intensity of activation. We also found symmetrical sensorimotor cortex activation between the damaged and undamaged hemispheres, while the activation of the cerebellum was shifted to the damaged hemisphere in the stroke group.

In the present study, we aimed to examine the relationship between measures of pedaling-related brain activation and locomotor performance in stroke subjects. Our

emphasis was on locomotor symmetry and velocity, i.e. pedaling and walking, as these are the main locomotor deficits for this population (Alexander et al., 2009; Balasubramanian et al., 2007; Bowden et al., 2006; Dettmann, Linder, Sepic 1987; Kautz and Hull 1993; Patterson et al., 2008; Perry et al., 1995; Turns, Neptune, Kautz 2007). Therefore, we developed three hypotheses. First, volume of activation is directly correlated to locomotor velocity. Second, symmetrical sensorimotor cortex activity in stroke subjects will result in symmetrical locomotion. Third, locomotor symmetry (non-paretic>paretic leg) will be directly related to the cerebellar activation symmetry (damaged>undamaged hemisphere).

4.2 MATERIALS AND METHODS

In this study, the relationship between locomotor performance and pedaling-related brain activity was examined in stroke survivors. Comparison was made to individuals without stroke. Locomotor performance was examined in both groups during pedaling and walking, after which these data were compared to pedaling-related brain activity recorded with fMRI. The fMRI data were obtained in a prior experiment (Chapter 3).

4.2.1 Subject Selection

The same subjects who completed the fMRI study described in Chapter 3 were examined here. These individuals included 12 stroke survivors (8 females, age 55.1±13.3 years) and 9 healthy controls (6 females; age 53.4±13.1 years). Five stroke subjects had cortical lesions and 7 had subcortical lesions. All stroke subjects had their stroke at least 1.1 years prior to testing. The mean (±SD) time since stroke was 12.91 (±13.47) years. Five out of 12 stroke subjects used a mobility aid such as a cane and/or an ankle-foot orthotic (AFO) to walk. There were 6 stroke subjects with right, 5 stroke subjects with left, and 1 stroke subjects with bilateral hemiparesis (Table 4-1). The definitions of subcortical and cortical lesion are described in Chapter 3. Control subjects had no signs or history of stroke or other neurological impairment. Each subject gave written informed consent according to the Declaration of Helsinki and institutional guidelines at Marquette University and the Medical College of Wisconsin.

Table 4-1. Descriptive characteristics for subjects with stroke.

Subject	Age (years)	Sex	Affected limb	Affected brain area	Time to scan (years)	Fugl-Meyer Score (56)
S01	60	F	R	Cortical	20.4	39
S03	62	F	L	Subcor	8.4	54
S05	56	M	L	Subcor	51.0	43
S06	64	F	R	Subcor	6.5	54
S07	20	F	L	Subcor	19.0	47
S08	73	F	R	Subcor	1.1	52
S10	58	F	L	Cortical	6.1	43
S11	53	F	R	Subcor	17.4	51
S13	46	M	R>L	Subcor	4.4	37
S15	48	M	R	Cortical	8.1	37
S17	65	F	L	Cortical	6.2	26
S19	55	M	R	Cortical	6.4	53

F=female, M=male, R=right, L=left, Cortical=stroke affecting cerebral cortex, Subcortical=stroke affecting subcortical structures.

4.2.2 Measurement of pedaling-related brain activity with fMRI

The procedures for fMRI data collection, processing, and analysis are described in Chapter 3 of this dissertation. Briefly, fMRI was used to examine the volume, intensity, and symmetry of brain activation in the sensorimotor cortex and cerebellum during pedaling. The sensorimotor cortex includs the primary somatosensory area (S1), primary motor area (M1), premotor area (PMA), and supplemental motor area (SMA). The cerebellum included cerebellar lobules IV, V, and VIII. fMRI signals were processed in Analysis of Functional NeuroImages (AFNI) software (Cox 1996) using general linear

modeling on the portion of the blood oxygen level-dependent (BOLD) signal recorded after pedaling stopped, as described previously (Mehta et al., 2009). Significantly active voxels at a familywise error rate of $p<0.05$ were identified using a Monte Carlo simulation (AlphaSim) to set an appropriate cluster size for a given individual voxel p-value. FMRI data were analyzed individually in their original coordinate system to avoid distortion arising from transformation to a standardized coordinate system (See Appendix C for more details).

Volume of activation was defined as the number of significantly active voxels in each brain region multiplied by voxel volume in microliters (μL). Intensity of activation was defined as the average percent signal change from baseline in the active portion of the region of interest. Laterality index in stroke subjects was defined as the difference in volume of activation between the damaged and undamaged sides of the brain as a proportion of total volume of activation on both sides of the brain. Laterality index for control subjects was the difference in volume of activation between the left and right sides of the brain as a proportion of total volume of activation.

4.2.3 Measurement of pedaling performance

4.2.3.1 Instrumentation

A custom-modified bicycle ergometer (EFI Sports Medicine, San Diego, CA) equipped with a frictional flywheel and rigid backboard was used to examine pedaling performance. The backboard was designed to support the subject's pelvis, trunk, and head and was oriented 39 degrees from horizontal. Each pedal was equipped with a 6-

degree of freedom force/torque transducer (ATI Industrial Automation, Apex, NC) that was used to measure shear and normal forces applied to the pedal. Optical position encoders (BEI industrial encoders, Goleta, CA) coupled to crank shaft and the pedal spindles were used record the angular position of the crank and the pedals. Force and position data were recorded at 2000 Hz using a 16-bit analog to digital converter (Micro 1401mkII, Cambridge Electronic Design (CED), Roma, Italy) and Spike2 software (Cambridge Electronic Design (CED), Roma, Italy).

4.2.3.2 Experimental Protocol

Subjects were positioned on the bicycle ergometer with their feet secured to the pedals with toe and heel clips. The tension on the ergometer was adjusted to a subject-selected moderate effort. Subjects were asked to pedal forward at a comfortable rate for approximately 3 minutes. Two minutes of data were collected after subjects achieved a constant pedaling rate. Rest breaks were offered.

4.2.3.3 Quantification of pedaling performance

Pedaling performance was characterized by mean pedaling rate and symmetry of mechanical work produced by the lower limbs. The mechanical work produced by each limb was computed as follows: The normal and shear forces recorded from each pedal were used in conjunction with crank and pedal position data to derive the tangential forces applied to each crank arm. These tangentially oriented forces created a torque (referred to as crank torque) about the crank center that contributed to angular acceleration or deceleration. The crank torque produced by each limb was plotted as a

function of crank angle for each pedaling cycle (Figure 4-1). The total area under the resulting curve was the net mechanical work. The area under the positive and negative portions of the curve was also computed to measure propulsive and retarding work. These values were referred to as positive and negative work, respectively. For each subject, the positive, negative, and net mechanical work produced by each limb was computed for each cycle. Average values for each subject were then computed and used in subsequent analysis.

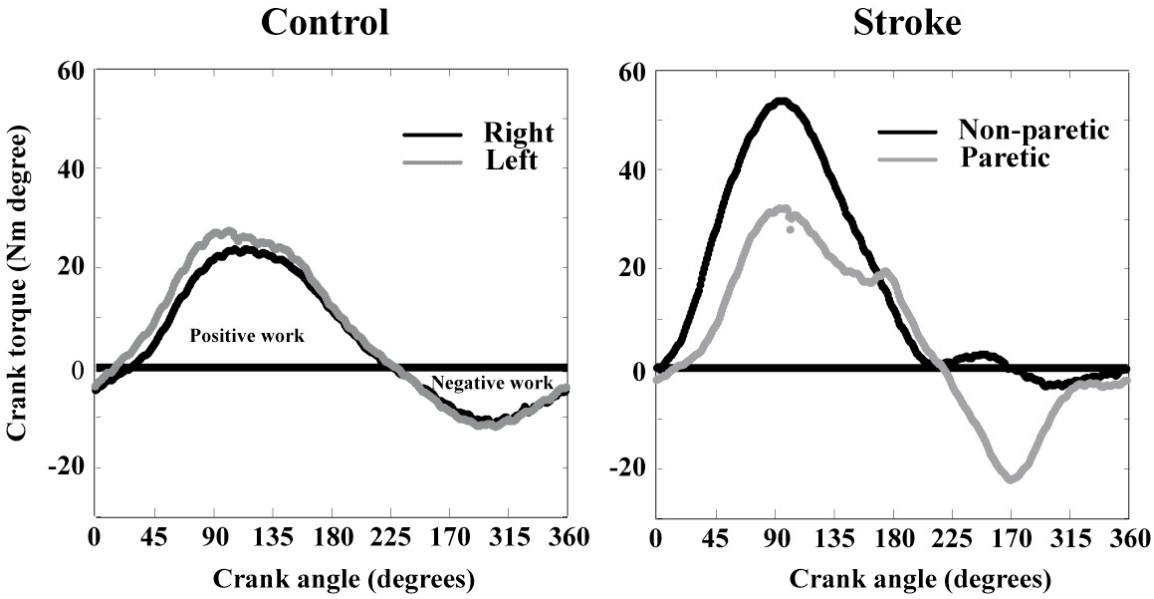

Figure 4-1. Crank torque versus crank angle for the right and left leg of a representative control subject and for the non-paretic and paretic leg of a representative stroke survivor.

Symmetry of mechanical work produced during pedaling (PEDSYM) was calculated for stroke subjects as the ratio of paretic leg work to total work, expressed in percent (Eq. 3). Hence, a value of 50% would indicate perfect symmetry of work output between the paretic and non-paretic leg. The same calculation was used in the control group using work produced by the right leg in the numerator (Eq. 4). PEDSYM was computed for positive (PEDSYM(+)), negative (PEDSYM(-)), and net mechanical work (PEDSYM(-)).

$$\text{PEDSYM(Stroke)} = \frac{\text{Work(paretic)}}{\text{Work(paretic)} + \text{Work(non - paretic)}} \times 100 \qquad \text{Eq.3}$$

$$\text{PEDSYM(control)} = \frac{\text{Work(right)}}{\text{Work(right)} + \text{Work(left)}} \times 100 \qquad \text{Eq.4}$$

Each the dependent variable of pedaling (PEDSYM and pedaling rate) was computed for each pedaling cycle. The mean of each subject's performance was used for group analysis.

4.2.4 Measurement of walking performance

4.2.4.1 Instrumentation

A motion capture system (Vicon Motion Systems Ltd., Oxford, England) with six cameras (model Vicon Mx-3+) was used to measure the spatiotemporal profile of the lower extremities during walking, namely swing and stance phase time and step length. Two force plates (Advanced Mechanical Technology Inc., model OR6-7-1000, Watertown, MA) mounted under a walkway were used to record anteroposterior ground

reaction forces (AP-GRF) during walking. The sampling frequency of the camera system was 100 Hz. Heel markers were used to define the phases of each gait cycle. Force data were acquired at 1000 Hz.

An acquisition system (MX Giganet, Oxford, England) was configured with a 64-channel analog card to connect and sync signals from the force plates and the cameras. Vicon Nexus software was used to capture the heel markers during walking and to process the AP-GRFs.

4.2.4.2 Experimental Protocol

In preparation for recording the spatiotemporal and kinetic characteristics of walking, subject's weight was measured. Reflective markers were attached bilaterally with double-sided tape to the posterior aspect of the calcaneus. If an orthosis was required to walk safely, the markers were placed on the shoes. A safety harness was provided, if needed. Subjects were asked to walk at a self-selected comfortable velocity along a 6-m walkway without the use of walking aids, if possible. We recorded 15-100 walking trials for each subject to ensure that we obtained approximately ten trials in which the foot contacted the force plate. Rest breaks were offered frequently to minimize fatigue.

4.2.4.3 Quantification of walking performance

To eliminate the influences of acceleration and deceleration at the beginning and end of each trial, only recordings obtained mid-trial were used in analysis.

Walking performance was characterized by velocity and between-limb symmetry

with respect to the kinematics and kinetics of lower limb movement. Walking velocity was calculated by a stride length (m) divided by a stride time (s) with a unit of meters per second (m/s). The temporal symmetry of the lower limbs in stroke subjects was represented by the temporal symmetry ratio (TSR) which was defined as the ratio of the swing phase time to the stance phase time of the paretic to the non-paretic leg. (Eq. 5). Swing phase was defined as toe-off to heel-strike of the same foot. Stance phase was defined as heel-strike to toe-off of the same foot. Spatial symmetry in stroke subjects was represented by step length ratio (SLR), which was the ratio of the paretic leg to the non-paretic leg step length. (Eq. 7). Step length was defined as the distance between heel-strike of one foot and heel-strike of the other foot. Temporal symmetry ratio and SLR calculations were also done in the control group where right leg data was used in the numerator. (Eq. 6 and 8). These measures were selected because they are sensitive to stroke-related locomotor impairments (Alexander et al., 2009; Patterson et al., 2008).

$$\text{TSR (Stroke)} = \frac{\text{swing time (paretic)/ stance time (paretic)}}{\text{swing time (non - paretic) / stance time (non - paretic)}} \qquad \text{Eq. 5}$$

$$\text{TSR (Control)} = \frac{\text{swing time (right)/ stance time (right)}}{\text{swing time (left) / stance time (left)}} \qquad \text{Eq. 6}$$

$$\text{SLR (Stroke)} = \frac{\text{step length (paretic)}}{\text{step length (non - paretic)}} \qquad \text{Eq. 7}$$

$$\text{SLR (Control)} = \frac{\text{step length (right)}}{\text{step length (left)}} \qquad \text{Eq. 8}$$

Between-limb symmetry of walking kinetics (KINSYM) was calculated from the propulsive, braking, and net impulses generated by each leg as the ratio of the paretic leg impulse to the sum of the impulses generated by the paretic and non-paretic leg. Values were expressed as percent, with 50% representing perfect between-limb symmetry. (Eq. 9). The same calculations were done for the control group where the right leg impulse was used in the numerator. (Eq. 10).

$$\text{KINSYM (Stroke)} = \frac{\text{impulse (paretic)}}{\text{impulse (paretic)} + \text{impulse (non - paretic)}} \times 100 \qquad \text{Eq. 9}$$

$$\text{KINSYM (Control)} = \frac{\text{impulse (right)}}{\text{impulse (right)} + \text{impulse (left)}} \times 100 \qquad \text{Eq. 10}$$

Impulses were computed from AP-GRFs as follows. AP-GRFs were filtered using a fourth-order zero lag Butterworth low-pass filter at with a 20 Hz cutoff frequency. These data were then normalized to bodyweight. AP-GRFs were plotted as a function of the percent stance phase time of each foot (Figure 4-2). The area under the resulting curve yielded the propulsive (positive area) and braking (negative area) impulses. The sum of the propulsive and braking impulses was referred as the net impulse (Bowden et al., 2008). KINSYM was computed for propulsive (KINSYM(+)), braking (KINSYM(-)), and net impulses (KINSYM(-)).

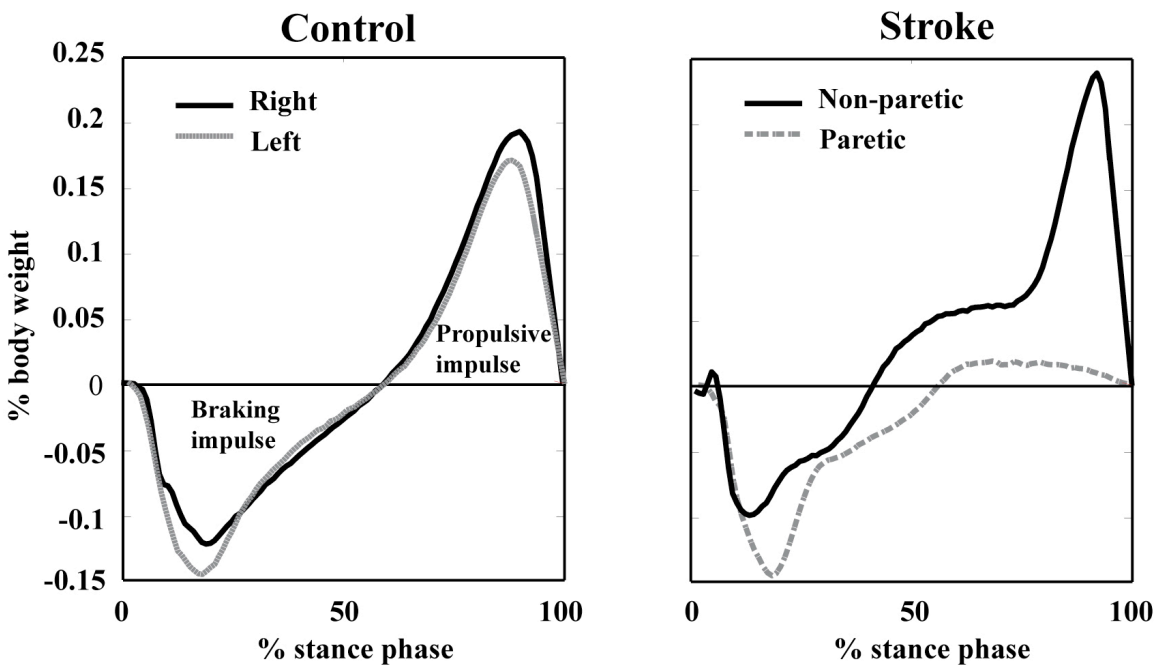

Figure 4-2. Anterioposterior ground reaction force (AP-GRF) showed as percentage of body weight versus percentage of stance phase for the right and left leg of a representative control subject and for the non-paretic and paretic leg of a representative stroke survivor.

Each dependent variable of walking (TSR, SLR, KINSYM, and walking velocity) was computed for each successful trial. The mean of each subject's responses was used for group analysis.

4.2.5 Statistical analysis

Group means (±SD) were computed for each of the 10 dependent variables describing pedaling and walking performance: pedaling rate, walking velocity, PEDSYM(+), PEDSYM(-), PEDSYM(net), TSR, SLR, KINSYM(+), KINSYM(-), and KINSYM(net). Independent t-tests were used to test for between-group differences (control versus stroke group) for each dependent variable. Volume, intensity, and laterality index (LI) of activation previously reported in Chapter 3 were used to examine

the association between brain activity and pedaling and walking performance in stroke and control subjects. Specifically, we examined the following relationship: LI and pedaling symmetry, LI and walking symmetry, intensity of activation and pedaling rate, volume of activation and pedaling rate, intensity of activation and walking velocity, volume of activation and walking velocity.

Pearson correlation coefficients (r) were used to examine the strength of these relationships. Finally, a paired t-test between the rate of pedaling during the fMRI experiment and the rate of pedaling during the ergometer experiment was performed to assure that pedaling performance during the two sessions was comparable. All statistical analyses were completed in SPSS (SPSS Inc, Chicago, IL), and effects were considered significant at $P<0.05$. Quantitative values are reported as mean ±1 standard deviation (SD).

4.3 RESULTS

All subjects performed the pedaling task on the ergometer as directed. During the walking session, 2 stroke subjects wore an ankle-foot orthosis (AFO) and shoes, 1 stroke subject used a cane, and 1 stroke subject used a fall-arrest harness. One stroke subject demonstrated insufficient step length required to record AP-GRFs, as the paretic and non-paretic feet must land on different force plates. Therefore, the kinetic characteristics of walking were computed for only 11 stroke subjects.

4.3.1 Pedaling and walking performance

4.3.1.1 Symmetry of pedaling and walking

As shown in Table 4-2 and Figure 4-3, pedaling and walking performance in stroke subjects was significantly less symmetrical than control subjects as evidenced by significant between-group differences in PEDSYM(+), PEDSYM(-), PEDSYM(net), TSR, KINSYM(+), and KINSYM(-) ($P \leq 0.007$). There was also a trend to suggest reduced symmetry in stroke subjects with respect to SLR and KINSYM(net), but these differences did not reach statistical significance ($P \geq 0.191$).

Table 4-2. Group mean (SD) values for pedaling on the ergometer and walking symmetry.

		Control	Stroke	P-value
Pedaling	PEDSYM(+) (%)	48.72 (1.87)	38.86 (5.29)	<0.001
	PEDSYM(-) (%)	47.96 (2.04)	67.49 (11.62)	<0.001
	PEDSYM(net) (%)	49.69 (4.08)	11.09 (24.04)	<0.001
Walking	TSR	0.97 (0.05)	1.38 (0.43)	0.007
	SLR	0.99 (0.03)	1.43 (1.10)	0.191
	KINSYM(+)(%)	51.40 (3.61)	37.00 (13.57)	0.006
	KINSYM(-)(%)	49.60 (2.69)	59.78 (8.53)	0.003
	KINSYM(net) (%)	35.13 (56.14)	19.79 (356.4)	0.604

P-value=P-value for between-group comparisons (control versus stroke group), PEDSYM(+), PEDSYM(-), and PEDSYM(net) =symmetry of positive, negative, and net mechanical work, respectively, produced during pedaling, TSR=temporal symmetrical ratio, SLR=step length ratio, KINSYM(+), KINSYM(-), and KINSYM(net)=between-limb symmetry of propulsive impulse, braking impulse, and net impulse, respectively.

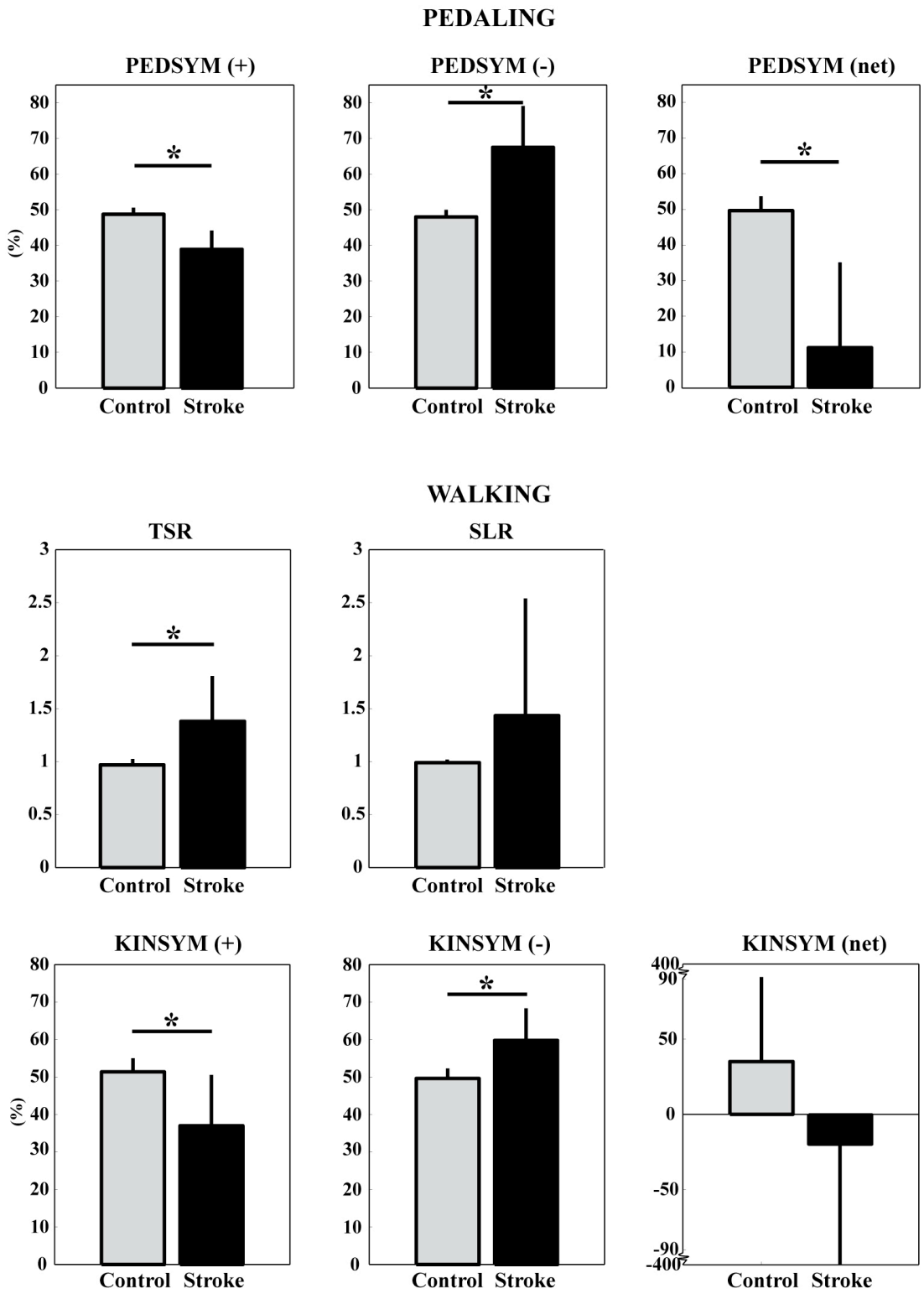

Figure 4-3. Bar plots showing pedaling and walking symmetry in individuals with and without stroke. Values are group means (±SD). Asterisks indicate significant between-group differences at $P<0.05$. See text for definitions of dependent variables.

4.3.1.2 Pedaling rate and walking velocity

As shown in Table 4-3, there was no difference between the control and stroke groups with respect to the rate of pedaling. Despite not controlling workload among subjects, there was also no between-group difference in the total work completed across the pedaling cycle (control group=51.43±23.53 Nm degree, stroke group=52.14±32.21 Nm degree, P=0.954). Within each group, there was no difference in the rate of pedaling between the fMRI session and the ergometer session (P=0.300 for control group, P=0.539 for stroke group). Walking velocity was significantly slower in stroke as compared to control subjects.

Table 4-3. Group mean (SD) values for pedaling rate on the ergometer and walking velocity.

	Control	Stroke	P-value
Pedaling rate (Hz)	0.88 (0.08)	0.78 (0.16)	0.084
Walking velocity (m/s)	1.00 (0.08)	0.80 (0.27)	*0.031*

P-value=P-value for between-group comparisons (control versus stroke group).

4.3.2 Relationships between the pedaling-related brain activity and locomotor performance

In the stroke group, there was a significant positive correlation between pedaling rate and intensity of activation in the sensorimotor cortex and cerebellum combined (SMC-Cb) and in sensorimotor cortex alone. When intensity of activation was examined for cerebellum alone, the correlation with pedaling rate did not reach statistical significance. We also found no significant correlation between pedaling rate and volume of brain activation among stroke subjects in any brain region examined. In the stroke group, there was no significant correlation between walking velocity and intensity or volume of activation in any region examined. In the control group, there was no significant correlation between pedaling rate or walking velocity and intensity or volume of activation for any region of interest. See Table 4-4 and Figure 4-4.

Table 4-4. Correlation coefficients (r) and P-values describing the relationship between the intensity or volume of activation and pedaling rate and waling velocity in control and stroke group.

		Control				**Stroke**			
		Rate of pedaling		**Walking velocity**		**Rate of pedaling**		**Walking velocity**	
		r	P	r	P	r	P	r	P
INT	SMC-Cb	0.052	0.894	0.438	0.238	0.704	*0.011*	-0.009	0.979
	SMC	-0.119	0.760	0.526	0.145	0.646	*0.023*	-0.078	0.810
	cerebellum	0.189	0.626	0.276	0.472	0.351	0.263	0.108	0.738
VOL	SMC-Cb	-0.029	0.940	0.176	0.650	0.416	0.178	-0.165	0.608
	SMC	-0.060	0.878	0.203	0.600	0.390	0.21	-0.152	0.636
	cerebellum	0.077	0.843	0.074	0.849	0.189	0.556	-0.081	0.803

r=correlation coefficient, P=P-value of the corresponding correlation analysis, INT= intensity of activation, VOL=volume of activation, SMC-Cb=sensorimotor cortex and cerebellum combined, SMC=sensorimotor cortex. Italic indicates significant correlation.

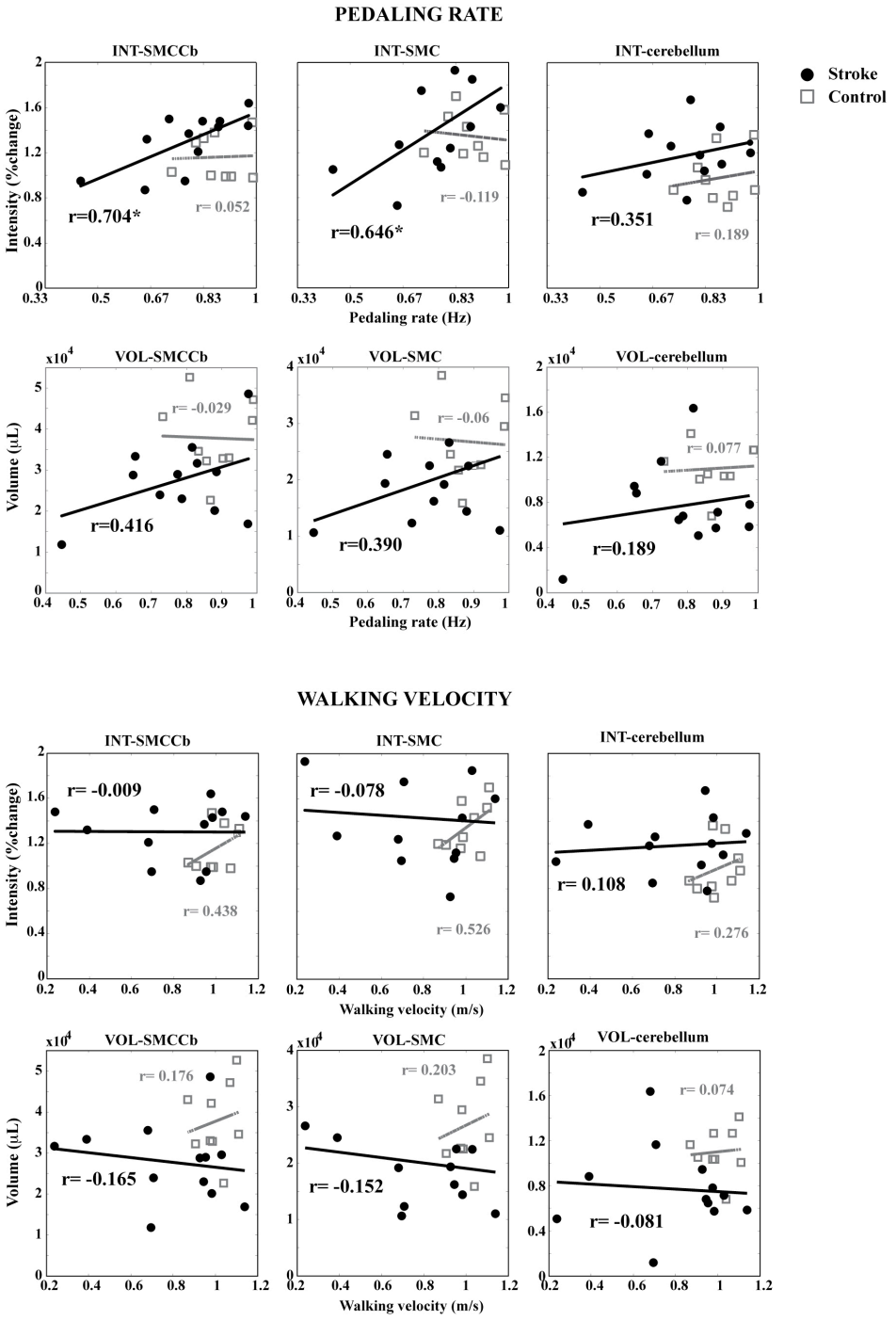

Figure 4-4. Scatter plots representing the correlations between pedaling rate and walking velocity and the volume and intensity of brain activity in control and stroke groups. Each plot represents a different brain region. Black and gray r values represent the correlation coefficients of the stroke and control group, respectively. Black and gray lines represent the least square fit of the stroke and control group, respectively. SMC=sensorimotor cortex, SMC-Cb=sensorimotor cortex and cerebellum combined, r=correlation coefficient. Asterisks indicate significance at $P<0.05$.

With respect to symmetry of brain activity and locomotor performance, there were no significant correlations between the LI in the sensorimotor cortex or cerebellum and any measure of pedaling or walking symmetry in the stroke or control group. (Figure 4-5 and Table 4-5).

Table 4-5. Correlation coefficients and P-values between LI of sensorimotor cortex and cerebellum and the PEDSYM, TSR, SLR, and KINSYM for control and stroke groups.

		Control				Stroke			
		LI-SMC		LI-Cerebellum		LI-SMC		LI-Cerebellum	
		r	P	r	P	r	P	r	P
Pedaling	PEDSYM(+) (%)	-0.094	0.810	-0.490	0.181	-0.168	0.601	-0.286	0.368
	PEDSYM(-) (%)	-0.126	0.747	0.134	0.731	-0.156	0.628	0.125	0.698
	PEDSYM(net) (%)	0.045	0.907	-0.633	0.067	-0.414	0.181	-0.340	0.280
Walking	TSR	0.219	0.572	-0.143	0.713	0.159	0.623	0.487	0.108
	SLR	-0.157	0.687	0.250	0.516	-0.174	0.589	0.321	0.308
	KINSYM(+) (%)	0.161	0.679	0.261	0.497	-0.291	0.385	-0.482	0.133
	KINSYM(-) (%)	-0.232	0.547	-0.265	0.491	-0.257	0.445	-0.375	0.256
	KINSYM(net) (%)	-0.033	0.933	-0.34	0.371	-0.124	0.701	-0.361	0.249

LI-SMC=laterality index of sensorimotor cortex, LI-Cerebellum=laterality index of cerebellum, r=correlation coefficient, P=P-value of the corresponding correlation analysis, PEDSYM=symmetry of positive mechanical work produced during pedaling, TSR=temporal symmetrical ratio, SLR=step length ratio, KINSYM=between-limb symmetry of walking kinetics.

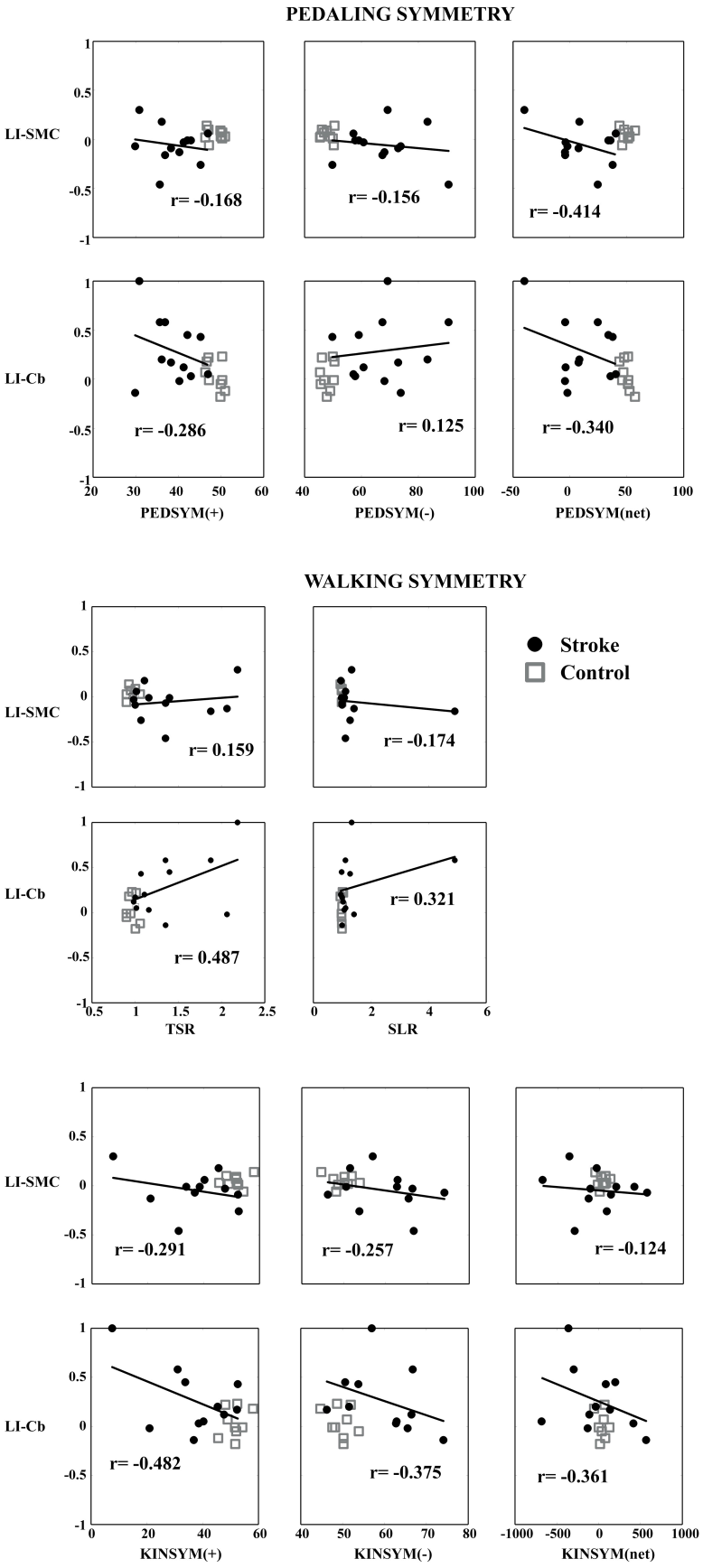

Figure 4-5. Scatter plots represent correlations of the LI of sensorimotor cortex and cerebellum and the pedaling and walking symmetry. Lines represent least square fit of the stroke group. LI-SMC=laterality index of sensorimotor cortex, LI-Cb=laterality index of cerebellum, r=correlation coefficient. PEDSYM(+), PEDSYM(-), PEDSYM(net) = symmetry of positive work, negative, and net work, respectively. TSR=temporal symmetrical ratio, SLR=step length ratio. KINSYM(+), KINSYM(-), KINSYM(net)=symmetry of propulsive, braking, and net impulse, respectively.

4.4 DISCUSSION

The most prominent finding from our previous brain activation study (Chapter 3) was that the stroke group displayed reduced volume of activation associated with pedaling. In this aim, stroke group demonstrated slower locomotor velocity and locomotor asymmetry. Taken together, this suggests that impaired locomotion was associated with reduced volume of activation. In this aim, we also found that intensity of brain activation and the rate of pedaling showed a positive relationship, suggesting that increased intensity of activation in active brain areas may compensate for reduced volume of activation in the production of hemiparetic locomotion. Both control and stroke subjects showed symmetrical sensorimotor cortex activity, however the stroke subjects did not demonstrate symmetrical locomotion. While the control subjects demonstrated symmetrical locomotion that was directly associated with symmetrical sensorimotor cortex activity, the asymmetry of locomotion in the stroke subjects was not directly associated with their sensorimotor cortex activity. We also found no correlation between the cerebellar activity symmetry and locomotor symmetry, suggesting that increased cerebellar activation on the damaged hemisphere was not directly responsible for the greater activity of the non-paretic leg in compensation for the paretic leg.

4.4.1 Locomotor impairments in stroke survivors

Slow velocity and asymmetrical patterns are the main deficits in hemiplegic locomotion. During pedaling, previous studies have shown that stroke subjects are able to pedal at a comparable rate to control subjects, but the mechanical work exertion between the two legs is asymmetrical (Brown, Kautz, Dairaghi 1997; Kautz and Brown

1998). Our result was consistent with the previous findings for both rate and asymmetry of mechanical work done. The stroke subjects could pedal at a similar rate to the control subjects because pedaling is a coupled action that requires both legs to move the crank. This allows the stronger leg to do compensatory work for the weaker leg to accomplish a given rate, especially at a low load, where the non-paretic leg could solely accomplish the task (Chen et al., 2005).

The asymmetrical work generation between the two legs is characterized by less positive work and more negative work generated by the paretic leg, resulting in less net mechanical work compared to the non-paretic leg. Positive work reflects a propulsion force to propel the crank against the load (Kautz and Hull 1993), which is confounded by the weight of the leg, load of the bike, and resistance from the opposite leg. In stroke subjects, the lesser positive work produced by the paretic leg could be caused by a combination of reduced knee extensor muscle activity and phase-advanced knee flexor muscle activity during the extension phase of pedaling cycles (Chen et al., 2005; Schindler-Ivens, Brown, Brooke 2004). Negative work reflects a resistance to the crank propulsion (Kautz and Hull 1993). Schindler et al. (2004) suggested that in stroke subjects the greater negative work produced by the paretic leg could be caused by a prolonged activity of knee and ankle extensor muscles during the flexion phase of pedaling cycles (Schindler-Ivens, Brown, Brooke 2004).

During walking in stroke subjects, previous studies have shown slow velocity (Hsu, Tang, Jan 2003; Perry et al., 1995; Turns, Neptune, Kautz 2007), asymmetry of spatiotemporal characteristics (Alexander et al., 2009; Balasubramanian et al., 2007; Hsu, Tang, Jan 2003; Lin et al., 2006; Patterson et al., 2008; Turns, Neptune, Kautz 2007), and

asymmetry of gait kinetics (Balasubramanian et al., 2007; Turns, Neptune, Kautz 2007). Our findings were mostly in an agreement with the previous work. Our stroke subjects walked significantly slower than the control subjects, and less symmetrical with the exception of the spatial characteristic of walking.

The asymmetrical temporal characteristic of walking in stroke subjects, measured by TSR, is caused by increased stance phase time of the non-paretic leg accompanied with decreased stance phase time of the paretic leg (Alexander et al., 2009; Patterson et al., 2008). This could be caused by a weakness of the paretic leg during stance phase. Therefore in stroke subjects, to maintain a given velocity the non-paretic leg has to stay in the stance phase longer, allowing the paretic leg to gain some distance during the swing phase.

Our stroke subjects demonstrated symmetrical SLR, similar to the control subjects. Previous reports demonstrated a mixed result of either asymmetry or symmetry in SLR. The asymmetrical SLR could be a longer or shorter paretic step length compared to the non-paretic leg (Balasubramanian et al., 2007; Dettmann, Linder, Sepic 1987; Dettmann, Linder, Sepic 1987; Hsu, Tang, Jan 2003; Turns, Neptune, Kautz 2007). The mixed results from the previous research suggest that step length might not be an essential indicator for the hemiparetic locomotion.

Symmetry of gait kinetics was measured using the calculated impulses. Stroke survivors showed significantly increased braking impulse and decreased propulsive impulse on the paretic leg, resulting in a negative net impulse (Bowden et al., 2008; Turns, Neptune, Kautz 2007). Our results were consistent with this finding. The propulsive impulse is the net positive, anteriorly directed force generated by the legs to

accelerate (propel) the body center of mass forward (Turns, Neptune, Kautz 2007). Therefore, reduction of this impulse could result in slower walking velocity (Bowden et al., 2008). The braking impulse is the net negative, posteriorly directed force generated to decelerate the body center of mass (Turns, Neptune, Kautz 2007). An increase of this impulse suggests an increased impact at heel-strike.

These findings lead us to a conclusion that our stroke subjects demonstrated residual locomotor deficits, which can be measured during both pedaling and walking.

4.4.2 Relationship between the brain activation and the locomotor impairments

4.4.2.1 Volume of activation and the locomotor velocity

We hypothesized that if reduced volume of activation was responsible for impaired locomotor velocity, then volume of activation would be directly related to locomotor velocity. Inconsistent with our prediction, volume of activation was not correlated to locomotor velocity. A possible explanation could be that the entire supraspinal network of neurons involved in locomotor velocity would be equally active for similar perceived difficulty in pedaling for each stroke subject, as they were asked to pedal at their comfortable pace. Dobkin et al. (2004) demonstrated that increasing volume of activation associated with foot-tapping in stroke survivors stopped after two weeks of body weight support treadmill training, even though walking velocity continued improving (Dobkin et al., 2004). This suggests that for each individual stroke survivor, once the maximum number of neurons were recruited the volume of activation would not be altered, even though the behaviors continuing to change. On the other hand, it is possible that the brain tissue that was active in the control subjects but suppressed in the

stroke subjects might be important in controlling locomotion. The reduced activity of the tissue might cause locomotor deficits in stroke subjects. We conclude that even though volume of activation did not reveal a direct relationship with the locomotor velocity, as a group volume of activation showed the most prominent difference between the control and stroke subjects, implying that impaired locomotion could be associated with reduced volume of activation.

Surprisingly, intensity of sensorimotor cortex activation and the rate of pedaling showed a positive relationship. This surprised us because the intensity of sensorimotor cortex activation associated with pedaling was not different between the control and stroke groups, but the positive relationship with pedaling rate was shown only in the stroke and not in control group, suggesting that this relationship might involve the reduced volume of activation that has been shown in the stroke group. It could be implied that increased intensity of activation in active brain areas may compensate for reduced volume of activation in the production of hemiparetic locomotion. Supporting evidence came from a previous study that demonstrated a positive correlation between intensity of the brain activation and movement velocity. Miyai et al. showed that increased brain signal during treadmill waking is correlated with greater cadence when a body weight support was applied to the stroke subjects (Miyai et al., 2006). Increased intensity of activation is thought to reflect an increased neuronal synaptic activity (Logothetis et al., 2001), and as a result enhances the neural firing frequencies in the brain in order to generate higher muscle forces to increase movement velocity (Lutz et al., 2005; Rao et al., 1996). This scheme was supported by a single cell recording study in monkeys, which showed that the firing rate of M1 neurons is positively correlated with

the increased force and velocity needed to produce faster finger movement (Humphrey 1972). Therefore, our results suggest that neurons in the sensorimotor cortex increased their synaptic activity and/or firing frequency, which is responsible for the increased rate of pedaling in stroke survivors.

4.4.2.2 Brain activation symmetry and the locomotor symmetry

Our hypotheses predicted that if the symmetrical sensorimotor cortex activity in the stroke subjects is directly related to the locomotor symmetry, then stroke subjects would demonstrate symmetrical locomotion; that if increased cerebellar activation on the damaged hemisphere is responsible for increased descending command to the non-paretic leg, then locomotor symmetry (non-paretic>paretic leg) would be directly related to the cerebellar activation symmetry (damaged>undamaged hemisphere). The former hypothesis was partially based on observations from the previous NIRS work, which showed that improved locomotor symmetry was directly correlated with enhanced symmetry of sensorimotor cortex activity in stroke survivors (Lin, Chen, Lin 2012; Miyai et al., 2002; Miyai et al., 2003; Miyai et al., 2006). Inconsistent with the first prediction, we observed that stroke subjects produced asymmetrical locomotion, suggesting that the symmetrical sensorimotor cortex activity during pedaling was not directly associated with the symmetrical locomotion. In addition, we found that the control subjects produced symmetrical sensorimotor cortex activation and balanced locomotion, suggesting that either symmetrical sensorimotor cortex activation does not play a role in symmetry of locomotion or that between groups the sensorimotor cortex controls symmetry of locomotion through different mechanisms.

An explanation that could account for the different contribution of sensorimotor cortex between the stroke and control subjects was that in stroke subjects, their brain injury could cause changes in the excitatory and inhibitory signals both for the descending commands and the interhemispheric interactions. Our hypothesis that we would find a direct correlation between the brain activity symmetry and the locomotor symmetry was based on an assumption that the brain activation represents excitatory descending commands. However, previous evidence has shown that motor cortex on the damaged hemisphere is associated with hyperactivity of cortical inhibitory interneurons (Classen et al., 1997), resulting in a distinct patterns of motor abnormalities. This suggested that the asymmetrical locomotion could be the exaggerated inhibitory activity from the motor cortex. Furthermore, the inhibitory signal between the two hemispheres could be altered after stroke. During normal motor tasks excitatory signals are sent from M1 as a down-regulation in order to generate a movement, but at the same time the M1 also sends an interhemispheric inhibition signal to the other hemisphere to inhibit its excitation command in order to allow dissociated movement between limbs (Daskalakis et al., 2002; 2002; Di Lazzaro et al., 1999). The balance between the two hemispheres is important in maintaining the symmetrical movement. However, previous evidence has shown abnormally high interhemispheric inhibitory drive from the M1 on the undamaged to the damaged hemisphere during a voluntary finger movement in stroke subjects (Murase et al., 2004). This process could be more complicated with motor movements that involve more components, such as rhythmic locomotor movement, where multiple joints of both legs are moving at the same time in a reciprocal, alternating fashion. fMRI shows the active brain areas with signal intensity, but it does not identify if the signal is

excitatory or inhibitory. We conclude that in stroke subjects, symmetrical sensorimotor cortex activation does not directly correlate with locomotor symmetry, but the activity seen is a consequence of changes in the excitatory and inhibitory commands after stroke. Further studies are needed to enhance our understanding of this issue.

Our finding was inconsistent with the second prediction as well. We found that no correlation existed between lateralized cerebellar activity and asymmetrical locomotion, suggesting that the increased cerebellar activation on the damaged hemisphere was not responsible for increased descending commands to the non-paretic leg. An explanation for this lack of correlation could be a change of the type of signals from the cerebellum to the motor cortex. Previous studies in healthy controls have shown that cerebellar activity could either inhibit (Ugawa et al., 1991) or facilitate (Di Lazzaro et al., 1994a; Di Lazzaro et al., 1994b) cortical excitability via the cerebellocortical loop of the sensorimotor network (Coffman, Dum, Strick 2011; Kelly and Strick 2003; Molinari, Filippini, Leggio 2002). No one has previously studied the adaptation of the type of signals between cerebellum and M1 after stroke. For our finding, we believe that the cerebellar activity could be modified after stroke, and become more inhibitory.

4.4.2.3 No correlation between the pedaling-related brain activation and walking velocity

We observed no correlation between the brain activation and the walking velocity. A possible reason could be that walking is composed of rhythmic locomotor movement, balance, weight bearing, and postural control. The brain activation measured during pedaling might be able to reflect mainly the rhythmic locomotor movement component, but not the other confounding components.

4.5 LIMITATION

Our work is based on the idea that an injured brain causes impaired locomotion. However this might be true only at the early stage of stroke. In the chronic stage, it is possible that locomotor impairments might also cause the abnormal brain activation. Unfortunately, our study could not identify which is the primary cause.

4.6 CONCLUSION

Our stroke subjects demonstrated poor locomotor performance and decreased volume of activation measured during pedaling, suggesting that impaired locomotion was associated with reduced volume of activation. Intensity of brain activity was associated with rate of pedaling in stroke subjects, suggesting that increased intensity of activation in the active brain areas may compensate for reduced volume of activation in the production of hemiparetic locomotion. Moreover, the symmetrical sensorimotor cortex activity was shown in both control and stroke groups, but the locomotor symmetry was shown in only the control group, suggesting that the balanced sensorimotor cortex shown in the two groups did not contribute to the control of locomotion in a similar way. There was no correlation between either sensorimotor cortex or cerebellar symmetry and the locomotor impairments, suggesting that both brain areas are not directly responsible for the asymmetrical locomotion. It is possible that stroke causes changes of the types of interacting signals between hemispheres or descending commands. fMRI could show the active brain areas, but it could not identify if the signal is excitatory or inhibitory. Further studies are needed to address the type of brain signals we observed during

pedaling to enhance our understanding of the contribution of different types of the brain signals after stroke.

CHAPTER 5: INTEGRATION OF RESULTS

5.1 SUMMARY OF RESULTS

This chapter summarizes the results obtained from the previously described experiments (Chapter 2-5), outlines the unique contributions this study makes in the area of brain control of locomotion in stroke survivors, and provides suggestions for future research studies building on the present findings.

The results outlined in this dissertation provided evidence that hemodynamic responses post-stroke are different from controls, but these differences are not substantial enough to alter detection of locomotor-related brain activation as measured with blood-oxygenated level dependent-functional magnetic resonance imaging (BOLD-fMRI). The changes of the hemodynamic responses post-stroke were stroke lesion location-dependent and reproducible over days. Volume of brain activation associated with rhythmic locomotor movement in stroke survivors was decreased, while the intensity of activation was not different compared to control subjects. In contrast to the locomotor task, volume of activation associated with non-locomotor movement was not different between groups, but the intensity of activation was increased in stroke subjects. Our stroke subjects demonstrated poor locomotor performance and decreased volume of activation measured during pedaling, suggesting that impaired locomotion was associated with reduced volume of activation. Intensity of activation of brain activity was associated with rate of pedaling, suggesting that increased intensity of activation in the active brain areas may compensate for reduced volume of activation in the production of hemiparetic locomotion.

5.1.1 Changes in hemodynamic responses in stroke subjects do not affect fMRI signal detection in a block experimental design

The first aim, outlined in Chapter 2, was instrumental to this dissertation because it characterized the spatiotemporal characteristics of the hemodynamic responses post-stroke, which is important for fMRI analysis. We were concerned that using a canonical hemodynamic response function might cause inaccurate measurements in our movement-related brain activation data in stroke subjects, as previous studies have shown that using an inappropriate function could degrade the accuracy of brain activation maps (Bonakdarpour, Parrish, Thompson 2007; Kang et al., 2003; Mazzetto-Betti et al., 2010). Our result demonstrated that the spatiotemporal characteristics of hemodynamic responses post-stroke were different from that of control subjects. However, the differences in hemodynamic responses were not substantial enough to necessitate the use of individualized hemodynamic response functions. This is evident because using an individualized hemodynamic response function did not enhance the BOLD-fMRI signal detection of blocked, movement-related brain activity compared to a canonical hemodynamic response function. In addition, we found that the altered hemodynamic responses were more apparent in individuals with cortical as compared to subcortical stroke, suggesting that hemodynamic responses are dependent on stroke lesion location. Lastly, we found that hemodynamic responses were reproducible.

Our results differ from previous studies in that the hemodynamic response post-stroke was not substantially altered. One possible reason for this finding is that our stroke subjects may not have had cerebrovascular occlusive disease. The abnormal hemodynamic response in stroke subjects in the previous studies has been attributed to

changes in neurovascular coupling caused by poor cerebrovascular autoregulation, a characteristic in people with cerebrovascular occlusive disease.

We conclude that both cortical and subcortical stroke do not have a significant impact on the spatiotemporal characteristics of the hemodynamic response that could cause an inaccurate brain activation map. However, stroke-study investigators should be aware that some individual subjects may have an abnormal hemodynamic response, especially ones with a history of cerebrovascular occlusive disease, which could subsequently cause an inaccurate brain activation map. Specifically for our study, our conclusion provides us evidence that we can use the canonical hemodynamic response function to analyze our pedaling-related brain activation data in the next aims.

5.1.2 Decreased brain activity in stroke survivors during pedaling: an fMRI study

In the second aim, we examined changes in brain activation in controlling locomotion post-stroke. Our focus was on the locomotor component of gait, which involves the rhythmic, reciprocal, multi-joint flexion and extension of both lower limbs while negating other factors of walking such as balance and weight-bearing. Our results demonstrated that during locomotor movement, bilateral sensorimotor cortex and cerebellum were activated during pedaling in both stroke and control groups. The main findings were that in the stroke subjects, volume of these active areas were reduced while no significant intensity difference between groups was observed. Stroke subjects also showed symmetrical sensorimotor cortex activity, while the cerebellar activity was asymmetrical. This suggests that reduced volume of activation and asymmetrical cerebellar activation might be responsible for locomotor asymmetry seen in stroke

subjects. The reduced volume of activation in the stroke subjects compared to the control subjects also suggests that the motor-related brain areas were not abnormally involved in control of locomotion post-stroke. In addition, we were able to compare supraspinal control mechanisms across locomotor and non-locomotor task because we also measured brain activity with fMRI during foot-tapping movements. In the foot-tapping task, the volume of activation of the sensorimotor cortex and cerebellum were not different from the control subjects, whereas the intensity was reduced. This suggests that the brain's plasticity after stroke was task-dependent.

The changes in the supraspinal control of locomotion post-stroke could be a compensatory mechanism in response to cortical damage. Increased spinal center control of locomotion may be a result of reduced supraspinal inputs (volume of activation). Spinal centers may be able to produce an immature form of rhythmic locomotor movement, as seen in human infants. Gait impairment therefore may be caused by the decreased supraspinal input and resulting increase in spinal control of locomotion. In addition, supraspinal centers may produce lower fMRI signals as a result of reduced sensory input. The lateralized activity in the damaged hemisphere of the cerebellum may facilitate the primary motor cortex (M1) on the contralesional hemisphere, via corticocerebellar pathways, to enhance the cortical motor drive to the non-paretic leg. As a result, the non-paretic leg may compensate for the poor performance of the paretic leg. We conclude that spinal centers of locomotion and the cerebellum might have a major role in compensatory mechanism for hemiplegic locomotion.

Compared to the locomotor task, the non-locomotor movement (i.e. foot tapping) demonstrated different changes of supraspinal control after stroke. Intensity of activation

was decreased in stroke subjects, while no difference was observed in volume of activation between stroke and control subjects. The sensorimotor cortex was the primary contributor to this phenomenon, with lesser contribution from the cerebellum. The different changes of supraspinal control between the locomotor and non-locomotor task could be attributed to the dissimilarities in the underlying mechanisms of supraspinal control of the two tasks. Locomotion is an automatic rhythmic action, which could mainly be controlled by spinal centers, but requires constant supraspinal inputs for maintaining an ongoing rhythmic, reciprocal movement (Jain et al., 2012; Petersen et al., 2001). In contrast, unilateral paretic foot tapping, which is not an automatic movement, might require higher levels of involvement from the supraspinal centers than automatic movements. Different engagement of the supraspinal control between the two tasks might cause different brain adaptations after stroke.

5.1.3 Relationship between locomotor impairment and pedaling-related brain activity post-stroke

In the last aim (Chapter 4) we investigated the relationship between locomotor impairments, i.e. pedaling and walking, and the pedaling-related brain activity in stroke survivors. Because of our finding in the second aim (Chapter 3) that the brain activation in the stroke subjects was different from the control subjects and our suspicion that the stroke subjects would have impaired locomotion, we were interested to see if the locomotor impairments would be associated with abnormal brain activity during pedaling. Our emphasis was on locomotor velocity and symmetry, i.e. pedaling and walking, as both of these deficits are major locomotor issues for this population.

The most prominent finding from our brain activation study in aim 2 (Chapter 3) was that the stroke group displayed reduced volume of activation associated with pedaling. In aim 3, the stroke subjects demonstrated slower gait velocity and locomotor asymmetry. Relating these two results suggested that impaired locomotion was associated with reduced volume of activation. In aim 3, we also found that intensity of brain activation and the rate of pedaling showed a positive relationship, suggesting that increased intensity in active brain areas may compensate for reduced volume of activation in the production of hemiparetic locomotion. Both control and stroke groups showed symmetrical sensorimotor cortex activity, however the stroke group did not demonstrate symmetrical locomotion. The control group's symmetrical locomotion and brain activity were shown to be directly associated, whereas the asymmetry of locomotion in stroke subjects was not directly associated with their sensorimotor cortex activity. This suggests that either symmetrical sensorimotor cortex activation does not play a role in symmetry of locomotion or that between groups, or the sensorimotor cortex controls symmetry of locomotion through different mechanisms. One possible difference in mechanism is that, in stroke subjects, the types of signals interacting between hemispheres undergo changes in facilitatory or inhibitory functions. It is also possible that the supraspinal center has self-normalized its activation between the two hemispheres, resulting in a balanced activation of the sensorimotor cortex.

We also found no correlation between the cerebellar activity symmetry and the locomotor symmetry, suggesting that increased cerebellar activation on the damaged hemisphere was not directly responsible for the greater activity of the non-paretic leg in compensation for the paretic leg. Similarly, the changes in types of brain signals between

the sensorimotor cortex and cerebellum via cerebrocerebellar pathways might account for not finding any correlation.

5.2 UNIQUE CONTRIBUTIONS

This study has many unique contributions that can be used to further understand supraspinal control of locomotion after stroke. To our knowledge, this is the first study that provides the brain reorganization during locomotion in ST and compares this locomotor-related brain organization to that of the non-locomotor (foot-tapping) brain activation in the same subjects. This allows us to make a direct comparison of the tasks without the confounding factors among different subjects such as lesion size, lesion locations, time post-stroke, age, underlying conditions, and medicine, which can all be contributing factors to brain reorganization after stroke.

Our study characterized the spatiotemporal profiles of the hemodynamic responses in stroke survivors and performed an experiment to ensure that the hemodynamic response functions we used were appropriate for our stroke fMRI studies. To date, this is the first and only study that characterizes the hemodynamic response profile in the leg representation of the sensorimotor cortex collected during foot movement. The sensorimotor cortex also controls locomotion, which is beneficial because our result not only provides the characteristics of hemodynamic response post-stroke for foot movement tasks, but it could also provide useful information for further fMRI locomotor studies. Another contribution drawn from this study was that since the slightly different hemodynamic response post-stroke was reproducible over days, one could save time and cost of the scans by investigating the characteristics of the

hemodynamic response on one day and apply it during analysis on fMRI data collected on different days.

Lastly, this study demonstrated the capability of using fMRI to study locomotion in stroke survivors using an fMRI analysis technique that uses only the portion of the BOLD time-series after movement stopped to identify voxels containing pedaling-related brain activity. This is called the delayed non-movement technique. The success in using this analysis technique has previously been reported in healthy control data (Mehta et al., 2009). For stroke data, this is the first study that shows this technique can also be applied to accommodate movement artifacts created by stroke survivors while pedaling. This new signal processing technique is a significant contribution to the field that will enhance the future of fMRI motor control studies.

5.3 FUTURE RESEARCH

This dissertation outlines evidence of the change in suprapinal control of locomotion in stroke survivors. Given the current experimental paradigm, our result suggests reduced volume of activation was associated with locomotor impairments, but we were unable to identify the exact contributions of each hemisphere (damaged and undamaged) in controlling the locomotion involving the two legs. For example, we found symmetrical activity of sensorimotor cortex in both control and stroke subjects, but while the mechanical work effort between the two legs was symmetrical in the control group, it was asymmetrical in the stroke group. This might suggest that the symmetrical sensorimotor cortex activity in stroke subjects functions or contributes differently than that in control subjects. Therefore, future research will need to address the contribution

of each hemisphere during locomotion. To address this issue, unilateral versus bilateral pedaling paradigm should be studied. Unilateral pedaling should be experimentally set up to maintain the multijoint and alternating flexion and extension components of locomotion, similar to that of bilateral pedaling.

Another issue that we encountered in using the pedaling paradigm was the coupled crank of the bike allowed the non-paretic leg to compensate for the movement for the paretic leg. To be able to investigate the performance of each leg separately, experiments using a split-crank bike should be used.

Also, because the brain is a complex system including inhibition and facilitation mechanisms, fMRI produces maps of active neurons, but is unable to identify whether the activity is inhibitory or facilitatory. Therefore, using transcranial magnetic stimulation (TMS) could provide evidence of inhibitory and facilitatory actions of the motor cortex and might enhance our understanding of the change in supraspinal control of locomotion in stroke survivors.

To confirm that the decreased volume of activation in stroke subjects during pedaling was an effect of stroke and was not due to poor performance, a passive pedaling paradigm should be performed. Previous studies have shown that the volume of activation during active and passive pedaling was not different in control subjects (Mehta et al., 2012). If our finding was an effect of stroke, then the brain activation during passive pedaling should also be reduced.

One common issue in most human post-stroke studies is variations of lesion location and lesion size.. Our study excluded people whose lesion involved the leg representation of the primary motor and sensory area or cerebellum because we did not

have a large enough sample size for each of these groups. An examination of locomotor-related brain reorganization in stroke survivors whose movement-related brain areas are damaged would provide us a further understanding of the brain reorganization and its compensatory connections.

Interestingly, our study demonstrated a slight difference in the spatiotemporal characteristics of hemodynamic responses between control and stroke subjects. Our proposed reason was our stroke subjects did not have cerebrovascular occlusive disease, or if they did the condition had been cured before they participated in our study. This hypoperfusion condition causes impaired autoregulation. To confirm this hypoperfusion condition, an examination of the absolute cerebral blood flow or its velocity using arterial spin labeling (ASL) or transcranial doppler (TCD), respectively, should be performed. Another way to confirm our assumption is by performing an examination of hemodynamic responses in people with cerebrovascular occlusive disease.

This work focused only on the locomotor movement component of walking. However, balance and body weight support are another important problem in stroke populations, and might cause changes in the brain activation. Future studies should investigate the alterations of the brain activity associated with balance and body weight support in the same subjects.

BIBLIOGRAPHY

Aguirre GK, Zarahn E, D'esposito M. (1998). *The variability of human, BOLD hemodynamic responses*. NeuroImage 8(4):360-369.

Alexander LD, Black SE, Patterson KK, Gao F, Danells CJ, McIlroy WE. (2009). *Association between gait asymmetry and brain lesion location in stroke patients.* Stroke 40(2):537-544.

Altamura C, Reinhard M, Vry MS, Kaller CP, Hamzei F, Vernieri F, Rossini PM, Hetzel A, Weiller C, Saur D. (2009). *The longitudinal changes of BOLD response and cerebral hemodynamics from acute to subacute stroke. A fMRI and TCD study.* Neuroscience 10:151.

Ances BM. (2004). *Coupling of changes in cerebral blood flow with neural activity: What must initially dip must come back up*. Journal of Cerebral Blood Flow and Metabolism 24(1):1-6.

Armstrong DM and Drew T. (1984). *Discharges of pyramidal tract and other motor cortical neurones during locomotion in the cat*. The Journal of Physiology 346:471-495.

Balasubramanian CK, Bowden MG, Neptune RR, Kautz SA. (2007). *Relationship between step length asymmetry and walking performance in subjects with chronic hemiparesis*. Archives of Physical Medicine and Rehabilitation 88(1):43-49.

Barbeau H and Rossignol S. (1991). *Initiation and modulation of the locomotor pattern in the adult chronic spinal cat by noradrenergic, serotonergic and dopaminergic drugs.* Brain Research 546(2):250-260.

Barbeau H and Rossignol S. (1987). *Recovery of locomotion after chronic spinalization in the adult cat.* Brain Research 412(1):84-95.

Barbeau H, Chau C, Rossignol S. (1993). *Noradrenergic agonists and locomotor training affect locomotor recovery after cord transection in adult cats.* Brain Research Bulletin 30(3-4):387-393.

Bastiaanse CM, Duysens J, Dietz V. (2000). Modulation of cutaneous reflexes by load receptor input during human walking Experimental Brain Research 135(2):189-198.

Belanger M, Drew T, Provencher J, Rossignol S. (1996). *A comparison of treadmill locomotion in adult cats before and after spinal transection*. Journal of Neurophysiology 76(1):471-491.

Bonakdarpour B, Parrish TB, Thompson CK. (2007). *Hemodynamic response function in patients with stroke-induced aphasia: Implications for fMRI data analysis*. NeuroImage 36(2):322-331.

Bowden MG, Balasubramanian CK, Behrman AL, Kautz SA. (2008). *Validation of a speed-based classification system using quantitative measures of walking performance poststroke*. Neurorehabilitation and Neural Repair 22(6):672-675.

Bowden MG, Balasubramanian CK, Neptune RR, Kautz SA. (2006). *Anterior-posterior ground reaction forces as a measure of paretic leg contribution in hemiparetic walking.* Stroke 37(3):872-876.

Boynton GM, Engel SA, Glover GH, Heeger DJ. (1996). *Linear systems analysis of functional magnetic resonance imaging in human V1.* The Journal of Neuroscience 16(13):4207-4221.

Brown DA, Kautz SA, Dairaghi CA. (1997). *Muscle activity adapts to anti-gravity posture during pedalling in persons with post-stroke hemiplegia.* A Journal of Neurology 120:825-837.

Brown TG. (1911). *The intrinsic factors in the act of progression in the mammal.* Proceedings of the Royal Society B: Biological Sciences 84(572):308-319.

Burke D, Hicks RG, Stephen JP. (1990). *Corticospinal volleys evoked by anodal and cathodal stimulation of the human motor cortex*. The Journal of Physiology 425:283-299.

Bussel B, Roby-Brami A, Azouvi P, Biraben A, Yakovleff A, Held JP. (1988). *Myoclonus in a patient with spinal cord transection. possible involvement of the spinal stepping generator.* A Journal of Neurology 111:1235-1245.

Buurke JH, Nene AV, Kwakkel G, Erren-Wolters V, Ijzerman MJ, Hermens HJ. (2008). *Recovery of gait after stroke: What changes?* Neurorehabilitation and Neural Repair 22(6):676-683.

Calancie B, Needham-Shropshire B, Jacobs P, Willer K, Zych G, Green BA. (1994). *Involuntary stepping after chronic spinal cord injury. evidence for a central rhythm generator for locomotion in man*. A Journal of Neurology 117:1143-1159.

Capaday C, Lavoie BA, Barbeau H, Schneider C, Bonnard M. (1999). *Studies on the corticospinal control of human walking. I. responses to focal transcranial magnetic stimulation of the motor cortex*. Journal of Neurophysiology 81(1):129-139.

Carey JR, Anderson KM, Kimberley TJ, Lewis SM, Auerbach EJ, Ugurbil K. (2004). *fMRI analysis of ankle movement tracking training in subject with stroke.* Experimental Brain Research 154(3):281-290.

Carusone LM, Srinivasan J, Gitelman DR, Mesulam MM, Parrish TB. (2002). *Hemodynamic response changes in cerebrovascular disease: Implications for functional MR imaging.* American Journal of Neuroradiology 23(7):1222-1228.

Chen HY, Chen SC, Chen JJ, Fu LL, Wang YL. (2005). *Kinesiological and kinematical analysis for stroke subjects with asymmetrical cycling movement patterns*. Journal of Electromyography and Kinesiology 15(6):587-595.

Christensen LO, Morita H, Petersen N, Nielsen J. (1999). *Evidence suggesting that a transcortical reflex pathway contributes to cutaneous reflexes in the tibialis anterior muscle during walking in man.* Experimental Brain Research 124(1):59-68.

Christensen LO, Johannsen P, Sinkjaer T, Petersen N, Pyndt HS, Nielsen JB. (2000). *Cerebral activation during bicycle movements in man.* Experimental Brain Research 135(1):66-72.

Classen J, Schnitzler A, Binkofski F, Werhahn KJ, Kim YS, Kessler KR, Benecke R. (1997). *The motor syndrome associated with exaggerated inhibition within the primary motor cortex of patients with hemiparetic.* A Journal of Neurology 120:605-619.

Coffman KA, Dum RP, Strick PL. (2011). *Cerebellar vermis is a target of projections from the motor areas in the cerebral cortex.* Proceedings of the National Academy of Sciences of the United States of America 108(38):16068-16073.

Cox RW. (1996). *AFNI: Software for analysis and visualization of functional magnetic resonance neuroimages.* Computers and Biomedical Research, an International Journal 29(3):162-173.

Dancause N. (2006). *Vicarious function of remote cortex following stroke: Recent evidence from human and animal studies.* The Neuroscientist 12(6):489-499.

Daskalakis ZJ, Christensen BK, Fitzgerald PB, Roshan L, Chen R. (2002). *The mechanisms of interhemispheric inhibition in the human motor cortex*. The Journal of Physiology 543(1):317-326.

Den Otter AR, Geurts AC, Mulder T, Duysens J. (2006). *Gait recovery is not associated with changes in the temporal patterning of muscle activity during treadmill walking in patients with post-stroke hemiparesis.* Clinical Neurophysiology 117(1):4-15.

Desrosiers J, Malouin F, Bourbonnais D, Richards CL, Rochette A, Bravo G. (2003). *Arm and leg impairments and disabilities after stroke rehabilitation: Relation to handicap.* Clinical Rehabilitation 17(6):666-673.

Dettmann MA, Linder MT, Sepic SB. (1987). *Relationships among walking performance, postural stability, and functional assessments of the hemiplegic patient.* American Journal of Physical Medicine 66(2):77-90.

Di Lazzaro V, Oliviero A, Profice P, Insola A, Mazzone P, Tonali P, Rothwell JC. (1999). *Direct demonstration of interhemispheric inhibition of the human motor cortex produced by transcranial magnetic stimulation.* Experimental Brain Research 124(4):520-524.

Di Lazzaro V, Molinari M, Restuccia D, Leggio MG, Nardone R, Fogli D, Tonali P. (1994a). *Cerebro-cerebellar interactions in man: Neurophysiological studies in patients with focal cerebellar lesions.* Electroencephalography and Clinical Neurophysiology 93(1):27-34.

Di Lazzaro V, Restuccia D, Molinari M, Leggio MG, Nardone R, Fogli D, Tonali P. (1994b). *Excitability of the motor cortex to magnetic stimulation in patients with cerebellar lesions.* Journal of Neurology, Neurosurgery, and Psychiatry 57(1):108-110.

Dietz V, Muller R, Colombo G. (2002). *Locomotor activity in spinal man: Significance of afferent input from joint and load receptors.* A Journal of Neurology 125:2626-2634.

Dietz V, Colombo G, Jensen L. (1994). *Locomotor activity in spinal man*. Lancet 344(8932):1260-1263.

Dietz V, Colombo G, Jensen L, Baumgartner L. (1995). *Locomotor capacity of spinal cord in paraplegic patients.* Annals of Neurology 37(5):574-582.

Dimitrijevic MR, Gerasimenko Y, Pinter MM. (1998). *Evidence for a spinal central pattern generator in humans.* Annals of the New York Academy of Sciences 860:360-376.

Dobkin BH, Firestine A, West M, Saremi K, Woods R. (2004). *Ankle dorsiflexion as an fMRI paradigm to assay motor control for walking during rehabilitation.* NeuroImage 23(1):370-381.

Drew T. (1993). *Motor cortical activity during voluntary gait modifications in the cat. I. cells related to the forelimbs.* Journal of Neurophysiology 70(1):179-199.

Drew T. (1988). *Motor cortical cell discharge during voluntary gait modification.* Brain Research 457(1):181-187.

Duysens J and Van de Crommert HW. (1998). *Neural control of locomotion; the central pattern generator from cats to humans.* Gait & Posture 7(2):131-141.

Duysens J and Pearson KG. (1980). *Inhibition of flexor burst generation by loading ankle extensor muscles in walking cats.* Brain Research 187(2):321-332.

Earhart GM and Bastian AJ. (2001). *Selection and coordination of human locomotor forms following cerebellar damage.* Journal of Neurophysiology 85(2):759-769.

Fair DA, Snyder AZ, Connor LT, Nardos B, Corbetta M. (2009). *Task-evoked BOLD responses are normal in areas of diaschisis after stroke.* Neurorehabilitation and Neural Repair 23(1):52-57.

Fedirchuk B, Nielsen J, Petersen N, Hultborn H. (1998). *Pharmacologically evoked fictive motor patterns in the acutely spinalized marmoset monkey.* Experimental Brain Research 122(3):351-361.

Feeney DM and Baron JC. (1986). *Diaschisis.* Stroke 17(5):817-830.

Fine EJ, Ionita CC, Lohr L. (2002). *The history of the development of the cerebellar examination.* Seminars in Neurology 22(4):375-384.

Forssberg H. (1985). *Ontogeny of human locomotor control. I. infant stepping, supported locomotion and transition to independent locomotion.* Experimental Brain Research 57(3):480-493.

Forssberg H. (1979). *Stumbling corrective reaction: A phase-dependent compensatory reaction during locomotion.* Journal of Neurophysiology 42(4):936-953.

Forssberg H and Grillner S. (1973). *The locomotion of the acute spinal cat injected with clonidine i.v.* Brain Research 50(1):184-186.

Forssberg H, Grillner S, Rossignol S. (1977). *Phasic gain control of reflexes from the dorsum of the paw during spinal locomotion.* Brain Research 132(1):121-139.

Fransson P, Kruger G, Merboldt KD, Frahm J. (1998). *Temporal characteristics of oxygenation-sensitive MRI responses to visual activation in humans.* Magnetic Resonance in Medicine 39(6):912-919.

Fridriksson J, Rorden C, Morgan PS, Morrow KL, Baylis GC. (2006). *Measuring the hemodynamic response in chronic hypoperfusion.* Neurocase 12(3):146-150.

Fukuyama H, Ouchi Y, Matsuzaki S, Nagahama Y, Yamauchi H, Ogawa M, Kimura J, Shibasaki H. (1997). *Brain functional activity during gait in normal subjects: A SPECT study.* Neuroscience Letters 228(3):183-186.

Gordon KE, Wu M, Kahn JH, Dhaher YY, Schmit BD. (2009). *Ankle load modulates hip kinetics and EMG during human locomotion.* Journal of Neurophysiology 101(4):2062-2076.

Grillner S and Zangger P. (1979). *On the central generation of locomotion in the low spinal cat.* Experimental Brain Research 34(2):241-261.

Grillner S and Rossignol S. (1978). *On the initiation of the swing phase of locomotion in chronic spinal cats.* Brain Research 146(2):269-277.

Grillner S and Zangger P. (1975). *How detailed is the central pattern generation for locomotion?* Brain Research 88(2):367-371.

Gwin JT, Gramann K, Makeig S, Ferris DP. 2011. *Electrocortical activity is coupled to gait cycle phase during treadmill walking.* NeuroImage 54(2):1289-1296.

Hamzei F, Knab R, Weiller C, Rother J. (2003). *The influence of extra- and intracranial artery disease on the BOLD signal in FMRI.* NeuroImage 20(2):1393-1399.

Hansen NL, Hansen S, Christensen LO, Petersen NT, Nielsen JB. (2001). *Synchronization of lower limb motor unit activity during walking in human subjects.* Journal of Neurophysiology 86(3):1266-1276.

Harada T, Miyai I, Suzuki M, Kubota K. (2009). *Gait capacity affects cortical activation patterns related to speed control in the elderly.* Experimental Brain Research 193(3):445-454.

Heeger DJ and Ress D. (2002). *What does fMRI tell us about neuronal activity?* Nature Reviews. 3(2):142-151.

Horak FB and Diener HC. (1994). *Cerebellar control of postural scaling and central set in stance.* Journal of Neurophysiology 72(2):479-493.

Hsu AL, Tang PF, Jan MH. (2003). *Analysis of impairments influencing gait velocity and asymmetry of hemiplegic patients after mild to moderate stroke.* Archives of Physical Medicine and Rehabilitation 84(8):1185-1193.

Huda S, Rodriguez R, Lastra L, Warren M, Lacourse MG, Cohen MJ, Cramer SC. (2008). *Cortical activation during foot movements: II effect of movement rate and side.* Neuroreport 19(16):1573-1577.

Huettel, S.A., Song, A.W., McCarthy, G.J. (2004). *Functional magnetic resonance imaging.* Sunderland, Mass: Sinauer Associates, c2004.

Hultborn H and Nielsen JB. (2007). *Spinal control of locomotion--from cat to man.* Acta Physiologica 189(2):111-121.

Humphrey DR. (1972). *Relating motor cortex spike trains to measures of motor performance.* Brain Research 40(1):7-18.

Hund-Georgiadis M, Mildner T, Georgiadis D, Weih K, von Cramon DY. (2003). *Impaired hemodynamics and neural activation? A fMRI study of major cerebral artery stenosis.* Neurology 61(9):1276-1279.

Jain S, Gourab K, Schindler-Ivens SM, Schmit BD. (2012). *EEG during pedaling: Evidence for cortical control of locomotor tasks.* Clinical Neurophysiology [Epub ahead of print]

Jayaram G, Galea JM, Bastian AJ, Celnik P. (2011). *Human locomotor adaptive learning is proportional to depression of cerebellar excitability* Cerebral Cortex 21(8):1901-1909.

Kang JK, Bénar C, Al-Asmi A, Khani YA, Pike GB, Dubeau F, Gotman J. (2003). *Using patient-specific hemodynamic response functions in combined EEG-fMRI studies in epilepsy.* NeuroImage 20(2):1162-1170.

Kapreli E, Athanasopoulos S, Papathanasiou M, Van Hecke P, Strimpakos N, Gouliamos A, Peeters R, Sunaert S. (2006). *Lateralization of brain activity during lower limb joints movement. an fMRI study.* NeuroImage 32(4):1709-1721.

Kautz SA and Brown DA. (1998). *Relationships between timing of muscle excitation and impaired motor performance during cyclical lower extremity movement in post-stroke hemiplegia.* Brain 121:515-526.

Kautz SA and Hull ML. (1993). *A theoretical basis for interpreting the force applied to the pedal in cycling.* Journal of Biomechanics 26(2):155-165.

Kelly RM and Strick PL. (2003). *Cerebellar loops with motor cortex and prefrontal cortex of a nonhuman primate*. The Journal of Neuroscience 23(23):8432-8444.

Kim YH, You SH, Kwon YH, Hallett M, Kim JH, Jang SH. (2006). *Longitudinal fMRI study for locomotor recovery in patients with stroke.* Neurology 67(2):330-333.

Kwong KK, Belliveau JW, Chesler DA, Goldberg IE, Weisskoff RM, Poncelet BP, Kennedy DN, Hoppel BE, Cohen MS, Turner R. 1992. *Dynamic magnetic resonance imaging of human brain activity during primary sensory stimulation.* Proceedings of the National Academy of Sciences of the United States of America 89(12):5675-5679.

Lin PY, Chen JJ, Lin SI. (2012). *The cortical control of cycling exercise in stroke patients: An fNIRS study.* Human Brain Mapping [Epub ahead of print].

Lin PY, Yang YR, Cheng SJ, Wang RY. (2006). *The relation between ankle impairments and gait velocity and symmetry in people with stroke.* Archives of Physical Medicine and Rehabilitation 87(4):562-568.

Lloyd-Jones D, Adams R, Carnethon M, De Simone G, Ferguson TB, Flegal K, Ford E, Furie K, Go A, Greenlund K, and others. (2009). *Heart disease and stroke statistics--2009 update: A report from the american heart association statistics committee and stroke statistics subcommittee.* Circulation 119(3):e21-181.

Logothetis NK, Pauls J, Augath M, Trinath T, Oeltermann A. (2001). *Neurophysiological investigation of the basis of the fMRI signal.* Nature 412(6843):150-157.

Lord SE, McPherson K, McNaughton HK, Rochester L, Weatherall M. (2004). Community ambulation after stroke: How important and obtainable is it and what measures appear predictive? Archives of Physical Medicine and Rehabilitation 85(2):234-239.

Luft AR, Forrester L, Macko RF, McCombe-Waller S, Whitall J, Villagra F, Hanley DF. (2005). *Brain activation of lower extremity movement in chronically impaired stroke survivors.* NeuroImage 26(1):184-194.

Lutz K, Koeneke S, Wustenberg T, Jancke L. (2005). *Asymmetry of cortical activation during maximum and convenient tapping speed.* Neuroscience Letters 373(1):61-66.

Marchand-Pauvert V and Nielsen JB. (2002). *Modulation of heteronymous reflexes from ankle dorsiflexors to hamstring muscles during human walking*. Experimental Brain Research 142(3):402-408.

Marshall RS. (2004). *The functional relevance of cerebral hemodynamics: Why blood flow matters to the injured and recovering brain*. Current Opinion in Neurology 17(6):705-709.

Matthews PM and Jezzard P. (2004). *Functional magnetic resonance imaging.* Journal of Neurology, Neurosurgery & Psychiatry 75(1):6-12.

Mazzetto-Betti KC, Leoni RF, Pontes-Neto OM, Santos AC, Leite JP, Silva AC, de Araujo DB. (2010). *The stability of the blood oxygenation level-dependent functional MRI response to motor tasks is altered in patients with chronic ischemic stroke.* Stroke 41(9):1921-1926.

McVea DA, Donelan JM, Tachibana A, Pearson KG. (2005). *A role for hip position in initiating the swing-to-stance transition in walking cats.* Journal of Neurophysiology 94(5):3497-3508.

Mehta JP, Verber MD, Wieser JA, Schmit BD, Schindler-Ivens SM. (2012). *The effect of movement rate and complexity on functional magnetic resonance signal change during pedaling.* Motor Control 16(2):158-175.

Mehta JP, Verber MD, Wieser JA, Schmit BD, Schindler-Ivens SM. (2009). *A novel technique for examining human brain activity associated with pedaling using fMRI.* Journal of Neuroscience Methods 179(2):230-239.

Miezin FM, Maccotta L, Ollinger JM, Petersen SE, Buckner RL. (2000). *Characterizing the hemodynamic response: Effects of presentation rate, sampling procedure, and the possibility of ordering brain activity based on relative timing.* NeuroImage 11(6 Pt 1):735-759.

Mihara M, Miyai I, Hatakenaka M, Kubota K, Sakoda S. (2007). *Sustained prefrontal activation during ataxic gait: A compensatory mechanism for ataxic stroke?* NeuroImage 37(4):1338-1345.

Miyai I, Suzuki M, Hatakenaka M, Kubota K. (2006). *Effect of body weight support on cortical activation during gait in patients with stroke.* Experimental Brain Research 169(1):85-91.

Miyai I, Yagura H, Hatakenaka M, Oda I, Konishi I, Kubota K. (2003). *Longitudinal optical imaging study for locomotor recovery after stroke.* Stroke 34(12):2866-2870.

Miyai I, Yagura H, Oda I, Konishi I, Eda H, Suzuki T, Kubota K. (2002). *Premotor cortex is involved in restoration of gait in stroke.* Annals of Neurology 52(2):188-194.

Miyai I, Tanabe HC, Sase I, Eda H, Oda I, Konishi I, Tsunazawa Y, Suzuki T, Yanagida T, Kubota K. (2001). *Cortical mapping of gait in humans: A near-infrared spectroscopic topography study.* NeuroImage 14(5):1186-1192.

Molinari M, Filippini V, Leggio MG. (2002). *Neuronal plasticity of interrelated cerebellar and cortical networks.* Neuroscience 111(4):863-870.

Mori S, Matsui T, Mori F, Nakajima K, Matsuyama K. (2000). *Instigation and control of treadmill locomotion in high decerebrate cats by stimulation of the hook bundle of russell in the cerebellum.* Canadian Journal of Physiology and Pharmacology 78(11):945-957.

Morton SM and Bastian AJ. (2004). *Cerebellar control of balance and locomotion.* The Neuroscientist 10(3):247-259.

Morton SM and Bastian AJ. (2003). *Relative contributions of balance and voluntary leg-coordination deficits to cerebellar gait ataxia.* Journal of Neurophysiology 89(4):1844-1856.

Murase N, Duque J, Mazzocchio R, Cohen LG. (2004). *Influence of interhemispheric interactions on motor function in chronic stroke.* Annals of Neurology 55(3):400-409.

Murata Y, Sakatani K, Hoshino T, Fujiwara N, Kano T, Nakamura S, Katayama Y. (2006). *Effects of cerebral ischemia on evoked cerebral blood oxygenation responses and BOLD contrast functional MRI in stroke patients.* Stroke 37(10):2514-2520.

Newton J, Sunderland A, Butterworth SE, Peters AM, Peck KK, Gowland PA. (2002). *A pilot study of event-related functional magnetic resonance imaging of monitored wrist movements in patients with partial recovery.* Stroke 33(12):2881-2887.

Nielsen JB. (2003). *How we walk: Central control of muscle activity during human walking.* The Neuroscientist 9(3):195-204.

Nirkko AC, Ozdoba C, Redmond SM, Burki M, Schroth G, Hess CW, Wiesendanger M. (2001). *Different ipsilateral representations for distal and proximal movements in the sensorimotor cortex: Activation and deactivation patterns.* NeuroImage 13(5):825-835.

Noll DC and Vazquez A. (2004). *Contrast mechanisms and acquisition methods in functional MRI.* Conference Proceedings: Annual International Conference of the IEEE Engineering in Medicine and Biology Society 7:5219-5222.

Ogawa S, Lee TM, Kay AR, Tank DW. (1990). *Brain magnetic resonance imaging with contrast dependent on blood oxygenation.* Proceedings of the National Academy of Sciences of the United States of America 87(24):9868-9872.

Ogawa S, Tank DW, Menon R, Ellermann JM, Kim SG, Merkle H, Ugurbil K. (1992). *Intrinsic signal changes accompanying sensory stimulation: Functional brain mapping with magnetic resonance imaging.* Proceedings of the National Academy of Sciences of the United States of America 89(13):5951-5955.

Patterson KK, Parafianowicz I, Danells CJ, Closson V, Verrier MC, Staines WR, Black SE, McIlroy WE. (2008). *Gait asymmetry in community-ambulating stroke survivors.* Archives of Physical Medicine and Rehabilitation 89(2):304-310.

Pauling L and Coryell CD. (1936). *The magnetic properties and structure of hemoglobin, oxyhemoglobin and carbonmonoxyhemoglobin.* Proceedings of the National Academy of Sciences of the United States of America 22(4):210-216.

Perry J, Garrett M, Gronley JK, Mulroy SJ. (1995). *Classification of walking handicap in the stroke population.* Stroke 26(6):982-989.

Petersen N, Christensen LO, Nielsen J. (1998). *The effect of transcranial magnetic stimulation on the soleus H reflex during human walking.* The Journal of Physiology 513:599-610.

Petersen NT, Butler JE, Marchand-Pauvert V, Fisher R, Ledebt A, Pyndt HS, Hansen NL, Nielsen JB. (2001). *Suppression of EMG activity by transcranial magnetic stimulation in human subjects during walking.* The Journal of Physiology 537:651-656.

Pineiro R, Pendlebury S, Johansen-Berg H, Matthews PM. (2002). *Altered hemodynamic responses in patients after subcortical stroke measured by functional MRI.* Stroke 33(1):103-109.

Pyndt HS and Nielsen JB. (2003). *Modulation of transmission in the corticospinal and group ia afferent pathways to soleus motoneurons during bicycling.* Journal of Neurophysiology 89(1):304-314.

Ramnani N. (2006). *The primate cortico-cerebellar system: Anatomy and function*. Nature Review 7(7):511-522.

Rao SM, Bandettini PA, Binder JR, Bobholz JA, Hammeke TA, Stein EA, Hyde JS. (1996). *Relationship between finger movement rate and functional magnetic resonance signal change in human primary motor cortex.* Journal of Cerebral Blood Flow and Metabolism 16(6):1250-1254.

Roc AC, Wang J, Ances BM, Liebeskind DS, Kasner SE, Detre JA. (2006). *Altered hemodynamics and regional cerebral blood flow in patients with hemodynamically significant stenoses.* Stroke 37(2):382-387.

Rossini PM, Altamura C, Ferretti A, Vernieri F, Zappasodi F, Caulo M, Pizzella V, Del Gratta C, Romani GL, Tecchio F. (2004). *Does cerebrovascular disease affect the coupling between neuronal activity and local haemodynamics?* Brain 127:99-110.

Rother J, Knab R, Hamzei F, Fiehler J, Reichenbach JR, Buchel C, Weiller C. (2002). *Negative dip in BOLD fMRI is caused by blood flow--oxygen consumption uncoupling in humans.* NeuroImage 15(1):98-102.

Sakamoto M, Nakajima T, Wasaka T, Kida T, Nakata H, Endoh T, Nishihira Y, Komiyama T. (2004). *Load- and cadence-dependent modulation of somatosensory evoked potentials and soleus H-reflexes during active leg pedaling in humans.* Brain Research 1029(2):272-285.

Schindler-Ivens S, Brown DA, Brooke JD. (2004). *Direction-dependent phasing of locomotor muscle activity is altered post-stroke.* Journal of Neurophysiology 92(4):2207-2216.

Schubert M, Curt A, Colombo G, Berger W, Dietz V. (1999). *Voluntary control of human gait: Conditioning of magnetically evoked motor responses in a precision stepping task.* Experimental Brain Research 126(4):583-588.

Sherrington CS. (1910). *Remarks on the reflex mechanism of the step.* Brain 33(1):1-25.

Shik ML, Severin FV, Orlovskii GN. (1966). *Control of walking and running by means of electric stimulation of the midbrain* Biofizika 11(4):659-666.

Sinkjaer T, Andersen JB, Ladouceur M, Christensen LO, Nielsen JB. (2000). *Major role for sensory feedback in soleus EMG activity in the stance phase of walking in man*. The Journal of Physiology 523:817-827.

Springer JA, Binder JR, Hammeke TA, Swanson SJ, Frost JA, Bellgowan PS, Brewer CC, Perry HM, Morris GL, Mueller WM. (1999). *Language dominance in neurologically normal and epilepsy subjects: A functional MRI study.* Brain 122:2033-2046.

Stoodley CJ and Schmahmann JD. (2009). *Functional topography in the human cerebellum: A meta-analysis of neuroimaging studies.* NeuroImage 44(2):489-501.

Suzuki M, Miyai I, Ono T, Kubota K. (2008). *Activities in the frontal cortex and gait performance are modulated by preparation. an fNIRS study.* NeuroImage 39(2):600-607.

Suzuki M, Miyai I, Ono T, Oda I, Konishi I, Kochiyama T, Kubota K. (2004). *Prefrontal and premotor cortices are involved in adapting walking and running speed on the treadmill: An optical imaging study.* NeuroImage 23(3):1020-1026.

Thach WT, Goodkin HP, Keating JG. (1992). *The cerebellum and the adaptive coordination of movement.* Annual Review of Neuroscience 15:403-442.

Thierry G, Ibarrola D, Demonet JF, Cardebat D. (2003). *Demand on verbal working memory delays haemodynamic response in the inferior prefrontal cortex.* Human Brain Mapping 19(1):37-46.

Turns LJ, Neptune RR, Kautz SA. (2007). *Relationships between muscle activity and anteroposterior ground reaction forces in hemiparetic walking.* Archives of Physical Medicine and Rehabilitation 88(9):1127-1135.

Ugawa Y, Day BL, Rothwell JC, Thompson PD, Merton PA, Marsden CD. (1991). *Modulation of motor cortical excitability by electrical stimulation over the cerebellum in man.* The Journal of Physiology 441:57-72.

Verstynen T, Diedrichsen J, Albert N, Aparicio P, Ivry RB. (2005). *Ipsilateral motor cortex activity during unimanual hand movements relates to task complexity.* Journal of Neurophysiology 93(3):1209-1222.

Wernig A and Muller S. (1992). *Laufband locomotion with body weight support improved walking in persons with severe spinal cord injuries.* Paraplegia 30(4):229-238.

Wexler BE, Fulbright RK, Lacadie CM, Skudlarski P, Kelz MB, Constable RT, Gore JC. (1997). *An fMRI study of the human cortical motor system response to increasing functional demands.* Magnetic Resonance Imaging 15(4):385-396.

Whelan PJ. (1996). *Control of locomotion in the decerebrate cat.* Progress in Neurobiology 49(5):481-515.

Williamson JW, Nobrega AC, McColl R, Mathews D, Winchester P, Friberg L, Mitchell JH. (1997). *Activation of the insular cortex during dynamic exercise in humans*. The Journal of Physiology 503:277-283.

Wu M, Gordon K, Kahn JH, Schmit BD. (2011). *Prolonged electrical stimulation over hip flexors increases locomotor output in human SCI.* Clinical Neurophysiology 122(7):1421-1428.

Yang JF and Gorassini M. (2006). *Spinal and brain control of human walking: Implications for retraining of walking.* The Neuroscientist 12(5):379-389.

Yang JF, Stephens MJ, Vishram R. (1998). *Infant stepping: A method to study the sensory control of human walking.* The Journal of Physiology 507(3):927-937.

You SH, Jang SH, Kim YH, Hallett M, Ahn SH, Kwon YH, Kim JH, Lee MY. (2005). *Virtual reality-induced cortical reorganization and associated locomotor recovery in chronic stroke: An experimenter-blind randomized study*. Stroke 36(6):1166-1171.

Ziemann U, Rothwell JC, Ridding MC. (1996). *Interaction between intracortical inhibition and facilitation in human motor cortex.* The Journal of Physiology 496:873-881.

APPENDIX A: COMPARISON OF fMRI ANALYSIS TECHNIQUES FOR PEDALING-RELATED BRAIN ACTIVATION

In the past, our laboratory has used a conventional analysis technique with averaged fMRI data. The conventional analysis technique refers to a technique that fit the entire canonical hemodynamic response model with the blood-oxygenated level dependent (BOLD) signal. This approach produced an "activation" signal across the entire brain, which was considered to be an artifact caused by movement of the leg that occurred concurrently with the BOLD signal. Therefore, they proposed a delayed non-movement technique. However, we later discovered that the use of either conventional or delayed non-movement technique could produce physiological meaningful data, suggesting that the leg movement during pedaling did not distort the magnetic field during the fMRI scan and subsequently did not cause the image artifact.

This supplementary report aimed to demonstrate the comparisons of pedaling-related brain activation results when using the different combination of analysis techniques. To address our aim, 10 fMRI datasets of the healthy controls from our previous study were used (Mehta et al., 2009). The data was collected while the subject performed audio-guided active pedaling at 30 rpm. General linear model analysis was performed on each individual's data to identify active voxels associated with the given task. To compare the various combinations of analysis techniques, combinations of general linear model analysis techniques both with and without head movement as regressors, a canonical versus delayed non-movement hemodynamic response model, and averaged versus concatenated data were applied to the each data of each subject. The 5 combinations of analysis techniques are as followed:

Technique 1: The three runs were averaged. The time-series was modeled by $y = \beta_0 + \beta_1 x_1 + \varepsilon$, where β_0 is baseline of the signal; x_1 is the conventional model; ε is noise.

Technique 2: The three runs were concatenated. The time-series was modeled by $y = \beta_0 + \beta_1 x_1 + \varepsilon$, where x_1 is the conventional model.

Technique 3: the three runs were concatenated. The time-series was modeled by $y = \beta_0 + \beta_1 x_1 + \beta_2 x_2 + ... + \beta_7 x_7 + \varepsilon$ where x_1 is the conventional model; $x_2 \ldots x_7$ are head movements in 6 directions and act as variables of no interest.

Technique 4: The three runs were concatenated. The time-series was modeled by $y = \beta_0 + \beta_1 x_1 + \varepsilon$, where x_1 is the delayed non-movement model.

Technique 5: the three runs were concatenated. The time-series was modeled by $y = \beta_0 + \beta_1 x_1 + \beta_2 x_2 + ... + \beta_7 x_7 + \varepsilon$, where x_1 is the delayed non-movement model; x_2-x_7 are head movement in 6 directions and act as variables of no interest.

Data from each subject was transformed into the standardized Talairach and Tournoux coordination system (Talairach and Tournoux 1988). Functional data was blurred using a 4 mm full width half maximum Gaussian filter for each individual subject. Next, a group analysis was performed using to a t-test to identify the voxels that are consistently active across subjects. A clustered threshold for the t-test was determined using a Monte Carlo simulation (AlphaSim) that maintain a familywise error at $p<0.05$.

The pedaling-related brain activations in healthy control group that was analyzed by the 5 combination techniques are shown in the Figure. As a group, we found that any combination of analysis technique could produce comparable results, suggesting that any

of these combinations of analysis techniques are viable for our fMRI pedaling paradigm in healthy controls. It should be noted that for Technique 1-3 the conventional model has a tendency to show negatively correlated data compared to the delayed non-movement model. In addition, for each individual subject, concatenated data tends to demonstrate a slightly bigger cluster and more connected than the averaged data (these figures are not shown).

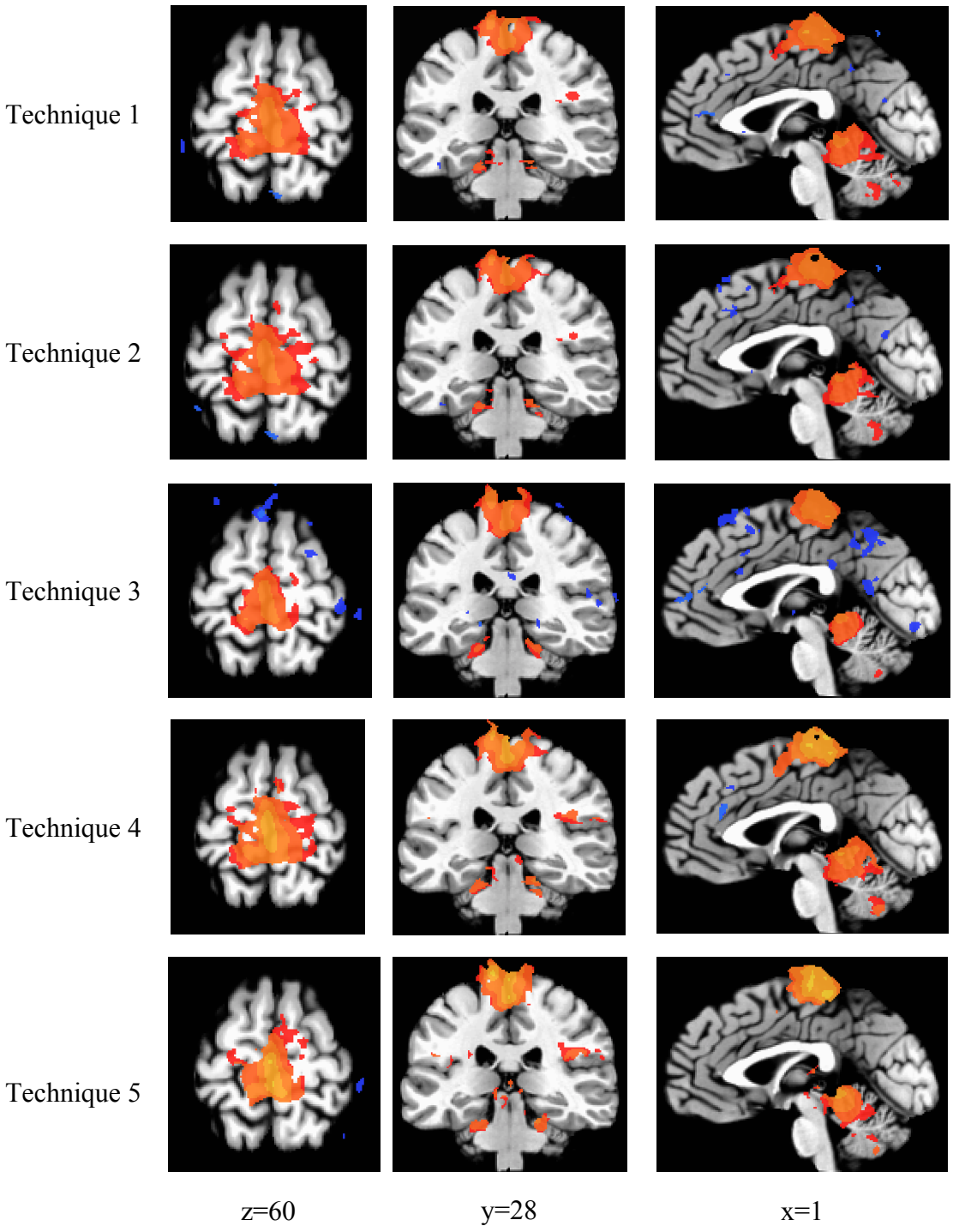

Figure. Group data represents the pedaling-related brain activation of group C analyzed by 5 different techniques, from top to bottom. The data shows the same slides in axial, coronal and sagittal view, from left to right.

APPENDIX B: DELAYED NON-MOVEMENT TECHNIQUE COULD ELIMINATE THE MOVEMENT ARTIFACTS IN THE IMAGES CAUSED BY A CONCURRENT HEAD MOVEMENT WITH A MOVEMENT OF INTEREST

B.1 INTRODUCTION

The delayed non-movement technique was first introduced in 2009, where it was used to analyze pedaling-related brain activation, as the task created highly concurrent head motion with pedaling (Mehta et al., 2009). It is an functional magnetic resonance imaging (fMRI) analysis technique that correlates only the portion of the blood oxygen level-dependent (BOLD) time-series after movement stopped (movement-free portion) to a canonical hemodynamic response function model. This approach was justified because the onset and termination of BOLD signals are delayed with respect to a given task (Bandettini and Cox 2000). The delayed non-movement technique has been validated in the healthy controls for pedaling and finger and foot tapping task (Mehta et al., 2009). However, this technique has never been explored in stroke survivors. Therefore, this supplementary study aims (1) to determine whether the delayed non-movement technique would be beneficial to the pedaling-related brain activation analysis in stroke subjects, and (2) to examine if there is a cutoff amplitude of the head movement where the delayed non-movement technique is unable to handle.

B.2 METHODS

Sixteen stroke survivors (9 females; age 55.3±11.6 years) and ten healthy controls (6 females; age 53.4±13.1 years) were recruited. Each subject gave written informed consent according to the Declaration of Helsinki and institutional guidelines at Marquette

University and the Medical College of Wisconsin. The experimental device, experimental protocols, and fMRI scanning sequences were as described in Chapter 3, experiment 1. Data analysis was performed using the delayed non-movement technique, then, reanalyzed using a conventional technique. As shown in Figure B-1, the delayed non-movement technique was a correlation between the canonical model and the BOLD signal in only the movement-free portions (gray), while the conventional technique was a correlation between the model and the signal for an entire signal (gray and white).

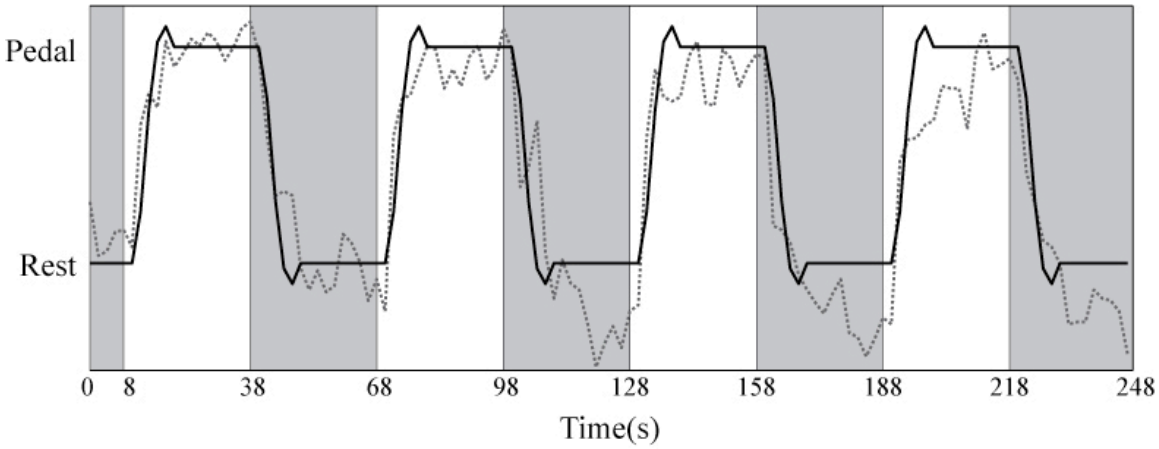

Figure B-1. A representative example from a single subject of the relationship between the canonical model and the BOLD signal. Time series voxels is from the sensorimotor cortex. The period of pedaling and rest is shown in the white and gray background, respectively. The BOLD signal is shown as a dotted line, and the canonical model is represented as a black line. The x-axis represents the number of repetition times (TRs), where 1 TR=2 s.

Head movement is one of the major causes of artifacts in the brain images. It is therefore important to monitor the movement to ensure the brain signals are not movement-contaminated. Head movement could also be used as an exclusion criteria for the sets of brain signal that show great head motions. Head movement is an indirect measurement that represents the amount of movement from the registered point. In this

analysis, the registered point is the head position at the beginning of the functional run that proceeds to the anatomical scan. The data were reported in three translational and three rotational directions. The three translational movements are superior-inferior (S-I), anterior-posterior (A-P), and left-right (L-R). The three rotational movements are roll (rotate around SI-axis), pitch (rotate around LR-axis), and yaw (rotate around AP-axis). All 6 runs were concatenated. To compare between subjects and groups, the head movement was quantified into three characteristics: displacement, drift, and oscillation. Figure B-2 shows the example of the three characteristics of the head movement data. Displacement is mean of the distance in translations or the degree in rotations of the head away from the registered position (Eq. 1). Drift is the changes in the head position from the beginning to the end position within a concatenated run (Eq. 2). Oscillation is calculated from the standard deviation of the residuals from the linear polynomial fit for each direction (Eq. 3)

$$\text{Displacement} = |\bar{x}| \qquad \text{Eq. 1}$$

$$\text{Drift} = |\bar{x}_{last} - \bar{x}_{first}| \qquad \text{Eq. 2}$$

$$\text{Oscillation} = \text{std}(\text{residuals}(\text{linear polynomial fit}) \qquad \text{Eq. 3}$$

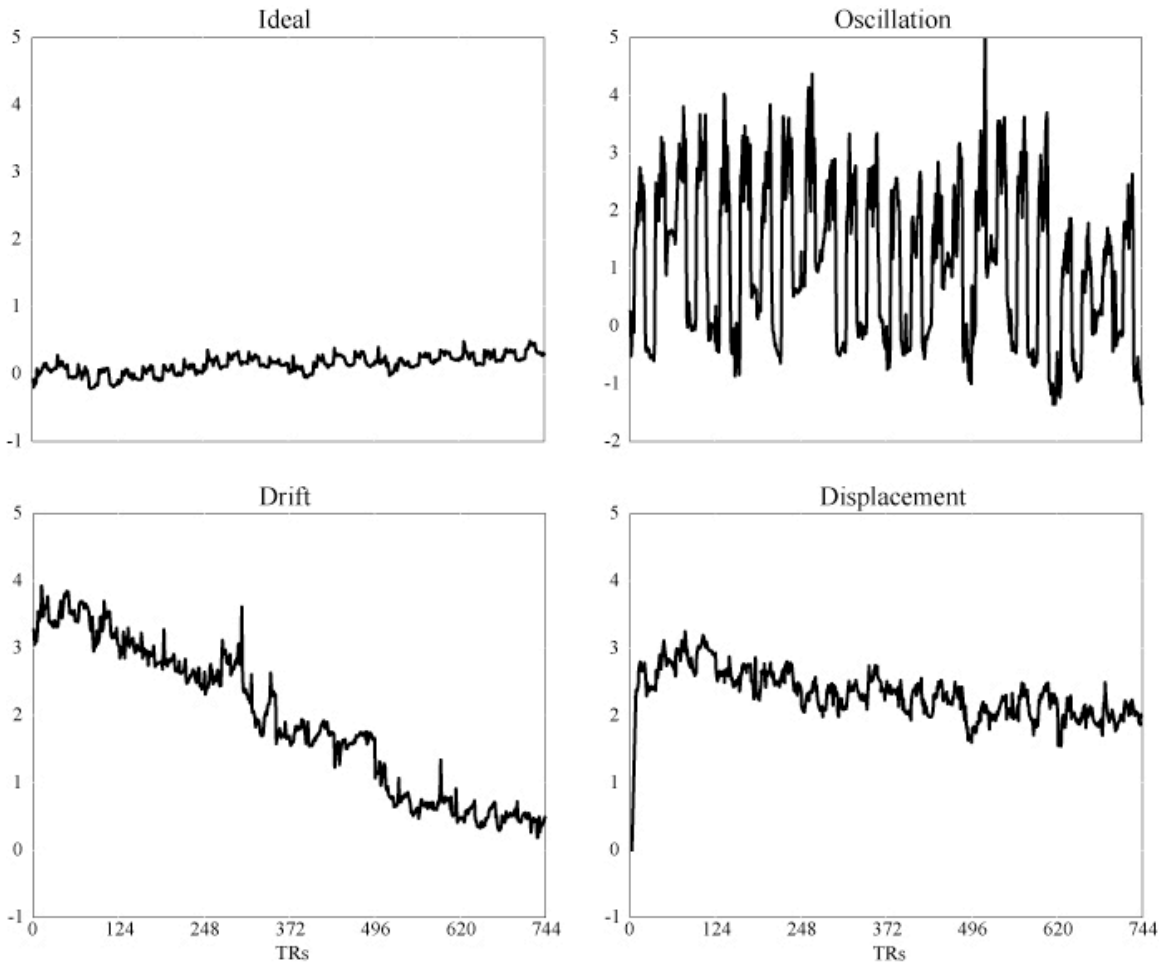

Figure B-2. Representative examples of (A) an ideal head movement, where the subject produced a small amount of head movement around the zero line, (B) oscillation, where the subject produced a larger amount of head movement around the zero line, (C) drift, where the subject produced small amount of head movement but drifted from the starting to the ending points and (D) displacement, where the subject moved to a different position at the beginning but stayed in that position and produced a small amount of head movement. The x-axis represents the number of TRs, where 1 TR=2 s. The y-axis represents the distance (mm) or degree of movement.

The maximal head movement of each characteristics of each subject, regardless of the direction, was extracted and used as a representative head movement for each subject. The representative head movement was then sorted for each of the three head motion characteristics.

B.3 RESULTS

B.3.1 Pedaling-related brain activation using delayed non-movement technique in stroke subjects

Comparing the pedaling-related brain activation analyzed by the delayed non-movement versus the conventional technique, we found that in some data, either technique could produce physiological meaningful data (Figure B-3 and B-4). Some data displayed either physiological meaningful data (Figure B-5 and B-6) or a greater specificity of the pedaling-related brain activation (Figure B-7) when delayed non-movement technique was used compared to when the conventional technique was used. However, there was a data that either analysis technique could not produce physiologically meaningful data (Figure B-8).

All the figures represent the data from a representative single subject, comparing the data analyzed by the conventional (top row) and the delayed non-movement technique (bottom row). The data shows the same slides in axial, coronal and sagittal view, from left to right. The figures show in the neurological convention: left is left).

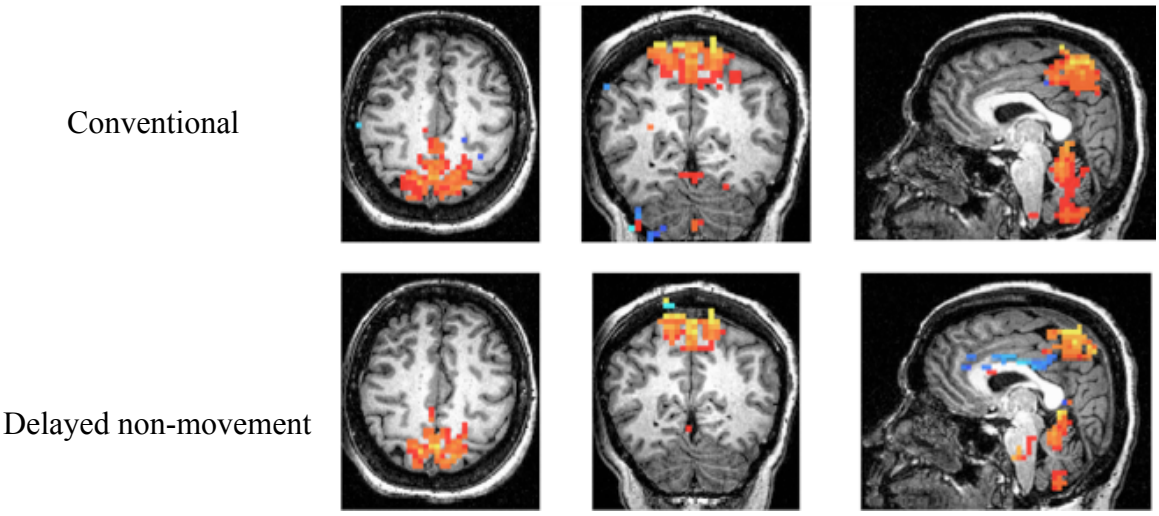

Figure B-3. A representative example from a single control subject (C6) shows that using either technique could produce physiologically meaningful data.

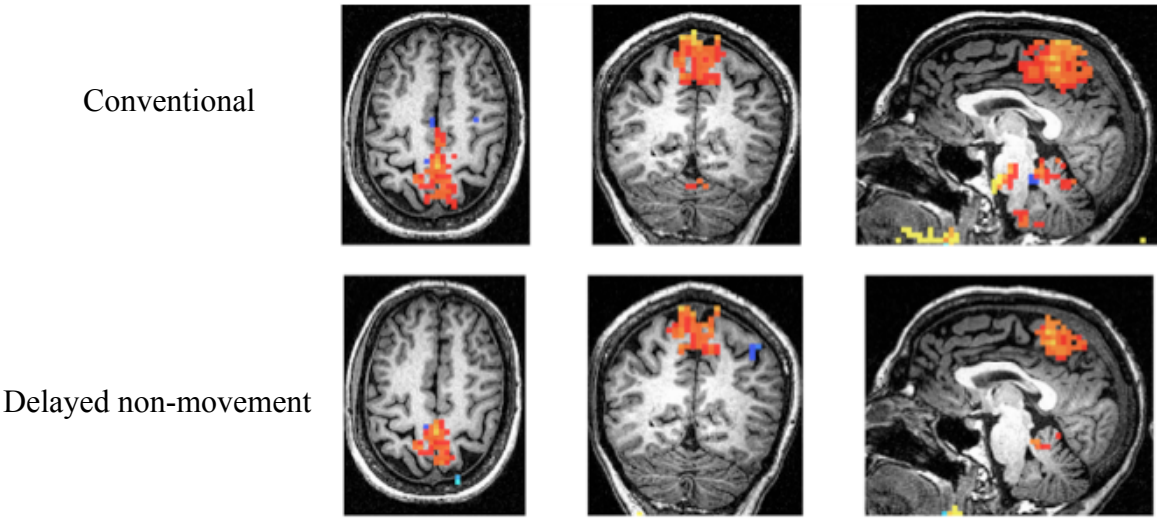

Figure B-4. A representative example from a single stroke subject (S10) shows that using either technique could produce physiologically meaningful data.

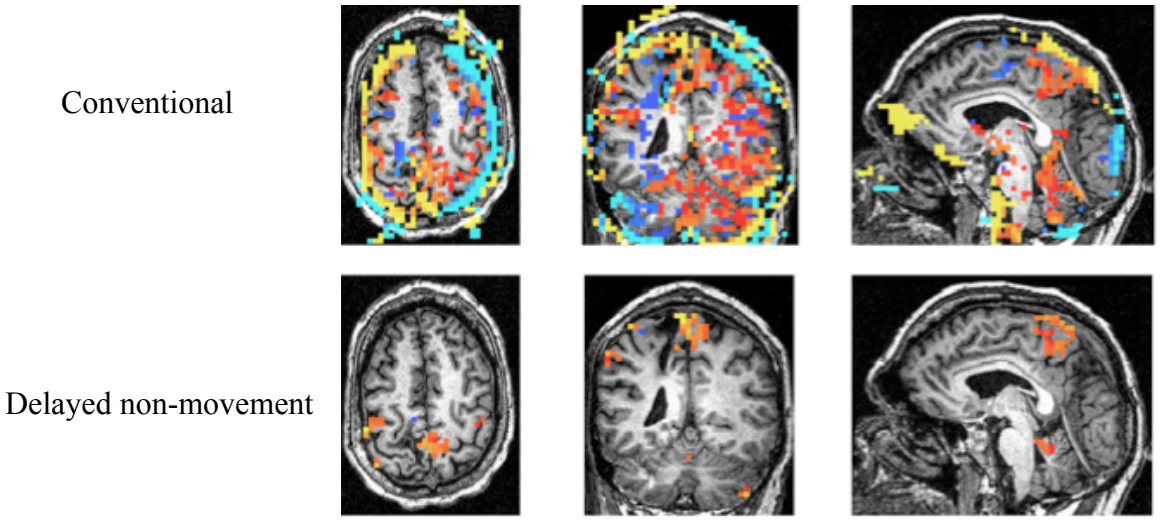

Figure B-5. A representative example from a single stroke subject (S4) shows that using the delayed non-movement technique could eliminate the circumferential ring artifacts, which is considered an artifact caused by head motions, while the conventional technique could not.

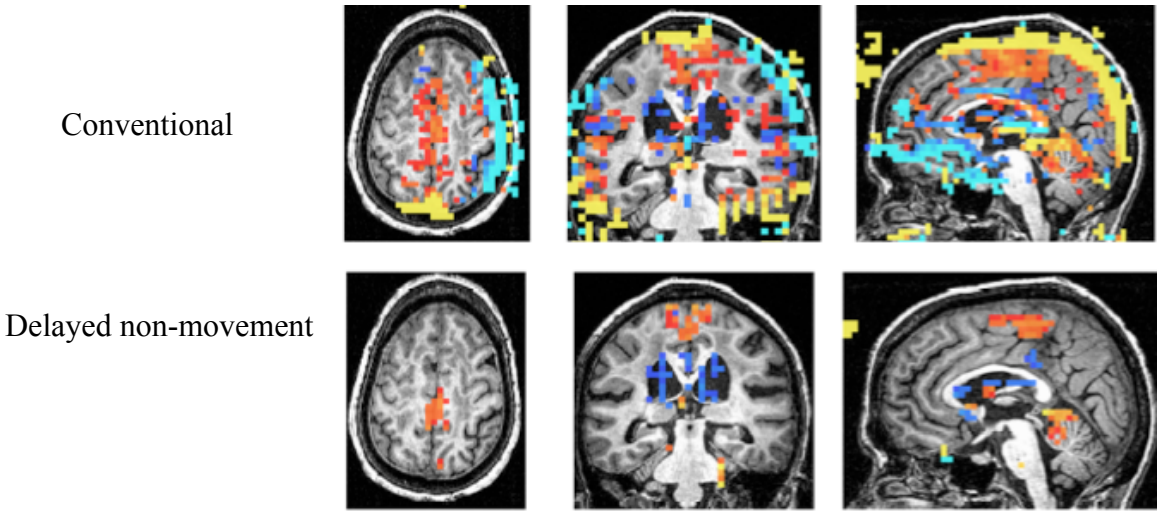

Figure B-6. A representative example from a single stroke subject (S3) shows that the delayed non-movement technique could eliminate the circumferential ring artifacts, which is considered an artifact caused by head motions, while the conventional technique could not.

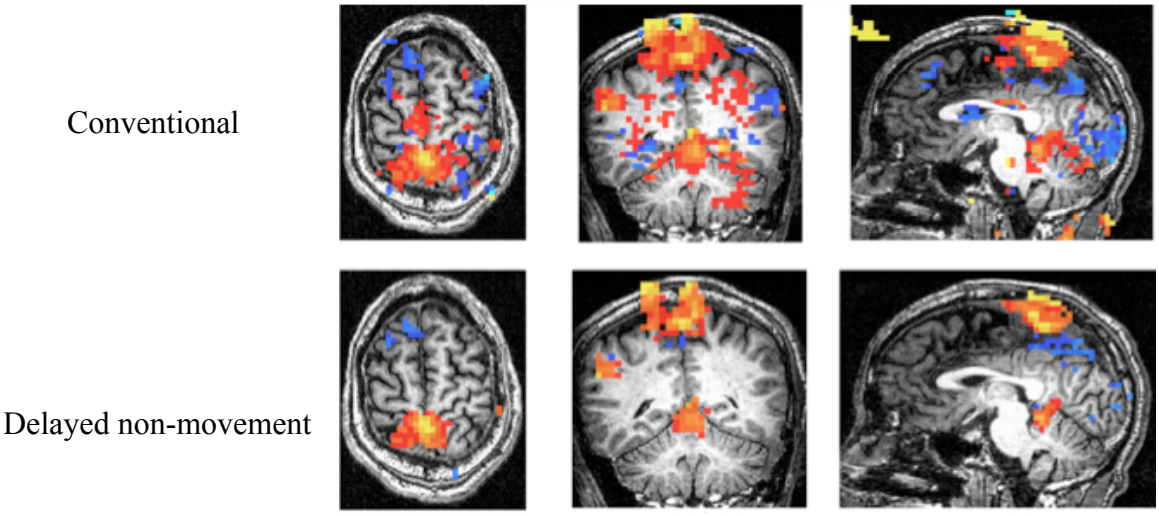

Figure B-7. A representative example from a single stroke subject (S12) shows that the delayed non-movement technique could increase the specificity of the pedaling-related brain activation compared to the conventional technique.

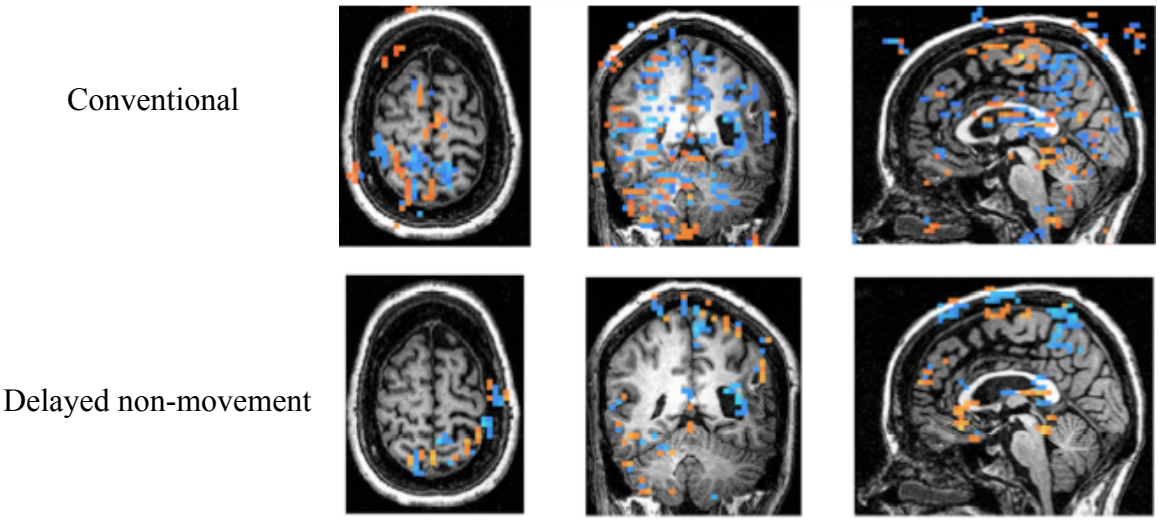

Figure B-8. A representative example from a single stroke subject (S13) shows that either analysis technique could not produce physiologically meaningful data.

B.3.2 Head movement data

As shown in Figure B-9, oscillation ranged from 0.21 to 0.90 mm/degrees for the control group and from 0.24 to 2.76 mm/degrees for the stroke group. The sorted plot of oscillation showed that 4 stroke subjects (S6, S4, S3 and S13) produced greater head motions than the range of the control subjects. Drift was ranged from 0.45 to 3.02 mm/degrees for the control group and from 0.45 to 9.10 mm/degrees for the stroke group. The sorted plot of drift demonstrated that 2 stroke subjects (S12, S13) produced greater head motions than the range of the control subjects. Displacement was ranged from 0.27 to 2.15 mm/degrees for the control group and from 0.40 to 5.10 mm/degrees for the stroke group. The sorted plot showed that 4 stroke subjects (S2, S15, S12, S13) created greater head motions than the range of the control subjects.

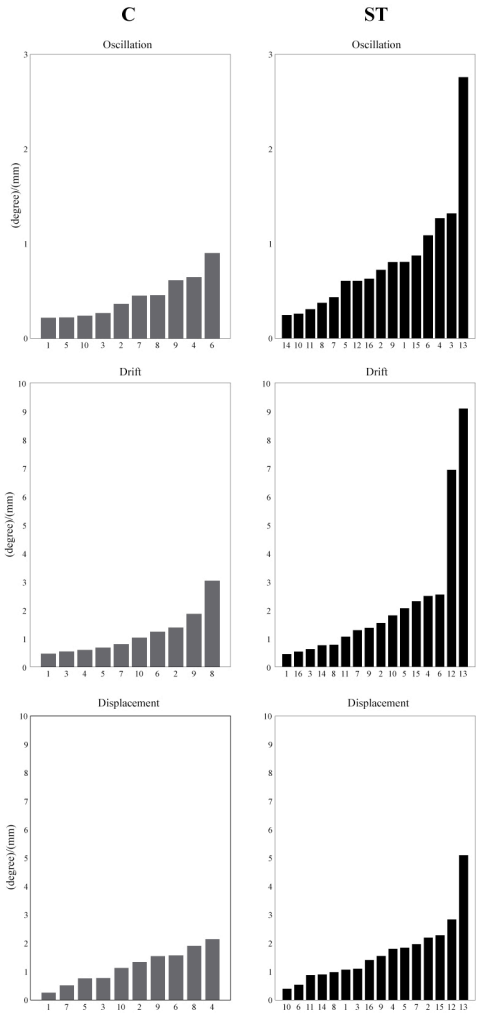

Figure B-9 shows sorted head movement data for (top) oscillation, (middle) drift and (bottom) displacement within each group. Each bar represents the amount of head motions for each individual subject. C=control group and ST=stroke group.

B.3.3 Relationship between the pedaling-related brain activation and head movement

Both C6 and S10 subjects, who displayed physiologically meaningful data of the pedaling-related brain activation, also demonstrated small amount of oscillation, drifting, and displacement of head movement, suggesting that if subjects produce small head movement, either fMRI analysis can be used. Meanwhile, S3 and S4 subject, whose their data showed that using the delayed non-movement technique could eliminate the motion artifacts in the images, leaving the likely physiological meaningful data. Their head movement results showed a great amount of oscillation, but moderate drifting and displacement. This suggested that increased oscillation could cause head motion artifact, which can be eliminated when using the delayed non-movement technique. S12 subject, who showed that the delayed non-movement technique could increase specificity of the brain images, demonstrated a great amount of drifting and displacement, but small oscillation. This data suggested that the delayed non-movement technique could enhance the specificity of the pedaling-related brain activation in subjects, who creates a great amount of drifting and displacement. Lastly, S13 subject, who showed that using either analysis technique could not extract a physiological meaning data, demonstrated the greatest head motions of all three characteristics of head motions, suggesting that the delayed non-movement technique could not enhance the quality of the functional brain images when the head movement is excessive.

B.4 CONCLUSION

This supplementary study shows that the delayed non-movement technique is beneficial for analyzing pedaling-related brain activation analysis in stroke subjects, specifically in the stroke subjects with a great amount of head oscillation, which likely causes a circumferential ring artifact when using a conventional analysis technique. However, the analysis technique did not have an advantage on the data that contained a great combination of oscillation, drift and displacement, i.e. S13. This suggests that the delayed non-movement technique could be beneficial to either a certain amount of head movement, or a to certain combinations of head motion characteristics.

We also showed that the delayed non-movement technique can account for head oscillation up to 1.32 mm; and it cannot account for oscillatory head movement at 2.76 mm. We do not know the exact cutoff of amount of head movement, as our experiment was not designed to answer this question specifically. Apart from that, the technique does not introduce adverse effects for the data carrying small head movement.

APPENDIX C: ANALYSIS OF FUNCTIONAL NEUROIMAGES (AFNI)

C.1 AFNI functions and scripts for generating a model and stimulus function

AFNI functions	Descriptions
Waver	Creates an ideal waveform time-series file with a given experimental design
RSFgen	Sample program to generate random stimulus functions
Nodata	Evaluate the quality of the experimental design only (no input data)

C.1.1 Waver

```
waver -TR 2 -peak .48 -input model104.1D > canonical100.1D
```

C.1.2 RSFgen

```
set seeds = (1 2 3 4 5 6 7 8 9 10 )
set reps = (20 30 40 50 60 70 80 90 100 110 120 130 140 150)
        foreach rep ($reps)
        foreach seed ($seeds)
                RSFgen \
                        -nt 60 -num_stimts 1 -nblock 1 1 -seed $seed \
                        -one_file -prefix test$seed -nreps 1 $rep\
                        $seed >>test_results
        end
        end
```

C.5.3 Nodata

```
        foreach seed ($seeds)
                3dDeconvolve \
                        -nodata 60 2 -polort A -num_stimts 1 -stim_file 1 test$seed.1D\
                        -stim_label 1 tap -stim_minlag 1 0 -stim_maxlag 1 8\
                        >> test_results
                        1dplot -yaxis -1:2:1:1  -plabel test120$seed.1D test$seed.1D &
        end
```

C.2 AFNI functions and scripts for estimating hemodynamic response functions and for generating the parametric map associated with foot tapping

AFNI functions	Descriptions
to3d	DICOM files (2D) containing fMRI signals are converted into 3D images
3dTshift	A time-series of each individual voxel is aligned to the same temporal origin within each repetition time (TR), so that the separate slices are aligned to the same temporal origin
3dToutcount	Calculating number of 'outliers' a 3D+timedataset, at each time point. These outliers can be eliminated later
3dTcat	Concatenating sub-bricks from input datasets into one 3D+time dataset and remove the first 4 TRs of each run to eliminate non-steady state magnetization artifacts
3dvolreg	Registering each functional scan to the first point of the functional scan obtained closest in time to the anatomical scan
3dDeconvolve	*To estimate hemodynamic response:* Estimate impulse response using deconvolution approach, and generate the fitted model using the least squares estimates of the linear regression coefficients
	To generate parametric brain activation map: General linear modeling (multiple linear regression) was used to fit a canonical hemodynamic response function to the measured blood oxygen level-dependent (BOLD) signal
3dREMLfit	Generalized least squares time-series fit, with restricted maximum likelihood (REML) estimation of the temporal auto-correlation structure
3dSkullStrip	Extract the brain from surrounding tissue from T1-weighted images
3dFWHMx	Functional data were blurred using a 4 mm full width half maximum Gaussian filter
AlphaSim	Performing a Monte Carlo simulation (alpha probability simulations) to compute the probability of a random noise producing a cluster of a given size after the noise is thresholded at a given level (‘-pthr’). In our case, we set individual voxel p-value at 0.005 and used a Monte Carlo simulation to identify an appropriate cluster size that

	maintain a familywise error rate of p<0.05 for each individual subject.
Percent signal change	Computing percent signal change relative to its baseline
3dmerge	Merging the clusterized threshold and the functional dataset
3dcalc	Eliminating any voxels with percent signal change greater than 10 percent, as these large changes were likely due to edge effects
3dBrickStat	Computing volume and mean and max intensity of activation
3dCM	Computing center of activation

C.2.1 Hemodynamic response (event-related experiment)

To3d

```
to3d -prefix anat_tap_day1 \
*MRDC
```

```
set conditions = (f_er_np_30s_1 f_er_np_30s_2 f_er_np_30s_3 f_er_p_30s_1
f_er_p_30s_2 f_er_p_30s_3)
        foreach condition ( $conditions )
                to3d -prefix $condition -time:zt 36 98 2000 alt+z \
                *MRDC*
        end
```

3dTshift

```
set conditions = (f_er_np_30s_1 f_er_np_30s_2 f_er_np_30s_3 f_er_p_30s_1
f_er_p_30s_2 f_er_p_30s_3)
        foreach condition ( $conditions )
                3dTshift -verb -tzero 0 -prefix $condition.tshift -ignore 4 -heptic \
                $condition+orig
        end
```

3dTcat

```
3dTcat \
f_er_np_30s_1.tshift+orig'[4..97]' \
f_er_np_30s_2.tshift+orig'[4..97]' \
f_er_np_30s_3.tshift+orig'[4..97]' \
-prefix f_er_np_30s_03.tshift.cat

3dTcat \
f_er_p_30s_1.tshift+orig'[4..97]' \
f_er_p_30s_2.tshift+orig'[4..97]' \
f_er_p_30s_3.tshift+orig'[4..97]' \
-prefix f_er_p_30s_03.tshift.cat
```

3dvolreg

```
set runs = (f_er_np_30s_03.tshift.cat f_er_p_30s_03.tshift.cat)
        foreach run ($runs)
                3dvolreg \
                -heptic \
                -prefix $run.volreg \
                -base 'f_er_p_30s_3.tshift+orig[0]' \
                -dfile $run.volreg.dfile \
                -1Dfile $run.volreg.1Dfile \
                $run+orig
                cp $run.volreg.1Dfile $run.volreg.1D
        end
```

3dDeconvolve

```
set runs = ( f_er_np_30s_03 f_er_p_30s_03)
        foreach run ($runs)
        3dDeconvolve \
        -float \
        -input $run.tshift.cat.volreg+orig \
        -concat er_30s_03.concat \
        -polort A \
        -num_stimts 7 \
        -stim_file 1 stimtimes_30s_03.1D \
        -stim_minlag 1 0 \
        -stim_maxlag 1 15 \
        -stim_label 1 tap \
        -stim_file 2 $run.tshift.cat.volreg.1Dfile'[0]' -stim_base 2 -stim_label 2 roll \
        -stim_file 3 $run.tshift.cat.volreg.1Dfile'[1]' -stim_base 3 -stim_label 3 pitch \
        -stim_file 4 $run.tshift.cat.volreg.1Dfile'[2]' -stim_base 4 -stim_label 4 yaw \
```

```
        -stim_file 5 $run.tshift.cat.volreg.1Dfile'[3]' -stim_base 5 -stim_label 5 dS \
        -stim_file 6 $run.tshift.cat.volreg.1Dfile'[4]' -stim_base 6 -stim_label 6 dL \
        -stim_file 7 $run.tshift.cat.volreg.1Dfile'[5]' -stim_base 7 -stim_label 7 dP \
        -iresp 1 $run.decon.glt.iresp_15 \
        -num_glt 1 \
        -glt_label 1 peak1 \
        -gltsym 'SYM: +tap[2..5]' \
        -fout \
        -tout \
        -bout \
        -full_first \
        -fitts $run.decon.glt.fitts_15 \
        -errts $run.decon.glt.errts_15\
        -bucket $run.decon.glt.bucket_15
        csh $run.REML_cmd
end
```

3dSkullStrip

```
        3dSkullStrip \
                -input anat_tap_day1+orig \
                -push_to_edge \
                -blur_fwhm 2 \
                -ld 100 \
                -prefix anat_tap_day1_strip_PTE_mesh


        3dcalc \
                -a anat_tap_day1_strip_PTE_mesh+orig \
                -expr "step(a-1700)" \
                -prefix anat_tap_day1_strip_1500_PTE_mesh


        3dfractionize \
                -template f_er_np_30s_03.tshift.cat+orig \
                -input anat_tap_day1_strip_1500_PTE_mesh+orig \
                -prefix anat_tap_day1_strip_1500_PTE_mesh_bigvoxels


        3dcalc \
                -a anat_tap_day1_strip_1500_PTE_mesh_bigvoxels+orig \
                -expr "step(a)" \
                -prefix anat_tap_day1_strip_1500_PTE_mesh_bigvoxels.mask
```

3dFWHMx

```
3dFWHMx \
        -dset pedal06_censor.tshift.cat.decon.errts+orig \
        -mask anat_pedal_strip_1500_bigvoxels.mask+orig \
        -out pedal06_censor.tshift.cat.FWHMx.

#Report from 3dFWHMx
-fwhmx 5.14  -fwhmy 4.10  -fwhmz 2.98
```

AlphaSim

```
AlphaSim \
        -quiet \
        -mask anat_pedal_strip_1500_bigvoxels.mask+orig \
        -fwhmx 5.14  -fwhmy 4.10  -fwhmz 2.98 \
        -rmm 6.6 \
        -pthr 0.005 \
        -iter 1000 \
        -out alphasim_0.005.txt

#Report from AlphaSim
#Alpha = 0.05   #of Cl = 6.6 i.e 371.25
```

Scaling and computing percent signal change (PSC)

```
set runs = (f_er_np_30s_03 f_er_p_30s_03)
set pieces = (19 21 23 25 27 29 31 33 35 37 39 41 43 45 47 49)
        foreach run ($runs)
        foreach piece ($pieces)
                3dcalc \
                        -fscale \
                        -a $run.decon.glt.bucket_15+orig'[1]' \
                        -b $run.decon.glt.bucket_15+orig'[7]' \
                        -c $run.decon.glt.bucket_15+orig'[13]' \
                        -d $run.decon.glt.bucket_15+orig'['$piece']' \
                        -expr "100 *(d/((a+b+c)/3))*step(1-abs((d/((a+b+c)/3))))" \
                        -prefix $run.decon.glt.bucket_15.$piece.PSC
        end
        end
```

Averaging the scaled coefficients (PSC) of the peak points [2nd..4th] of a hemodynamic response

```
foreach run ($runs)
        3dcalc \
                -a $run.decon.glt.bucket_15.23.PSC+orig'[0]' \
                -b $run.decon.glt.bucket_15.25.PSC+orig'[0]' \
                -c $run.decon.glt.bucket_15.27.PSC+orig'[0]' \
                -expr "((a+b+c)/3)" \
                -prefix $run.decon.glt.bucket_15.PSC.avg
end
```

Putting coef and stat data together

```
foreach run ($runs)
        3dbuc2fim \
                -prefix $run.decon.glt.bucket_15.PSC.avg.stat \
                $run.decon.glt.bucket_15.PSC.avg+orig'[0]'\
                $run.decon.glt.bucket_15_REML+orig'[35]'
end
```

C.2.2 Parametric map associated with foot tapping (block experiment)

To3d

```
        to3d -prefix anat_tap_day1 \
        *MRDC*

set conditions = (f_bl_np f_bl_p)
        foreach condition ( $conditions )
                to3d -prefix $condition -time:zt 36 104 2000 alt+z \
                *MRDC*
        end
```

3dTshift

```
set conditions = (f_bl_p f_bl_np)
        foreach condition ( $conditions )
                3dTshift -verb -tzero 0 -prefix $condition.tshift -ignore 4 -heptic \
                $condition+orig
        end
```

3dTcat

```
3dTcat \
f_bl_np.tshift+orig'[4..103]' \
-prefix f_bl_np.tshift.cat


3dTcat \
f_bl_p.tshift+orig'[4..103]' \
-prefix f_bl_p.tshift.cat
```

3dvolreg

```
set runs = ( f_bl_np.tshift.cat f_bl_p.tshift.cat)
        foreach run ($runs)
                3dvolreg \
                -heptic \
                -prefix $run.volreg \
                -base 'f_er_p_30s_3.tshift+orig[0]' \
                -dfile $run.volreg.dfile \
                -1Dfile $run.volreg.1Dfile \
                $run+orig
                cp $run.volreg.1Dfile $run.volreg.1D
        end
```

3dDeconvolve

```
set runs = (f_bl_np f_bl_p)
        foreach run ($runs)
        3dDeconvolve \
        -float \
        -input $run.tshift.cat.volreg+orig \
        -polort A -num_stimts 7 \
        -censor Mcensor100.1D -stim_file 1 Mcanonical100.1D \
        -stim_minlag 1 0 -stim_maxlag 1 0 -stim_label 1 tap \
        -stim_file 2 $run.tshift.cat.volreg.1Dfile'[0]' -stim_base 2 -stim_label 2 roll \
        -stim_file 3 $run.tshift.cat.volreg.1Dfile'[1]' -stim_base 3 -stim_label 3 pitch \
        -stim_file 4 $run.tshift.cat.volreg.1Dfile'[2]' -stim_base 4 -stim_label 4 yaw \
        -stim_file 5 $run.tshift.cat.volreg.1Dfile'[3]' -stim_base 5 -stim_label 5 dS \
        -stim_file 6 $run.tshift.cat.volreg.1Dfile'[4]' -stim_base 6 -stim_label 6 dL \
        -stim_file 7 $run.tshift.cat.volreg.1Dfile'[5]' -stim_base 7 -stim_label 7 dP \
        -fitts $run.tshift.cat.decon.fitts_Censor \
        -errts $run.tshift.cat.decon.errts_Censor \
        -fout -tout -bout -full_first \
```

```
        -bucket $run.tshift.cat.decon.bucket_Censor
        csh $run.REML_cmd
end
```

3dSkullStrip

```
        3dSkullStrip \
                -input anat_tap_day1+orig \
                -push_to_edge \
                -blur_fwhm 2 \
                -ld 100 \
                -prefix anat_tap_day1_strip_PTE_mesh


        3dcalc \
                -a anat_tap_day1_strip_PTE_mesh+orig \
                -expr "step(a-1700)" \
                -prefix anat_tap_day1_strip_1500_PTE_mesh


        3dfractionize \
                -template f_er_np_30s_03.tshift.cat+orig \
                -input anat_tap_day1_strip_1500_PTE_mesh+orig \
                -prefix anat_tap_day1_strip_1500_PTE_mesh_bigvoxels


        3dcalc \
                -a anat_tap_day1_strip_1500_PTE_mesh_bigvoxels+orig \
                -expr "step(a)" \
                -prefix anat_tap_day1_strip_1500_PTE_mesh_bigvoxels.mask
```

3dFWHMx

```
        3dFWHMx \
                -dset pedal06_censor.tshift.cat.decon.errts+orig \
                -mask anat_pedal_strip_1500_bigvoxels.mask+orig \
                -out pedal06_censor.tshift.cat.FWHMx

#Report from 3dFWHMx
-fwhmx 5.14  -fwhmy 4.10  -fwhmz 2.98
```

AlphaSim

```
AlphaSim \
        -quiet \
        -mask anat_pedal_strip_1500_bigvoxels.mask+orig \
        -fwhmx 5.14  -fwhmy 4.10  -fwhmz 2.98 \
        -rmm 6.6 \
        -pthr 0.005 \
        -iter 1000 \
        -out alphasim_0.005.txt

#Report from AlphaSim
#Alpha = 0.05   #of Cl = 6.6 i.e 371.25
```

Scaling and computing percent signal change (PSC)

```
set runs = (f_bl_np f_bl_p)
    foreach run ($runs)
        3dcalc \
            -fscale \
            -a $run.tshift.cat.decon.bucket_ Censor +orig'[1]' \
            -d $run.tshift.cat.decon.bucket_ Censor +orig'[7]' \
            -expr "100 *(d/((a)/1))*step(1 -abs((d/((a)/1))))" \
            -prefix $run.decon.bucket_ Censor.PSC
    end
```

Putting coef and stat data together

```
    foreach run ($runs)
        3dbuc2fim \
            -prefix $run.decon.bucket Censor.PSC.stat \
            $run.decon.bucket Censor.PSC+orig'[0]'\
            $run.tshift.cat.decon.bucket_" Censor "_REML+orig'[2]'

    end
```

3dmerge

```
foreach run ($runs)
foreach method ($methods)
    3dmerge \
        -1thresh 2.8 \
        -1clust 6.6 371.25 \
        -1dindex 0 \
```

```
		-1tindex 1 \
		-prefix $run.decon_"$method".PSC_AUC_thresh.REML_stat \
		$run.decon.bucket_"$method".PSC.stat+orig

	3dmerge \
		-1thresh 2.8 \
		-1clust_order 6.6 371.25  \
		-1dindex 0 \
		-1tindex 1 \
		-1noneg \
		-prefix $run.decon_"$method".PSC_AUC_order.thresh.REML_stat \
		$run.decon.bucket_"$method".PSC.stat+orig
end
end



foreach run ($runs)
foreach method ($methods)
	3dcalc \
		-a $run.decon_"$method".PSC_AUC_thresh.REML_stat+orig \
		-b anat_tap_day1_strip_1500_PTE_mesh_bigvoxels.mask+orig \
		-expr "step(b)*a" \
		-prefix $run.decon_"$method".PSC_AUC_thresh.REML_stat.mask

	3dcalc \
		-a $run.decon_"$method".PSC_AUC_order.thresh.REML_stat+orig \
		-b anat_tap_day1_strip_1500_PTE_mesh_bigvoxels.mask+orig \
		-expr "step(b)*a" \
		-prefix $run.decon_"$method".PSC_AUC_order.thresh.REML_stat.mask
end
end



foreach run ($runs)
foreach method ($methods)
	3dmerge \
	-1clust_order 6.6 371.25\
	-1erode 0 -1dilate \
	-prefix
	$run.decon_"$method".PSC_AUC_order.thresh.REML_stat.mask.ERODE \
	$run.decon_"$method".PSC_AUC_order.thresh.REML_stat.mask+orig
end
end



foreach run ($runs)
```

```
foreach method ($methods)
	3dmerge \
	-1clust_order 6.6 371.25\
	-prefix
$run.decon_"$method".PSC_AUC_order.thresh.REML_stat.mask.ERODE.CLUST \
	$run.decon_"$method".PSC_AUC_order.thresh.REML_stat.mask.ERODE+orig
end
end


foreach run ($runs)
foreach method ($methods)
3dcalc \
	-a
$run.decon_"$method".PSC_AUC_order.thresh.REML_stat.mask.ERODE.CLUST+orig
\
	-b $run.decon.bucket_"$method".PSC.stat+orig \
	-expr "step(a)*b" \
	-prefix $run.decon.bucket._"$method".PSC.STAT.MASK
end
end
```

3dcalc

```
foreach run ($runs)
foreach method ($methods)
3dcalc \
	-a $run.decon.bucket._"$method".PSC.STAT.MASK+orig'[0]' \
	-expr "a*within(a,-10,10) " \
	-prefix $run.decon.bucket._"$method".PSC.STAT.MASK_outlier
end
end


foreach run ($runs)
foreach method ($methods)
3dcalc\
	-a $run.decon.bucket._"$method".PSC.STAT.MASK+orig\
	-b $run.decon.bucket._"$method".PSC.STAT.MASK_outlier+orig\
	-expr "step(b)*a" \
	-prefix $run.decon.bucket._"$method".PSC.STAT.MASK_outlier_stat
end
end
```

```
# Manually define regions of interest


set runs = (f_bl_np.tshift.cat)
set methods = (Censor)
set regions = (0)
        foreach run ($runs)
        foreach method ($methods)
        foreach region ($regions)
                3dcalc\
                -a $run.decon.bucket._"$method".PSC.STAT.MASK_outlier_stat+orig \
                -b $run."$method".$region.outlier+orig \
                -expr "step(b)*a" \
                -prefix $run."$method".SM1
end
end
end


set runs = (f_bl_p.tshift.cat)
set methods = (Censor)
set regions = (1)
        foreach run ($runs)
        foreach method ($methods)
        foreach region ($regions)
                3dcalc\
                -a $run.decon.bucket._"$method".PSC.STAT.MASK_outlier_stat+orig \
                -b $run."$method".$region.outlier+orig \
                -expr "step(b)*a" \
                -prefix $run."$method".SM1
end
end
end
```

3dBrickStat

```
set runs = (f_bl_np.tshift.cat f_bl_p.tshift.cat)
set methods = (Censor)
        foreach run ($runs)
        foreach method ($methods)
                3dBrickStat \
                        -volume \
                        -max \
                        -mean \
                        -non-zero \
```

```
                $run."$method".SM1+orig \
                >$run."$method".orig.count.txt
        end
        end
```

3dCM

```
set runs = (f_bl_np.tshift.cat f_bl_p.tshift.cat)
set methods = (Censor)
        foreach run ($runs)
        foreach method ($methods)
                3dCM \
                        $run."$method".SM1+orig \
                        >$run."$method".orig.CM.txt
        end
        end
```

C.2 AFNI functions and scripts for generating the parametric map associated with pedaling (block experiment)

The AFNI functions and scripts are similar the scripts that used for processing parametric maps associated with foot-tapping.

To3d

```
    to3d -prefix anat_pedal \
    *MRDC*

set conditions = (pedal1 pedal2 pedal3 pedal4 pedal5 pedal6)
        foreach condition ( $conditions )
                to3d \
                        -prefix $condition -time:zt 36 128 2000 alt+z \
                        *MRDC*
        end
```

3dTshift

```
set conditions = (pedal1 pedal2 pedal3 pedal4 pedal5 pedal6)
        foreach condition ( $conditions )
                3dTshift \
                        -verb -tzero 0 -prefix $condition.tshift \
                        -ignore 4 -heptic
                        $condition+orig
        end
```

3dToutcount

```
set conditions = (pedal1 pedal2 pedal3 pedal4 pedal5 pedal6)
        foreach condition ( $conditions )
                3dTshift -verb -tzero 0 -prefix $condition.tshift \
                -ignore 4 -heptic \$condition+orig
        end
```

3dTcat

```
        3dTcat \
                pedal1.tshift+orig'[4..127]' \
                pedal2.tshift+orig'[4..127]' \
                pedal3.tshift+orig'[4..127]' \
                pedal4.tshift+orig'[4..127]' \
                pedal5.tshift+orig'[4..127]' \
                pedal6.tshift+orig'[4..127]' \
                -prefix pedal06.tshift.cat
```

3dvolreg

```
        3dvolreg \
                -heptic \
                -prefix pedal06.tshift.cat.volreg \
                -base 'pedal6.tshift+orig[0]' \
                -dfile pedal06.tshift.cat.volreg.dfile \
                -1Dfile pedal06.tshift.cat.volreg.1Dfile \
                pedal06.tshift.cat+orig
```

3dDeconvolve

```
3dDeconvolve \
        -float \
```

```
-input pedal06.tshift.cat.volreg+orig \
-concat concat.pedal.744\
-polort A -num_stimts 7 \
-censor Mcensor744.1D \
-stim_file 1 Mcanonical744.1D \
-stim_minlag 1 0 -stim_maxlag 1 0 \
-stim_label 1 pedal \
-stim_file 2 pedal06.tshift.cat.volreg.1Dfile'[0]' -stim_base 2 -stim_label 2 roll \
-stim_file 3 pedal06.tshift.cat.volreg.1Dfile'[1]' -stim_base 3 -stim_label 3 pitch \
-stim_file 4 pedal06.tshift.cat.volreg.1Dfile'[2]' -stim_base 4 -stim_label 4 yaw \
-stim_file 5 pedal06.tshift.cat.volreg.1Dfile'[3]' -stim_base 5 -stim_label 5 dS \
-stim_file 6 pedal06.tshift.cat.volreg.1Dfile'[4]' -stim_base 6 -stim_label 6 dL \
-stim_file 7 pedal06.tshift.cat.volreg.1Dfile'[5]' -stim_base 7 -stim_label 7 dP \
-fitts pedal06_censor.tshift.cat.decon.fitts \
-errts pedal06_censor.tshift.cat.decon.errts \
-fout -tout -bout -full_first \
-bucket pedal06_censor.tshift.cat.decon.bucket
csh pedal06_censor.REML_cmd
```

3dSkullStrip

```
3dSkullStrip \
        -input anat_pedal+orig \
        -push_to_edge \
        -ld 50 \
        -prefix anat_pedal_strip_PTE_mesh

3dcalc \
        -a anat_pedal_strip_PTE_mesh+orig \
        -expr "step(a-1500)" \
        -prefix anat_pedal_strip_1500_PTE_mesh

3dfractionize \
        -template pedal03.tshift.cat+orig \
        -input anat_pedal_strip_1500_PTE_mesh+orig \
        -prefix anat_pedal_strip_1500_PTE_mesh_bigvoxels

3dcalc \
        -a anat_pedal_strip_1500_PTE_mesh_bigvoxels+orig \
        -expr "step(a)" \
        -prefix anat_pedal_strip_1500_PTE_mesh_bigvoxels.mask
```

3dFWHMx

```
set runs = ( pedal06_censor.tshift.cat )
	foreach run ($runs)
		3dFWHMx \
			-dset $run.decon.errts+orig \
			-mask anat_pedal_strip_1500_bigvoxels.mask+orig \
			-out $run.FWHMx.
	end


#Report from 3dFWHMx
-fwhmx 5.14  -fwhmy 4.10  -fwhmz 2.98
```

AlphaSim

```
	AlphaSim \
		-quiet \
		-mask anat_pedal_strip_1500_bigvoxels.mask+orig \
		-fwhmx 5.14  -fwhmy 4.10  -fwhmz 2.98 \
		-rmm 6.6 \
		-pthr 0.005 \
		-iter 1000 \
		-out alphasim_0.005.txt

# Report from AlphaSim
#Alpha = 0.05   #of Cl = 6.6 i.e 371.25
```

Percent signal change

```
set runs = (pedal06_censor.tshift.cat)
set pieces = (37)
	foreach run ($runs)
	foreach piece ( $pieces )
		3dcalc \
		-fscale \
		-a $run.decon.bucket+orig'[1]' \
		-b $run.decon.bucket+orig'[7]' \
		-c $run.decon.bucket+orig'[13]' \
		-d $run.decon.bucket+orig'[19]' \
		-e $run.decon.bucket+orig'[25]' \
		-f $run.decon.bucket+orig'[31]' \
		-g $run.decon.bucket+orig'['$piece']' \
		-expr "100 * (g/((a+b+c+d+e+f)/6)) * step(1-abs((g/((a+b+c+d+e+f)/6))))"
		-prefix $run.decon.bucket.PSC
```

```
        end
        end


foreach run ($runs)
        3dbuc2fim \
                -prefix $run.decon.bucket.PSC.stat \
                $run.decon.bucket.PSC+orig'[0]'\
                $run.decon.bucket_REML+orig'[2]'
        end
```

3dmerge

```
set runs = (pedal06_censor.tshift.cat)
        foreach run ($runs)
                3dmerge \
                        -1thresh 2.8 -1clust 6.6 371.25 \
                        -1dindex 0 -1tindex 1 \
                        -prefix $run.decon.PSC_AUC_thresh.REML_stat \
                        $run.decon.bucket.PSC.stat+orig

                3dmerge \
                        -1thresh 2.8 -1clust_order 6.6 371.25  \
                        -1dindex 0 -1tindex 1 -1noneg \
                        -prefix $run.decon.PSC_AUC_order.thresh.REML_stat \
                        $run.decon.bucket.PSC.stat+orig
        end

        foreach run ($runs)
                3dcalc \
                        -a $run.decon.PSC_AUC_thresh.REML_stat+orig \
                        -b anat_pedal_strip_1500_PTE_mesh_bigvoxels.mask+orig \
                        -expr "step(b)*a" \
                -prefix $run.decon.PSC_AUC_thresh.REML_stat.mask

                3dcalc \
                        -a $run.decon.PSC_AUC_order.thresh.REML_stat+orig \
                        -b anat_pedal_strip_1500_PTE_mesh_bigvoxels.mask+orig \
                        -expr "step(b)*a" \
                        -prefix $run.decon.PSC_AUC_order.thresh.REML_stat.mask
        end
```

3dcalc

```
foreach run ($runs)
    3dcalc \
        -a $run.decon.bucket.PSC.STAT.MASK+orig'[0]' \
        -expr "a*within(a,-10,10) " \
        -prefix $run.decon.bucket.PSC.STAT.MASK_outlier
    end
```

Manually define regions of interest

3dBrickStat

```
foreach run ($runs)
foreach area ($areas)
    3dBrickStat \
        -volume \
        -max \
        -mean \
        -non-zero \
        $run.decon.bucket.PSC.STAT.MASK.$area+orig \
        >$run.$area.orig.count.txt
end
end
```